

**TECHNISCHE UNIVERSITÄT MÜNCHEN**

**Pankreas-Forschungslabor**

**Chirurgische Klinik und Poliklinik**

**Klinikum rechts der Isar**

**Aldh1a3 plays a context-dependent role in early pancreatic  
carcinogenesis**

Jing Cao

Vollständiger Abdruck der von der Fakultät für Medizin der Technischen Universität  
München zur Erlangung des akademischen Grades eines Doktors der Medizin  
genehmigten Dissertation.

Vorsitzender: Prof. Dr. Jürgen Schlegel

Prüfer der Dissertation: 1. Prof. Dr. Helmut Friess  
2. Priv.-Doz. Dr. Anna M. Schlitter

Die Dissertation wurden am 16.07.2019 bei der Technischen Universität München  
eingereicht und durch die Fakultät für Medizin  
am 01.01.2020 angenommen.

# Table of Contents

<b>1. INTRODUCTION</b>	3
1.1 ALDHs and its subfamily ALDH1A3	3
1.1.1 The function of ALDHs	3
1.1.2 The role of ALDHs in stem cells	4
1.1.3 ALDHs in cancer stem cells	4
1.1.4 ALDH1A3 and its role in normal tissues and malignancies	6
1.2 PDAC	7
1.2.1 Carcinogenesis of PDAC	8
1.2.2 Acinar-to-ductal metaplasia (ADM) and atypical flat lesions (AFLs) in PDAC	10
1.3 ALDH and PDAC	11
1.4 ALDH1A3 and PDAC	12
1.5 Cancer-associated fibroblasts (CAFs) and PDAC	13
<b>2. AIMS OF THIS STUDY</b>	15
<b>3. MATERIALS AND METHODS</b>	16
3.1 Materials	16
3.1.1 Mouse lines	16
3.1.2 List of the antibodies	20
3.1.3 Chemicals and Reagents	22
3.1.4 Buffers and Solutions	24
3.1.5 Kits	27
3.1.6 Laboratory consumables	28
3.1.7 Laboratory equipment	28
3.2 Methods	30
3.2.1 Caerulein treatment	30
3.2.2 Tamoxifen treatment	30
3.2.3 mouse primary pancreatic cell isolation and flow cytometry	30
3.2.4 Immunohistochemistry (IHC) analysis and quantification	31
3.2.5 Immunofluorescence (IF) analysis and quantification	32
3.2.6 Oil Red O staining	32
3.2.7 mRNA isolation	33

3.2.8 Quantitative Real-time Polymerase Chain Reaction (qRT-PCR, qPCR).....	33
3.2.9 Immunoblot analysis .....	34
3.3 Statistical analysis .....	35
<b>4. RESULTS .....</b>	<b>36</b>
4.1 The presence of ALDH1A3-positive cells in tumors rendered PDAC patients with a worse prognosis. ....	36
4.2 Aldh1a3 is also expressed in primary and metastatic murine PDAC .....	39
4.3 Aldh1a3 was expressed in pre-neoplastic lesions driven by oncogenic Kras <sup>G12D</sup> .....	40
4.4 Aldh1a3 ablation does not affect pancreatic physiology .....	42
4.5 Aldh1a3 deletion in pancreatic epithelial cells slightly promotes PanIN lesions in KC mice with acute pancreatitis .....	43
4.6 Aldh1a3 ablation promotes PanIN formation via suppressing p53 in the context of acute pancreatitis .....	48
4.7 Loss of Aldh1a3 reduced the “stemness” of pre-neoplastic lesions .....	51
4.8 Aldh1a3 promotes early pancreatic carcinogenesis in the absence of acute inflammation.....	53
4.9 ALDH1A3 labels a subgroup of mesenchymal cells. ....	55
<b>5. DISCUSSION .....</b>	<b>59</b>
<b>6. SUMMARY .....</b>	<b>65</b>
<b>7. ABBREVIATION.....</b>	<b>67</b>
<b>8. LIST OF FIGURES.....</b>	<b>69</b>
<b>9. REFERENCE .....</b>	<b>72</b>
<b>10. CURRICULUM VITAE .....</b>	<b>88</b>
<b>11. ACKNOWLEDGEMENTS.....</b>	<b>90</b>

# 1. INTRODUCTION

## 1.1 ALDHs and its subfamily ALDH1A3

### 1.1.1 The function of ALDHs

Aldehyde dehydrogenases (ALDHs) stand for a family of NAD(P)<sup>+</sup>-dependent enzymes, which exert their contributions in the metabolism of a broad range of endogenous and exogenous aliphatic and aromatic aldehydes (Vasiliou & Pappa, 2000). They catalyze the oxidation of aldehydes terminally to carboxylic acids. As aldehydes are commonly generated by metabolic processes (e.g. alcohol oxidation, lipid peroxidation), ALDHs mediate the detoxification of aldehydes thereafter.

Up to 19 isoforms of ALDHs have been hitherto identified in the human genome. A systematic nomenclature scheme for ALDH gene subfamily has been developed and updated based on divergent evolutions of aldehyde dehydrogenase amino-acid sequences and chromosome mapping (Sophos, Pappa, Ziegler, & Vasiliou, 2001; Sophos & Vasiliou, 2003; Vasiliou, Bairoch, Tipton, & Nebert, 1999; Ziegler & Vasiliou, 1999). The categorization of ALDH proteins is according to the percentage of amino acid identity. Proteins sharing 40% identity are classified to a subfamily designated by an Arabic number, and those exhibiting 60% identity are assigned into the same subgroup but with a letter as a further designation, the latter of which is expected to locate at the same sub-chromosome site. Accordingly, these isozymes harbour some similar amino acid sequences, hence some certain functions are shared among them, whereas their distributions differ in tissues/organs, in localization in cells and specificity to various substrates. Enzymes in ALDHs family play vital roles in physiological and toxicological function, covering the ranges from inflammation, metabolic disorders, metaplasia and malignancies.

### 1.1.2 The role of ALDHs in stem cells

Stem cells are undifferentiated cells with the distinguished ability of self-renewing and differentiating to mature progenies, including differentiated progenitor cells and terminally functional cells. Based on the developmental potentials, stem cells have been categorized into more specific subtypes, totipotent cells (able to generate embryonic and extra-embryonic cells), pluripotent cells (able to generate all cell types of embryo proper), multipotent cells (able to generate subtypes of cell lineages), oligopotent cells (able to generate more restricted subgroups of cell lineages), and unipotent cells (able to generate only certain mature cell type) (Wagers & Weissman, 2004). Stem cells have been identified in almost all tissues and suggested to share some common features including the habitation of ATP-binding cassette transporter G2 (Ding, Wu, & Jiang, 2010; Fatima, Zhou, & Sorrentino, 2012; Gangavarapu et al., 2013), harbor of high telomerase (Cai et al., 2004) and ALDH activity (Storms et al., 1999). High levels of ALDH activity, along with some other markers, have been demonstrated to identify stem/progenitor cells of high clonogenicity and multipotency in human bone marrow (Kastan et al., 1990) and blood (Christ et al., 2007; Pearce et al., 2005), hence the fact that ALDH activity, up to now, has been commonly used in sorting stem/progenitor cells in the haematopoietic system. Meanwhile, accumulated evidence has also supported partitioning stem cells upon ALDH level in other tissues such as brain-derived neural stem cell (Corti et al., 2006)

### 1.1.3 ALDHs in cancer stem cells

Cancer stem cells (CSCs), also known as tumour-initiating cells, have been identified in a growing amount of various human malignancies, including diverse solid tumors (Visvader & Lindeman, 2008), since the first prospective illustration of a CSC by Dick's research group for

AML in 1994 (Bonnet & Dick, 1997; Lapidot et al., 1994). One of the potential biological properties of CSCs underlies their role as a novel prognostic factor, yet their exact function in cancer progression remains to be further investigated. Two main functional features of CSCs are illustrated as 1) the ability to generate differentiated tumor cells with the same characteristics as the original tumor *in situ* or metastasis, 2) the ability of self-renewal (Grun, Hirose, Kawauchi, Ogura, & Umesono, 2000), suggesting that CSCs may serve as a central role in the initiation, progression and relapse of malignancies.

Even though CSCs share important properties with embryonic and normal stem cells, the capability to self-renewal and to further differentiate, CSCs do not necessarily derive from transformed normal stem cells. They may originate from progenitors or even differentiated cells that have acquired the ability of self-renewing (Tang, 2012). Regardless of their origins, CSCs are now generally defined in most cancers as distinct, isolatable tumor populations, and their prevalence is proposed to correlate with the aggressiveness of the malignancies (Marcato et al., 2011). Compared to the bulk of tumor, CSCs, though of a relatively small number, are believed to be the main and pivotal reason for recurrent and metastasis of cancer. Accordingly, CSC contributes as potential prognostic indicators in suffered patients.

In most experimental systems, the identification of CSCs has depended on the detection of particular cell surface antigens. Among those, ALDH activity is regarded as one of the main markers for discrete isolation of CSCs, and enhanced ALDH activity plays as a hallmark of CSCs. However, the expression of ALDH activity varies in different cancers, as multiple or distinct ALDH isoforms contribute to specific types of tumors and CSC markers, overall, are not universal for all types of cancers (Visvader & Lindeman, 2012). High ALDH activity has been described in tumorigenic cells among a few malignancies, involving acute myeloid leukemia (Cheung et al., 2007), primary breast tumor (Charafe-Jauffret et al., 2013; Ginestier et al., 2007; Tanei et al., 2009), hepatocellular carcinoma (Ma et al., 2008),

cholangiocarcinoma(Chen et al., 2016), colorectal cancer(Huang et al., 2009), pancreatic adenocarcinoma(Rasheed et al., 2010), prostate cancer(van den Hoogen et al., 2010), Hodgkin lymphoma(Jones et al., 2009) et cetera.

#### 1.1.4 ALDH1A3 and its role in normal tissues and malignancies

It is known that the ALDH activity in different organs and tissues is ascribed to differential subfamily isoforms, though some overlapping contributions exist, due to similar structures and functions shared by subgroups.

The ALDH1A subfamily, locating in the cytoplasm and mitochondria, consist of ALDH1A1, ALDH1A2 and ALDH1A3, which are essential in retinoic acid (RA) signalling through synthesizing retinaldehyde to RA. These isozymes have a high affinity for the oxidation of both *all-trans*- and *9-cis*-retinal.

ALDH1A3, firstly named as ALDH6 and discovered by Hsu et al. (Hsu, Chang, Hiraoka, & Hsieh, 1994), is involved in the biosynthesis of RA, particularly in the irreversible conversion of retinaldehyde to RA, hence another name Retinaldehyde Dehydrogenase 3 (RALDH3). It metabolizes *all-trans*-retinal, but not *9-cis*-retinal (Grun et al., 2000; Vasiliou, Pappa, & Estey, 2004).

ALDH1A3 expresses at distinct periods and locations throughout embryogenesis (Blentic, Gale, & Maden, 2003), and it is found, postnatal, to exert its main contributions to ALDH activity in both normal tissues and malignancies. Its expressions distribute highly in the ventral retina, nasal epithelium and nasolacrimal groove(Dupe et al., 2003), hair follicle(Everts, King, Sundberg, & Ong, 2004), prostate, trachea, and intestine(Fu, Selwyn, Cui, & Klaassen, 2016), faintly in Leydig cells in testis(Vernet et al., 2006). It is also reported that ALDH1A3 plays a key role in ALDH level in cardiac atrial appendage progenitor cells(Puttini et al., 2018).

Global Aldh1a3 knockout mouse model causes respiratory distress and death of Aldh1a3-null mutants at birth, due to choanal atresia, a malformation restricted to ocular and nasal regions resulted from suppressed RA synthesis(Dupe et al., 2003), underlying the importance of Aldh1a3 in *all-trans*-retinoic acid (atRA) formation during fetal development.

As ALDH level is enriched in CSCs and tumours, ALDH1A3 subtype is rationally enhanced in some malignancies. It is reported that ALDH1A3 contributes to the ALDH activity in most non-small cell lung cancer (NSCLC), while ALDH1A1 makes such contribution in small cell lung cancer (SCLC)(Shao et al., 2014). Moreover, consistently, ALDH1A3 knockdown reduced the ALDH activity of NSCLC cells. In human melanoma tumors, ALDH1A3 is expressed over 15-fold more in ALDH<sup>+</sup> cells than in ALDH<sup>-</sup> melanoma cells and is ranked second to ALDH1A1 in xenograft melanomas, but the most abundant isoform in ALDH<sup>+</sup> cell(Luo et al., 2012). Researches on breast cancers also showed ALDH1A3 is of primary importance for aldehyde activity in breast cancer cell lines and patient-derived samples(Marcato et al., 2011). The similar contributing role of ALDH1A3 was found in human cholangiocarcinoma (Chen et al., 2016) and malignant pleural mesothelioma (MPM) cells(Canino et al., 2015) as well.

## 1.2 PDAC

Pancreatic ductal adenocarcinoma (PDAC), the most common type of pancreatic neoplasm, covers more than 85% cases of pancreatic malignancy. It is the fourth most common cause of cancer-related death in the United States and is expected to become the second leading cause by 2030 (Rahib et al., 2014).

Several factors contribute to the poor prognosis of PDAC. Firstly, early detection of high-risk susceptible population is not available yet due to the absence of specific biomarkers(Lankadasari, Mukhopadhyay, Mohammed, & Harikumar, 2019). Secondly,



patients are always diagnosed with an advanced stage as the clinical symptoms are nonspecific in most cases before an advanced stage is reached. Finally, surgical resection, up to now, remains the only clinically curative method to PDAC but is unfortunately only possible to a small group of patients without radiological signs or distant metastasis(Wagner et al., 2004). Chemotherapy, despite the active application of novel chemotherapeutic regimens, resulted in merely a slight improvement of overall survival (OS).

### 1.2.1 Carcinogenesis of PDAC

Unlike tissues from colon, breast, prostate, and cervix, pancreatic tissue is not readily accessible to biopsy. As a result, the study to trace how pancreatic cancer progresses, histologically and genetically, was carried out much later than those of other cancers.

Surgical resection and the development in histology evaluation has facilitated the understanding of the morphology of dysplastic lesions and has further allowed for the identification and morphological classification of precursor lesions of pancreatic cancer. The putative precursors are described as pancreatic intraepithelial neoplasia (PanIN), intraductal papillary-mucinous neoplasm (IPMN), and mucinous cystic neoplasm (MCN)(Vincent, Herman, Schulick, Hruban, & Goggins, 2011). Among them, proliferations of PanINs are widely accepted to give rise to most pancreatic cancers. Mucin production, loss of cellular polarity, and graded nuclear atypia were gradually acquired during PanIN progression as characterized morphological changes. Cells in PanIN1 (1A and-1B) stage are assigned with elongated, flat or papillary architecture along with enhanced mucin production. Later they acquire moderate (PanIN2) and severe nuclear abnormalities (PanIN3) as the atypia progress (Schneider, Siveke, Eckel, & Schmid, 2005).

Since the identification of Kras oncogene mutation was released as the first significant gene altered in pancreatic cancer in 1988(Almoguera et al., 1988), an explosion of understanding

the genetic alteration has been seen in the last three decades. Moreover, pancreatic cancer has now become one of the better-characterized malignancies at genetic levels.

Up to date, two typical predictions have been commonly believed as the characterized progression model of PDAC, based on analyses of pancreatic intraepithelial neoplasm lesions: genetic alterations, which contribute crucially to PDAC, are acquired through a particular sequence (KRAS > CDKN2A > TP53/SMAD4) (Luttges et al., 2001; Moskaluk, Hruban, & Kern, 1997; Wilentz et al., 1998; Wilentz et al., 2000); each alteration is obtained independently, and the evolutionary trajectory is, therefore, gradual. This theory of tumorigenesis indicates the notion that PDAC evolves slowly and presents at a late stage, which, however, contradicts strongly the fact that PDAC has a high propensity to metastasize early and rapidly and early detection is so far not yet available (Chari et al., 2015). Notably, a new analysis upon tumour-enriched genomes revealed that tumorigenesis of pancreatic cancer is not gradual and does not follow the prevailing mutation order (Notta et al., 2016). Their novel finding challenges the previous model by arguing that two-thirds of pancreatic tumours contain complex rearrangement patterns associated with mitotic errors, and these errors eventually lead to simultaneous knockout of canonical tumour-suppressor genetic, instead of sequential gene knockout.

The putative KRAS mutations were demonstrated to prevail lesions from low-grade PanINs to advanced PDAC. Though CDKN2A, TP53, and SMAD4 alterations were well accepted to arise after KRAS, the explicit timing of their emergence was presented by contradictory results. While CDKN2A and TP53 were reported to be frequently altered in PanINs by Murphy S.J *et al.* (Murphy et al., 2013), a recent study in precancerous pancreatic lesions presented the data of whole-exome sequencing showing that CDKN2A mutations were relatively frequent in high-grade PanINs but absent in low-grade PanINs, besides, TP53 alterations were seen rarely in PanINs but in tumors and predominantly in invasive PDAC (Hosoda et al., 2017). An

updating knowledge in the genetic prospective of pancreatic precursor lesions will give insights into a better understanding of early carcinogenesis and facilitate the clinical approaches for early detection of PDAC as well as the therapeutic interventions.

### 1.2.2 Acinar-to-ductal metaplasia (ADM) and atypical flat lesions (AFLs) in PDAC

Acinar-to-ductal metaplasia (ADM) is defined as the process that acinar cells undergo trans-differentiation to a progenitor-like cell type that expresses ductal marker. ADM mediation has been ascribed to multiple factors, including KRAS hyperactivation and metabolic stress, as well as increased inflammatory signalling (Liou et al., 2016; Logsdon & Ji, 2009).

The presence of ADM was implicated *in vivo* firstly in transgenic mice model with overexpression of transforming growth factor-alpha (TGF-  $\alpha$ ) (Sandgren, Luetkeke, Palmiter, Brinster, & Lee, 1990) but was also demonstrated *in vitro* upon the presence of oncogenic KRAS, growth factor, stress, inflammatory cytokines and so forth (Liou et al., 2015; Pinho et al., 2011; Shi et al., 2013). ADM process exists commonly in pancreatitis, or other injuries that happened to both mouse and human tissues (Houbracken et al., 2011), and is putatively believed to facilitate pancreas regeneration and repopulation. The transition process is reversible until cells acquire oncogenic Kras mutation (Kong et al., 2018) or persistent aberrant of growth factor signalling, which results in irreversible ADM cells and progressing to further precancerous lesions, PanIN 1A or 1B (early dysplastic), or PanIN2 lesions (increasing levels of dysplasia). However, oncogenic Kras alone is not sufficient enough to push tumorigenesis beyond the initiation level. Secondary events, including inflammation (Guerra et al., 2011), acquisition of additional gene mutations, and activation of wild-type KRAS alleles through EGFR signalling (Ji et al., 2009; Navas et al., 2012), are required for driving precursor lesions to carcinoma *in situ* (PanIN 3, high-grade dysplasia) and eventually PDAC.(Storz, 2017)

Although ADM has been well accepted as an initiating event for the development of pancreatic cancer in mice, the evidence for the similar process of ADM in human PDAC remains insufficient. Few studies indicated that the malignance of PDAC might arise from ADM lesions in patients with a strong family history of PDAC (Aichler et al., 2012).

An additional promising alternative PDAC precursor, arising from ADM areas has been recently defined as atypical flat lesions (AFLs). AFLs have been identified in  $Ptf1a-Cre^{ex1/+}; LSL-Kras^{G12D/+}$  mouse model and in human patients with familial pancreatic cancer. AFLs display tubular structures lined by cuboidal cells with cytological atypia. More remarkably, AFLs are surrounded by a loose but highly cellular stroma consisting of whorls of spindle cells (Aichler et al., 2012). Their emergence from the ADM area suggests that the origin of AFLs derives from adult pancreatic acinar cells. It was also demonstrated that the expression of oncogenic  $Kras^{G12D}$  alone is sufficient to induce AFLs in the adult pancreas (von Figura et al., 2017). Of note, AFLs, compared to other lesions, present an increased proliferation rate and more nuclear expression of p53, which could imply that the cell cycle in AFLs begins to dysregulate. It was also proposed that AFLs could be precancerous lesions which bypass the stage of PanIN and developed in PDAC directly.

### 1.3 ALDH and PDAC

ALDH expression was reported to label pancreatic cancer cells that have stem cell traits and mesenchymal features. ALDH-positive pancreatic cancer cells, with enhanced clonogenic growth and migratory properties, indicate their crucial role in the development and metastatic capacity of PDAC. The ALDH level in pancreatic adenocarcinoma was demonstrated to correlate with worse survival in patients that received surgical resection for early-stage cancer (Rasheed et al., 2010). Those researchers also revealed that ALDH+ cells were detected more

in metastases than in the primary tumour, which is in line with the other finding showing ALDH+ cells were significantly tumorigenic both *in vitro* and *in vivo*.

Although the origin of metastasis of pancreatic cancer is still under debate, circulating tumour cells (CTCs), which was well accepted in many other cancers and was also defined in pancreatic cancer (Poruk et al., 2016; Tjensvoll, Nordgard, & Smaaland, 2014), are regarded as a possible source. A study described that CTCs in pancreatic cancer based on *LSL-Kras<sup>G12D/+</sup>;Trp53<sup>flox/flox</sup>* or *Trp53<sup>flox/+</sup>;Pdx1-Cre* mouse model was enriched with markers in ALDH1 subfamilies (especially *Aldh1a1* and *Aldh1a2*), with single-cell RNA sequencing technique (Ting et al., 2014) supporting a possible influence of high ALDH1 levels for metastasis formation.

#### 1.4 ALDH1A3 and PDAC

Rovira et al. reported that in adult mouse pancreas, in centroacinar and terminal ductal epithelial cells, which were of high aldefluor activity, *Aldha1a1* and *Aldh1a7* were enriched while *Aldh1a2*, *Aldh1a3*, and *Aldh8a1* only present low-level expression (Rovira et al., 2010).

However, transcriptome and epigenome data described that ALDH1A3 was abundantly expressed in human pancreatic cancer cell lines and human tumor tissues compared to normal derived tissue (1,630 fold and 78.5 fold on mRNA level, respectively), indicating that ALDH1A3 could prospectively mark pancreatic stem cancer cells (Jia et al., 2013).

In addition, reports from several groups presented that ALDH-positive, CD44+/CD24+, and CD133-positive pancreatic cancer cell harboured highly tumorigenic capabilities, and ALDH-positive cells take on a more-invasive feature (Hermann et al., 2007; Li et al., 2007; Rasheed et al., 2010).

A previous study of our group on PDAC revealed an aggressive subtype of PDAC labelled by

ALDH1A3, as ALDH1A3 was shown to be significantly upregulated on mRNA level in bulk PDAC tissue, and furthermore, patients with positive ALDH1A3 expressions had a significantly shorter survival after surgery compared to those with negative ALDH1A3 expressions (14.0 vs 22.8 months, respectively) (Kong et al., 2016).

### 1.5 Cancer-associated fibroblasts (CAFs) and PDAC

The aggressive feature, late diagnosis, and resistance to chemotherapy join together to contribute to PDAC lethality. Despite the complicated genetic mutation and epigenetic factors behind cancer formation and progression, tumor microenvironment also plays an important role. Among the components of tumor microenvironment, the stroma constitutes almost 90% of the tumor entity (Moir, Mann, & White, 2015). The stroma, characterized with poorly vascularization, denseness, and extensiveness, acts as a physical barrier to drug delivery (Diop-Frimpong, Chauhan, Krane, Boucher, & Jain, 2011; Provenzano et al., 2012), and cytokines and growth factors secreted by non-neoplastic stromal cells have been shown to contribute to pancreatic cancer initiation and progression (Fukuda et al., 2011; Hwang et al., 2008). Cancer-associated fibroblasts (CAFs) have been well accepted as the prominent components of the complex tumor microenvironment of PDAC. CAFs are involved in various fields of tumorigenesis, including desmoplasia, immunosuppression, and secretion of cytokines and factors that modulate the ability of proliferation and apoptosis (Feig et al., 2013; Provenzano et al., 2012; Sherman et al., 2014).

Pancreatic stellate cells (PSCs) have been well accepted as the major source of CAFs (Bachem et al., 2005; Erkan et al., 2012), acting as important mediators of the desmoplastic response. While desmoplasia acts as a barrier to drugs *per se*, PSCs also produce extracellular matrix, which could further provide nutrients to starved cancer cells (Kamphorst et al., 2015). The abundance of PSCs, therefore, suggests that they may be involved in the

metabolism of cancer cells as well. Studies have revealed a cooperative metabolism between cancer cells and PSCs, PSC-derived alanine acted as an alternative carbon source in this novel metabolic interaction (Sousa et al., 2016). Autophagy was unravelled in this interaction. Thus, inhibition of autophagy and other lysosomal degradation pathways may have a great therapeutic utility in PDAC. Additionally, human PSCs were found to produce factors, e.g. cytokines, chemokines and growth factors, to enhance myeloid-derived suppressor cell (MDSC) differentiation and its function to further promote an immunosuppressive microenvironment (Mace et al., 2013).

Recent studies have identified two characteristic subtypes of CAFs derived from PSCs, myofibroblastic CAFs and inflammatory CAFs (Ohlund et al., 2017). Myofibroblastic CAFs locate adjacent to neoplastic cells and are characterized with elevated expression of alpha-smooth muscle actin ( $\alpha$ -SMA), while inflammatory CAFs stay distant from neoplastic cells and are featured with elevated Interleukin 6 (IL6) and contrarily low expression of  $\alpha$ -SMA. The researcher further demonstrated the mechanism underlying the diverse differentiations (Biffi et al., 2019), where Interleukin 1 (IL1) induced LIF/JAK/STAT activation to facilitate differentiation from PSCs to inflammatory CAFs and transforming growth factor-beta (TGF- $\beta$ ) downregulates Interleukin 1 Receptor Type 1 (ILR1) and promotes the generation of myofibroblasts. The coexistence of these two subgroups constitutes the heterogeneity of CAFs and provides implications for the development of therapeutic approaches.

## 2. AIMS OF THIS STUDY

Pancreatic ductal adenocarcinoma is underlined with robust expression of mammalian target of rapamycin (mTOR) (Cancer Genome Atlas Research Network. Electronic address & Cancer Genome Atlas Research, 2017). Kras/Mek/Erk-mediated mTOR signalling was reported to rely on Aldh1a3 in murine PDAC model, and a subgroup of human PDAC with ALDH1A3 expression was found to have aggressive malignancy (Kong et al., 2016). However, it remains unclear what is the role of ALDH1A3 in the development of PDAC. Moreover, although the ALDHs family contribute highly to cell stemness, the distinct contribution of ALDH1A3 to cancer cell stemness in pancreatic cancer has not been unravelled yet.

Our previous data *in vitro* has illustrated the positive effect of Aldh1a3 in the growth of mouse pancreatic cancer cell lines, regardless of oncogenic Kras mutation. Besides, a dynamic pattern for early pancreatic carcinogenesis driven by oncogenic Kras<sup>G12D</sup> under the circumstance of acute pancreatitis was previously demonstrated (Kong et al., 2018). Therefore, we would like to investigate the role of Aldh1a3 in the early pancreatic carcinogenesis by answering the following questions.

Q1: What is the effect of knockout or overexpression of Aldh1a3 in murine pancreas development?

Q2: What is the role of Aldh1a3 in Kras<sup>G12D</sup>-driven pancreatic carcinogenesis?

Q3: what is the molecular mechanism responsible for potential function of Aldh1a3 in early pancreatic carcinogenesis?



### 3. MATERIALS AND METHODS

#### 3.1 Materials

##### 3.1.1 Mouse lines

###### *Ptf1a<sup>Cre/+</sup>; LSL-Kras<sup>G12D/+</sup>; Aldh1a3<sup>flox/flox</sup> mouse line*

Mice containing two floxed alleles of Aldh1a3 were obtained from IGBMC, France, the exon 8-9 of Aldh1a3 allele on chromosome 7 in mice are flanked by two loxP sites, as previously described (Dupe et al., 2003; Matt et al., 2005). The Loxp-STOP-Loxp-Kras<sup>G12D/+</sup> (LSL-Kras<sup>G12D/+</sup>; 008179) mutated mouse line, originally obtained from Jackson Laboratory (Bar Harbor, USA), and the pancreas-specific Cre recombinase line Ptf1a<sup>Cre/+</sup> (known as p48<sup>Cre/+</sup> as well) (Burlison, Long, Fujitani, Wright, & Magnuson, 2008; Magnuson & Osipovich, 2013) were passaged in our previous researches (Department of Surgery, Technical University of Munich). The wild type (hereafter WT or C57BL/6J) were obtained from Charles River Laboratory (Calco, Italy).

###### *Ptf1a<sup>Cre/+</sup>; LSL-Kras<sup>G12D/+</sup>; Rosa<sup>R26-CAG-Aldh1a3</sup> mouse line*

Rosa26 Conditional Knockin line was generated by Cyagen Biosciences (Suzhou, China) Inc. Mouse genomic fragments containing homology arms (HAs) were amplified from bacterial artificial chromosome (BAC) clone by using high fidelity Taq, and sequentially assembled into a targeting vector together with inward-facing loxP recombination sites and selection markers. This targeting vector was inserted between exon 1 and exon 2 of wild type Rosa26 allele to generate Rosa<sup>R26-LSL-Aldh1a3</sup>, led by a CAG promoter (*Figure 1A*). The vector was further linearized with NotI (*Figure 1B*) and subsequently delivered to embryonic stem (ES) cells (C57BL/6) via electroporation, followed by drug selection, PCR screening, and Southern Blot confirmation. The confirmed correctly targeted ES clones were selected for blastocyst microinjection, followed by chimaera production. Founders were confirmed as germline-transmitted via crossbreeding with wild type.

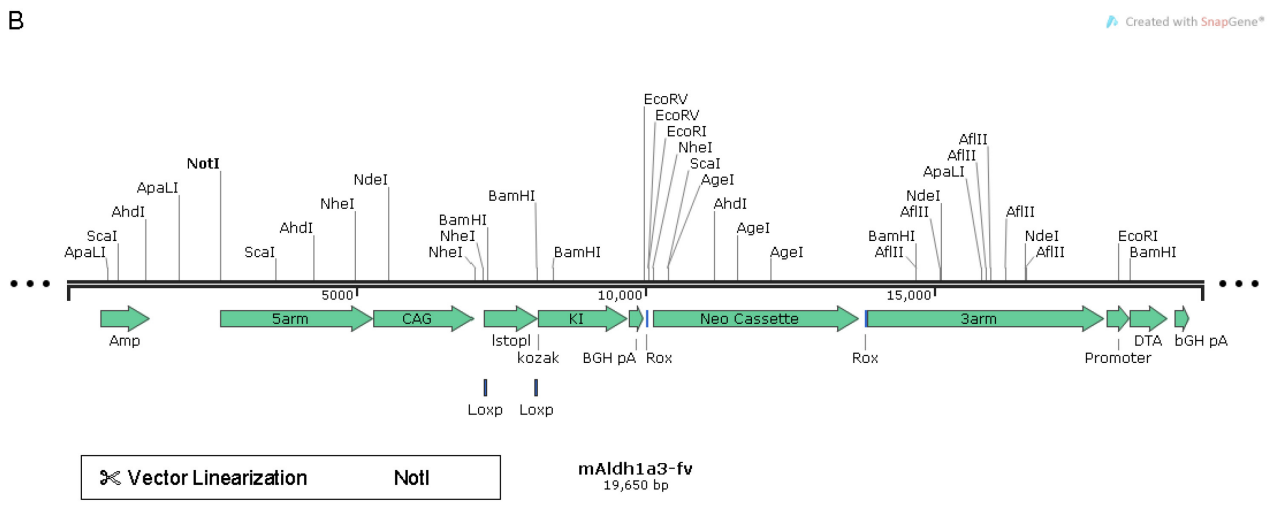
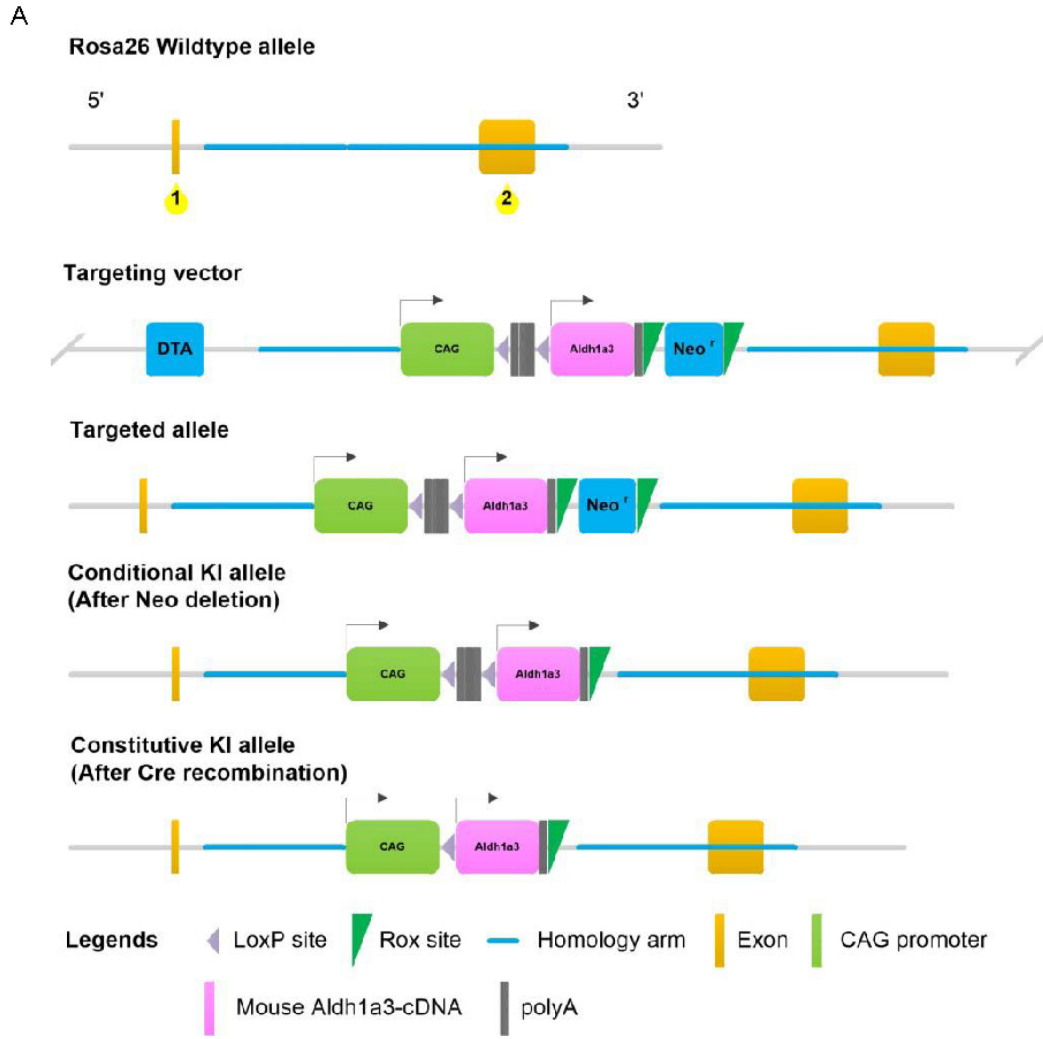


**Figure 1.** (A) Schematic diagrams of the targeting strategy for conditional knockin line to overexpress Aldh1a3. (B) Vector linearization with NotI for *Rosa<sup>R26-CAG-Aldh1a3</sup>* mouse line.

*Aldh1a3<sup>CreERT2</sup>; Rosa<sup>R26-CAG-tdTomato</sup>*

*Aldh1a3<sup>CreERT2</sup>* mouse line was generated by Cyagen Biosciences (Suzhou, China) Inc. In brief, amplified mouse genomic fragments containing HAs were sequentially assembled into a targeting vector together with loxP recombination sites and selection markers (*Figure 2A*). This targeting vector was inserted upstream of exon 13 of wild type *Aldh1a3* allele and further linearized with NotI (*Figure 2B*). The linearized vector was subsequently electroporated into ES cells (C57BL/6). Drug selection, PCR screening, and Southern Blot confirmation were carried out to confirm targeted clones, which were later proceeded for blastocyst microinjection and chimaera production.

After crossbreeding with wild type C57BL/6 mice, this line was further crossed with *Rosa26/tdTomato* line as a reporter gene. With this strategy, we were able to trace the cells labelled with *Aldh1a3* after Cre recombinase-induction by Tamoxifen. Mouse breeding was set up and husbandry was maintained at the specific pathogen free (SPF) and specific and opportunistic pathogen free (SOPF) mouse facility at Technische Universität München (Munich, Germany) and Charle River Laboratories Italia (Calco, Italy).

For all the experiments in this study, mice were housed under specific pathogen free (SPF) or specific and opportunistic pathogen free (SOPF) conditions. All animal procedures were approved by the Zentrum für Präklinische Forschung of the Technische Universität München, which follows the federal German guidelines for ethical animal treatment (Regierung von Oberbayern) with the proposal (Tierversuchsantrags TVA -83-2017).

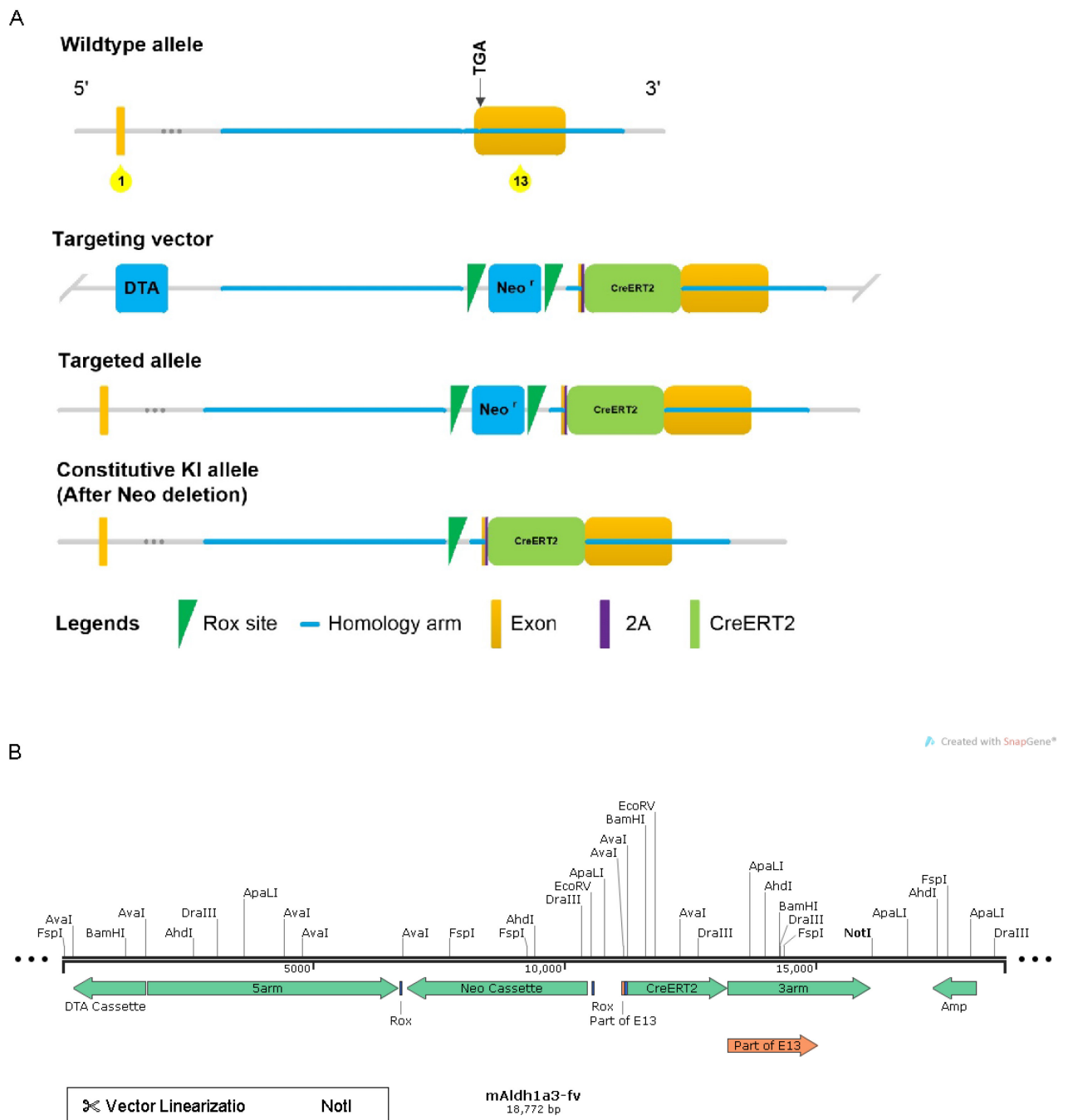


**Figure 2.** (A) Schematic diagrams of the targeting strategy for  $Aldh1a3^{CreERT2}$  mouse generation. (B) Vector linearization with NotI for  $Aldh1a3^{CreERT2}$  mouse line.

### 3.1.2 List of the antibodies

#### Primary antibodies

Antibody	Catalogue number	Application (Reactivity)	Source
a-Amylase	3796	IHC(H, M)	Cell signalling Technology (Europe B.V. Frankfurt am Main, Germany)
ALDH1A1	HPA002123	WB,IHC(H)	Sigma-Aldrich Chemie GmbH (Munich, Germany)
Aldh1a1	Ab52492	WB,IHC(M)	Abcam (Cambridge, UK)
ALDH1A3	HPA046271	WB(H,M) IHC(H,M)	Sigma-Aldrich Chemie GmbH
p-Ampk alpha	2535	WB(M)	Cell signalling Technology
Ampk alpha	2603	WB(M)	Cell signalling Technology
Beta-Actin	Sc-69879	WB(H, M)	Santa Cruz Biotechnology (Heidelberg, Germany)
B220/CD45R	MAB1217	IHC(M)	R&D system (Minneapolis, US)
BrdU	5292	IHC(M)	Cell signalling Technology
Claudin 18	700178	IHC(M)	Invitrogen (California, US)
C-MYC	5605	WB(M)	Cell signalling Technology
GAPDH	Sc-32233	WB(H, M)	Santa Cruz
Krt19	TROMA-III	IHC(M)	DHSB (Iowa, US)
Lc3b	3868	WB(M)	Cell signaling Technology
Met	3127	IHC(M)	Cell signalling Technology

p-Met	3129	IHC(M)	Cell signalling Technology
Muc5ac	MA5-12178	IHC(M)	Invitrogen
P21	556430	WB(M)	BD Bioscience (New Jersey, US)
P21	Ab188224	IHC(M)	Abcam
p53	2524	WB(M)	Cell signalling Technology
p53	NCL-p53-CM5p	IHC(M)	Leica (Wetzlar, Germany)
tdTomato	TA180009	IF	Origene (Rockville, US)
p-Akt(S473)	4060	WB(M)	Cell signaling Technology
p-p44/42 Mapk(T202/Y204)	9101	WB(M)	Cell signaling Technology
p-Stat 3(Try705)	9131	WB(M)	Cell signaling Technology

### Secondary antibodies

Antibody	Catalogue number	Application	Source
Alexa Fluor 488 Goat-anti-Rabbit	A11034	IF	Invitrogen
Alexa Fluor 488 Goat-anti-Mouse	A1101	IF	Invitrogen
Alexa Fluor 488 Goat-anti-Rat	A1106	IF	Invitrogen
Alexa Fluor 594 Goat-anti-Rabbit	A11012	IF	Invitrogen
Alexa Fluor 594 Goat-anti-Mouse	A11005	IF	Invitrogen
Anti-Rabbit IgG HRP Conjugate	W401B	WB	Promega (Wisconsin, US)

Anti-Mouse IgG HRP Conjugate	W402B	WB	Promega
EnVision+System-HRP Labelled Polymer Anti-Rabbit	K4003	IHC	Dako (Santa Clara, US)
EnVision+System-HRP Labelled Polymer Anti-Mouse	K4001	IHC	Dako
Simple Stain Rat MAX PO Universal immuno-peroxidase polymer	H1608	IHC	N-Histofine (Tokyo, Japan)

### 3.1.3 Chemicals and Reagents

Chemical/Reagent	Product number	Source
Albumin Fraction V (BSA)	T844.3	Carl Roth GmbH
Ammonium persulfate (APS)	215589	Sigma-Aldrich Chemie GmbH
Agarose Tablets	BIO-41027	BIOLINE
BCA protein assay	23225	Thermo Fisher Scientific
Albumin Fraction V	T844.3	Carl Roth GmbH
Cell lysis buffer(10x)	9803	Cell Signaling Technology
Citric acid (Monohydrate)	C1909	Sigma-Aldrich Chemie GmbH
Collagenase P	11249002001	Clostridium histolyticum (Roche)
Dulbecco's Phosphate Buffered Saline	D8537	Sigma-Aldrich Chemie GmbH
Dulbecco's Modified Eagle's Medium (DMEM)	D5796	Sigma-Aldrich Chemie GmbH
Advanced DMEM/F12	12634-010	Gibco
Advanced Fetal Bovine Serum	FBS-11A	CAPRICORN
Dimethylsulfoxid (DMSO)	A994.1	Carl Roth GmbH

ECL Plus Western Blotting Detection Reagents	32132	Amersham
Ethanol 70%	7078027	Fischar
Ethanol 96%	7138032	Fischar
Ethanol absolute	7127114	Fischar
Ethanol absolute	64-17-5	Merck KGaA
Fetal Bovine Serum	F7524	Sigma-Aldrich Chemie GmbH
Formaldehyde	4979.1	Carl Roth GmbH
Glycin	3908.3	Carl Roth GmbH
Haemalum (Mayer's) solution for microscopy	EM1.09249	VWr
Hank's BSS	H15-010	PAA
HCl(Hydrochloric acid) 37%	4625.1	Carl Roth GmbH
HEPES solution	H0887	Sigma-Aldrich Chemie GmbH
Hydrogen peroxide 30 %	9681.1	Carl Roth GmbH
Isoflurane CP	1214	CP-Pharma
KAPA SYBR FAST qPCR Master Mix(2x) for LightCycler 480	KM4107	KAPABIOSYSTEMS
L-Glutamine solution	G7513	Sigma-Aldrich Chemie GmbH
Methanol	4627.5	Carl Roth GmbH
Milk powder	T145.3	Carl Roth GmbH
Minimum Essential medium Eagle (MEM) media	M2279	Sigma-Aldrich Chemie GmbH
Natriumchlorid (NaCl)	3957.2	Carl Roth GmbH
Normal goat serum	50062Z	Life Technologies
NuPAGE LDS Sample Buffer (4x)	NP0007	Invitrogen
NuPAGE Sample reducing	NP0009	Invitrogen



Agent (10x)		
Oil Red O	O0625	Sigma-Aldrich Chemie GmbH
PBS Dulbecco	L182-50	Biochrom GmbH
Penicillin-Streptomycin	P0781	Sigma-Aldrich Chemie GmbH
phosphatase inhibitor	4906837001	Sigma-Aldrich Chemie GmbH
protease inhibitor	4693159001	Sigma-Aldrich Chemie GmbH
Red blood cell lysis buffer	R7757	Sigma-Aldrich Chemie GmbH
RIPA buffer(10x)	9806	Cell Signaling Technology
Roticlear	A538.1	Carl Roth GmbH
Rotiphorese Gel 30	3029.1	Carl Roth GmbH
SDS, ultra-pure	2326.2	Carl Roth GmbH
TEMED	2367.3	Carl Roth GmbH
Transfer Membrane 0.2 um	ISEQ00010	Merck Millipore
Tris base	T1503	Sigma-Aldrich Chemie GmbH
Tris-HCl	T3253	Sigma-Aldrich Chemie GmbH
Triton X 100	3051.2	Carl Roth GmbH
Tween 20	9127.2	Carl Roth GmbH
Trypsin-EDTA solution	T3924	Sigma-Aldrich Chemie GmbH

### 3.1.4 Buffers and Solutions

#### Immunohistochemistry & Immunofluorescence

##### 10x Tris Buffered Saline (TBS)

Tris base	24.2 g
-----------	--------

NaCl	85 g
Distilled Water	800 mL
Adjust pH to 7.4 with	5 M HCl
Constant volume with distilled water to	1000 mL

#### 10x Phosphate-buffered saline (PBS)

PBS	9.55 g
Tween 20	1 mL
Constant volume with distilled water to	1000 mL

#### 20x Citrate buffer

Citric acid (Monohydrate)	21 g
Distilled Water	300 mL
Adjust pH to 7.4 with	5 M NaOH
Constant volume with distilled water to	500 mL

#### Washing Buffer (1x TBST)

10x TBS	100 mL
Tween 20	1 mL
Constant volume with distilled water to	1000 mL

#### Washing Buffer (1x PBST)

10x PBS	100 mL
Tween 20	1 mL
Constant volume with distilled water to	1000 mL

### Western Blotting

## SDS PAGE

### Lower separating gel

percentage	10%	12.5%
H <sub>2</sub> O	4.1 ml	3.2 ml
Acrylamide 30%	3.3 ml	4.2 ml
Tris-HCl 1.5M pH8.8	2.6 ml	2.6 ml
SDS 10%	100 µl	100 µl
APS 10%	50 µl	50 µl
Temed	15 µl	15 µl
Total volume	10 ml	10 ml

### Upper stacking gel

H <sub>2</sub> O	3 ml
Acrylamide 30%	750 µl
Tris-HCl 0.5M pH6.8	1.3 ml
SDS 10%	50 µl
APS 10%	25 µl
Temed	10 µl
Total volume	5 ml

### 10% APS

APS	10 g
Constant volume with distilled water to	100 mL

### Electrophoresis buffer (10x)

Tris base	30.3 g
Glycin	144 g

SDS	10g
Constant volume with distilled water to	1000 mL

#### Running buffer

Electrophoresis buffer(10x)	100 mL
10% SDS	10 mL
Constant volume with distilled water to	1000 mL

#### Blotting buffer

Electrophoresis buffer(10x)	100 mL
Methanol	200 mL
Constant volume with distilled water to	1000 mL

#### Washing Buffer (1x TBST)

10x TBS	100 mL
Tween 20	1 mL
Constant volume with distilled water to	1000 mL

#### Blocking Buffer (1x TBST)

Skimmed milk powder or BSA	5 g
Washing buffer	100 mL

### 3.1.5 Kits

RNeasy Plus Mini Kit	QIAGEN
NucleoSpin RNA kit	MACHEREY-NAGEL
RevertAid H Minus First Strand cDNA Synthesis Kit	Thermo-scientific

### 3.1.6 Laboratory consumables

24/6-well plates	FALCON, Corning
96/48/24/6-well plates	Greiner Bio-one
6/10cm dishes	FALCON, Corning
Cell Strainer	FALCON, Corning
CellTrics 30µm	SYSMEX
Cover slips	MENZEL-GLÄSER
96-well PCR microplate, Lightcycler-type	STAR LAB
Syringe	Injekt, B/Braun

### 3.1.7 Laboratory equipment

Balance/Scale	SCAL TEC SBC 52
Biometra Tone	Analytik Jena
Centrifuge 5415R	Eppendorf
Freezer -20°C	LIEBHERR
Freezer -80°C	Heraeus, Thermo Fisher Scientific
Glass coverslips	Plano
GloMAX-Multi Detection System	Promega
HERAsafe hood	Thermo Fisher Scientific
HERAcell 150	Thermo Fisher Scientific
Imaging software	Olympus analysis software and Zeiss AxioVision
Magnetic mixer	IKA-COMBIMAG RET
Microscopes	Axiovert 40CFL Zeiss, Axiosko 40 Zeiss
Microtome	Leica JUNG RM2055

Multifuge 3SR PLUS	Heraeus, Thermo Fisher Scientific
PH-meter	BECKMAN (Washington, DC, USA)
Photometer	Thermo-Labsystem Opsys MR
Pipettes	Eppendorf
Power supple	Bio-RAD MODEL 200/2.0
Refrigerator 4°C	LIEBHERR
Shaker	IKA-Shaker MTS 4
Thermomixer	Eppendorf
Tissue embedding machine	Leica
Tissue processor	Leica
TissueLyser LT Adapter	Qiagen
Ultrasound processor	Hielscher
Vortex Mixer 7-2020	neoLab
Water bath	Lauda ecoline RE 104, MEDAX
X-ray films	Hyperfilm, Amersham Bioscience

## 3.2 Methods

### 3.2.1 Caerulein treatment

Mild acute pancreatitis model was applied on WT (C57BL/6J), KC (Ptf1 $\alpha$ <sup>Cre/+</sup>; LSL-Kras<sup>G12D/+</sup>) and KCAlhd1a3<sup>KO</sup> (Ptf1 $\alpha$ <sup>cre/+</sup>; LSL-Kras<sup>G12D/+</sup>; Aldh1a3<sup>fl/fl</sup>) animals. The mice were induced at the age of 8–9 weeks by administering caerulein through intraperitoneal (i.p.) injections (0.1 mg/kg body weight, in 100  $\mu$ l 0.9% NaCl), eight hourly on two consecutive days. Analgesia was carried out by applying Temgesic (0.1 mg/kg body weight) subcutaneously 30 min before and after the first injection every day and every 12 hours continuously afterwards until 72 hours after the last injection.

The first day of the first injection was considered as day 0, and the time point of the last injection was considered hour 0. Finally, experimental mice were injected with 2.5 mg BrdU (5-Bromo-2'-deoxyuridine) 2 hours before being sacrificed.

### 3.2.2 Tamoxifen treatment

Tamoxifen was dissolved in colza oil containing 10% absolute Ethanol. The experimental mice were induced at the age of 5-6 weeks by administering Tamoxifen (40 mg/ml, 100  $\mu$ l per injection) through oral gavage. The administration was conducted every other day, and three applications in total fulfil the procedure.

### 3.2.3 mouse primary pancreatic cell isolation and flow cytometry

Fresh mouse pancreas was minced in dissociation medium, containing 0.05% (weight/volume) Collagenase P), optional 0.125% (wt/vol) dispase in DMEM (4500 mg/L glucose) containing 1% FBS, and digested at 37°C for 30 minutes in a thermomixer or with pipetting cell pellets in 15ml falcon every 5 min. The sample was next trypsinized for 5min with 1x Trypsin and then quenched in 10% FBS/DMEM. Afterwards, the sample pellets were strained with 0.40  $\mu$ M strainer. Cells were collected by centrifuging the filtered suspension at 1200 rpm for 4 min.

Red blood cell lysis buffer (Sigma) was applied to eliminate the red blood cell and prepare sample ready for flow cytometry. FACS buffer, containing 3% FCS and 1 mM EDTA in 1xPBS (without Ca<sup>2+</sup> and Mg<sup>2+</sup>), was used to resuspend the cells before flow cytometry. Flow cytometry was performed using BD FACSAria™ Fusion.

### 3.2.4 Immunohistochemistry (IHC) analysis and quantification

Fresh tissue was fixed with 4% formaldehyde, further embedded in paraffin and finally was cut into 2-2.5 um sections before use. Deparaffination and rehydration of the tissue section were performed according to routine methods and followed by antigen retrieval with heat-induced epitope retrieval method. Briefly, sections were emerged in preheated (at sub-boiling temperature) citrate acid buffer (10mM citrate acid, pH=6.0) and were kept at sub-boiling or boiling temperature in a microwave oven for 10 minutes. Endogenous peroxidase was blocked by incubation in methanol containing 3% hydrogen peroxide at room temperature for 10 minutes. Blocking of nonspecific reactivity was performed with 10% goat serum in TBS (pH 7.4; 0.1M Tris Base, 1.4M NaCl). Afterwards, tissue sections were incubated with primary antibodies overnight at 4°C. Following that, second antibodies conjugated by horseradish peroxidase were applied onto sections, and Diaminobenzidine (Liquid DAB+ Substrate Chromogen System, Dako) was adapted for colour-detection and Mayer's hematoxylin for counterstaining, subsequently. Dehydration and mounting with Permount (Vector Laboratories) were finally performed to complete the procedure.

Permeabilization, if necessary, was applied by emerging sections in 0.1% TBS-Triton x100 buffer for 10 min. TBST buffer (0.1% Tween 20 was added into TBS above buffer) or TBSA buffer (0.1% BSA was added into TBS buffer) were used as washing buffer throughout the whole procedure.

For quantification, five pictures of random fields of view were taken for every slide with a Carl



Zeiss microscope under 20x or 40x objective lens. Cells were counted by two independent researchers with the ImageJ (1.51f).

### 3.2.5 Immunofluorescence (IF) analysis and quantification

We performed immunofluorescence also with paraffin-embedded tissue sections. Tissue sections were prepared according to the IHC protocol. Deparaffination, rehydration as well as antigen retrieval were performed in the same way as in IHC analysis. Sections were permeabilized with 0.1% PBS-Triton x100 buffer for 10 min. Blocking of nonspecific reactivity was performed with 10% goat serum in PBS (pH 7.4; 0.1M Tris Base, 1.4M NaCl). After incubation with primary antibodies overnight at 4°C, secondary fluorochrome-conjugated antibodies were applied. DAPI and mounting were completed together with Immunoselect Antifading Mounting Medium DAPI (Dianova, Germany). Sections with completed IF staining were kept at 4°C. PBST buffer (0.1% Tween 20 was added into PBS above buffer) was used as washing buffer throughout the whole procedure. Quantification of IF staining was performed similarly as described for quantifying IHC pictures.

### 3.2.6 Oil Red O staining

Preparing the Oil Red O staining working solution by dissolving 0.35 g Oil Red O in 100 ml isopropanol, which was then diluted in distilled water at a 3:2 ratio and filtered.

Cells in culture were fixed with 10% formalin for 10 min at room temperature, followed by 5 minutes incubation in 60% isopropanol. After drying, the cells were incubated with the working solution for 10 min. Afterwards, the cells were washed with water four times before images were taken.

### 3.2.7 mRNA isolation

The mRNA extraction from cells or fresh tissue was performed with the help of NucleoSpin RNA kit according to the manufacturer's instruction from MACHERY-NAGEL, respectively. cDNA reverse-transcription was performed with RevertAid H Minus First Strand cDNA Synthesis Kit from ThermoScientific.

### 3.2.8 Quantitative Real-time Polymerase Chain Reaction (qRT-PCR, qPCR)

Quantitative real-time PCR was performed using the LightCycler480 system with the SYBR Green 1 Master kit (Roche Diagnostics). Expression of the target gene was normalized to human housekeeping genes HPRT1 (Hypoxanthine phosphoribosyltransferase 1) or the mouse housekeeping gene RPS29 [Ribosomal Protein S29].

LightCycler480 software version 1.5.0.0801 (Roche Diagnostics) was used to analyze the data.

#### *List of primers used for qPCR*

Mouse Gene	Forward sense (5' ->3')	Reverse sense (5' -> 3')
Aldh1	CTGTGAAGGCTGCAAGACAGG	GTCAGCCAGCTTGTTTCAGCAG
Aldh1a1	GATGCCGACTTGGACATTGC	CACACTCCAGTTTGGCTCCT
Aldh1a3	CAGCAATTTCTCCCATCCG	CCTCCTAGCTCCAGTGTGAC
Epcam	TTAATGCCTAGCCGTGCTGAG	TCTGCAGTCCGAGCTCTTCTG
Nanog	TCTTCCTGGTCCCCACAGTTT	GCAAGAATAGTTCTCGGGATGAA
Cd24	TGACCGATAAGGCCATAGTGC	CGCCTGGTAGTTCCTTCCAAC
Cd44	CGGAATCTGCAGAGTGTGGAC	CAGGAATGACGTCTCCAATCG
Cd133	AATTCGCTCAGCAGCAGTGAC	TGCTTAGGCTTGGTCTGATGC
Cxcr4	GAAGTGGGGTCTGGAGACTAT	TTGCCGACTATGCCAGTCAAG
Gapdh	TGCACCACCAACTGCTTAG	GGATGCAGGGATGATGTTT
Oct4	GAGGAGTCCCAGGACATGAA	AGATGGTGGTCTGGCTGAAC
P21	TGAGGAGGAGCATGAATGGAG	CATCACCAGGATTGGACATGG
P27	GCCTGACTCGTCAGACAATCC	CTTCTGCAGCAGGTGCTTC

Sox2	GCGGAGTGGAACCTTTGTCC	GGGAAGCGTGACTTATCCTTCT
Sqstm1	GCTGCCCTATACCCACATCT	CGCCTTCATCCGAGAAAC
Trp53	GACCATCCTGGCTGTAGGTAGC	CAGTCTTCGGAGAAGCGTGAC

### 3.2.9 Immunoblot analysis

#### *Protein extraction from cells*

Cells were washed twice with ice-cold PBS (pH 7.4; 0.01M PBS). Cell lysis buffer (containing 20 mM Tris-HCl (pH 7.5), 150 mM NaCl, 1 mM Na<sub>2</sub>EDTA, 1 mM EGTA, 1% Triton, 2.5 mM sodium pyrophosphate, 1 mM β-glycerolphosphate, 1mM Na<sub>3</sub>VO<sub>4</sub>, 1 μg/ml leupeptin, Proteinase inhibitor added) was added onto cells, followed by sonication with Ultrasound Processor for 10-15 seconds for each sample. The cell homogenate was centrifuged at 16,100 g/13,200rpm in a pre-cooled centrifuge for 15 minutes. The supernatant was immediately transferred to fresh tubes and was aliquoted.

#### *Protein extraction from tissues*

RIPA buffer (20 mM Tris-HCl (pH 7.5), 150 mM NaCl, 1 mM Na<sub>2</sub>EDTA, 1 mM EGTA, 1% NP-40, 1% sodium deoxycholate, 2.5 mM sodium pyrophosphate, 1 mM β-glycerolphosphate, 1mM Na<sub>3</sub>VO<sub>4</sub>, 1 μg/ml leupeptin, Proteinase inhibitor added) was used to isolate protein from tissues. Sonication with UP100H ultrasound processor from Hielscher was regularly performed, followed by centrifugation with 16,100g/13,200rpm in a pre-cooled centrifuge for 15 minutes.

The concentration of the protein was determined using the BCA Protein Assay kit (Pierce, Thermo Scientific, USA) and analyzed by GloMAX-Multi-Detection system. Further, NuPAGE LDS Sample Buffer and Sample Reducing Agent were adapted to denature and reduce the protein disulfide bonds.

### *Western blotting*

20 µg of protein was loaded into 7.5-12.5% polyacrylamide gels and transferred to nitrocellulose membranes. Membranes were blocked in TBS-A (5% BSA) or TBS-T (3% or 5% skimmed milk powder) for 1 hour, followed by incubation with the primary antibody at 4°C overnight. A secondary horseradish peroxidase (HRP)-conjugated antibody was applied for 1h at room temperature. Signals were detected using the enhanced chemiluminescence system (ECL, Amersham Life Science Ltd., Bucks, UK). Films were scanned with a CanoScan 9900F scanner (Canon, Tokyo, Japan) and signals/bands were quantified with the help of software ImageJ (1.51f). TBS-T (0.1% Tween 20) buffer was used for washing membranes through the whole procedure.

### 3.3 Statistical analysis

Statistical analysis was performed with GraphPad Prism 7.0 (GraphPad, San Diego, California, USA). An unpaired Student's t-test was used for comparison between groups. P value <0.05 was set as the threshold of the significance level.

## 4. RESULTS

4.1 The presence of ALDH1A3-positive cells in tumors rendered PDAC patients with a worse prognosis.

As demonstrated previously (Kong et al., 2016), ALDH1A3 mRNA levels are significantly higher in human bulk PDAC compared to normal pancreas. In line, IHC staining demonstrated a subgroup of PDAC patients showing positive ALDH1A3 expression in cancer cells, while the ALDH1A3 staining was not detectable in pancreatic epithelial cells either in normal pancreas or in chronic pancreatitis tissues (*Figure 3A*). Consistently, survival analysis revealed that patients with high ALDH1A3 expression in cancer cells had significantly shorter survival than those with low ALDH1A3 expression (*Figure 3B*). Moreover, human PDAC cell lines presented elevated expression of ALDH1A3 (*Figure 3C*). To note, human pancreatic ductal epithelial cells (HPDE) showed a high level of ALDH1A3, indicating the expression of ALDH1A3 is acquired in the process as pancreas undergoes ductal metaplasia.

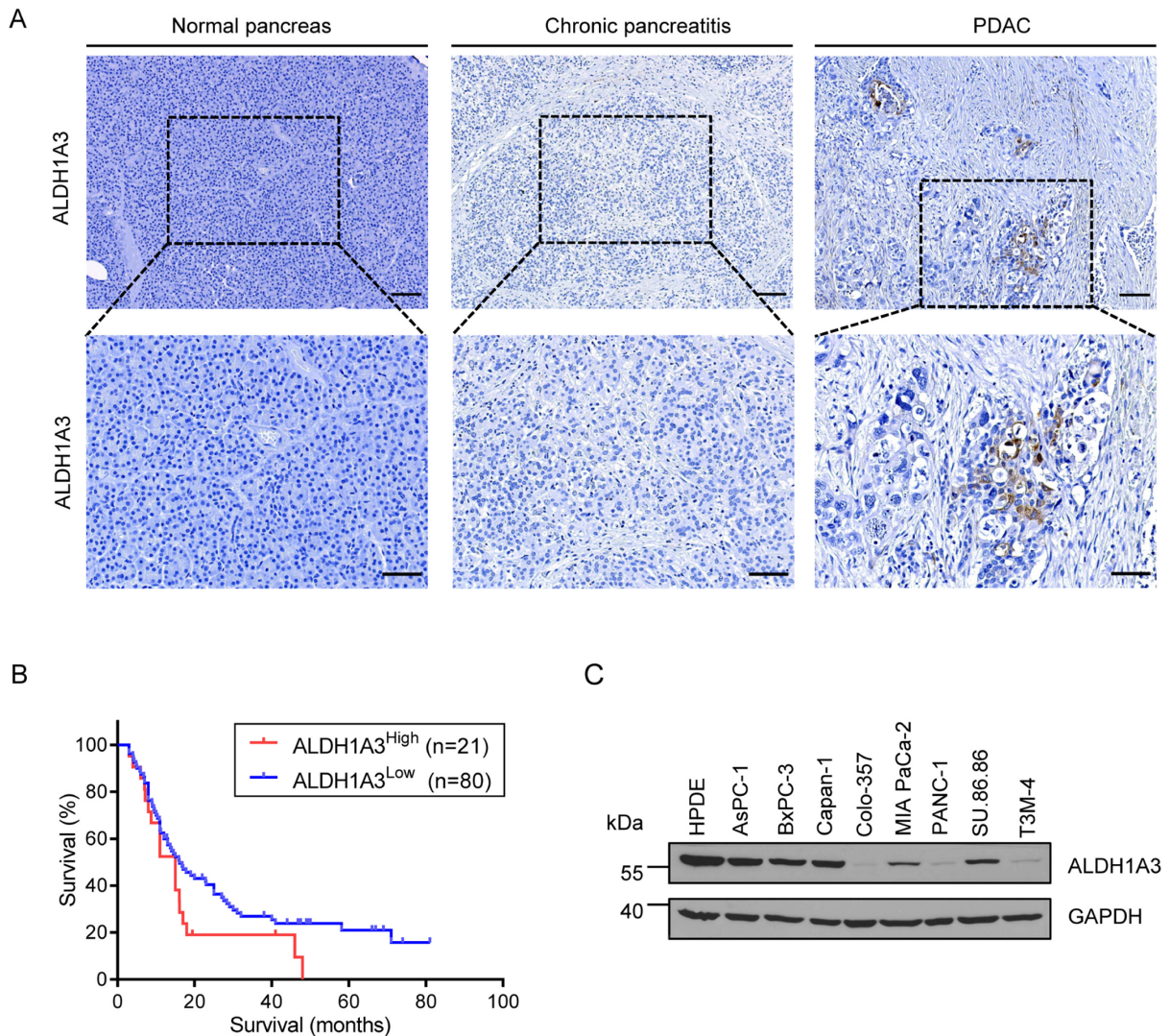
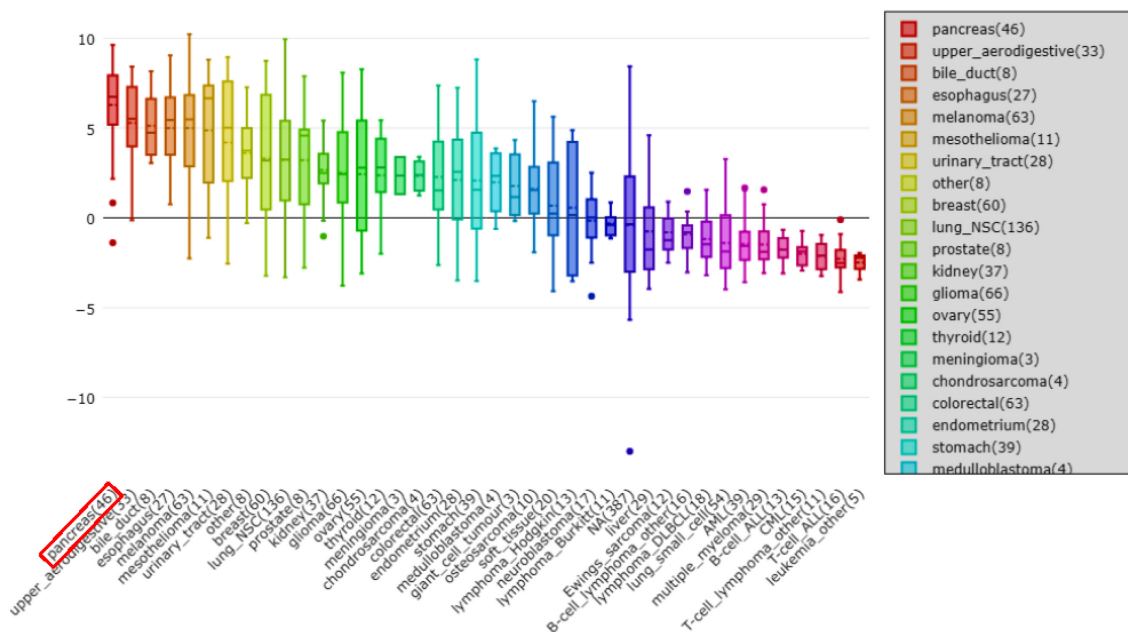


**Figure 3.** (A) Positive ALDH1A3 expression was detected in cancer cells in a subgroup of PDAC samples but not in normal pancreas or chronic pancreatitis tissues. Scale bar: upper 100 $\mu$ m, lower 50 $\mu$ m. (B) Patients with high ALDH1A3 expression in PDAC cells had shorter survival than those with low ALDH1A3 expression. (C) ALDH1A3 expression in HPDE and other 8 human PDAC cell lines.

Also, based on the database from Cancer Cell Line Encyclopedia (CCLE), authorized to Barretina J *et al.* (Barretina *et al.*, 2012), <https://portals.broadinstitute.org/ccle>, PDAC cell lines exhibit the highest ALDH1A3 mRNA expression and the lowest DNA methylation of ALDH1A3 among all accessible human malignancy cell lines (Figure 4A, B).

A

Copy Number: ALDH1A3



B

DNA methylation (RRBS): ALDH1A3

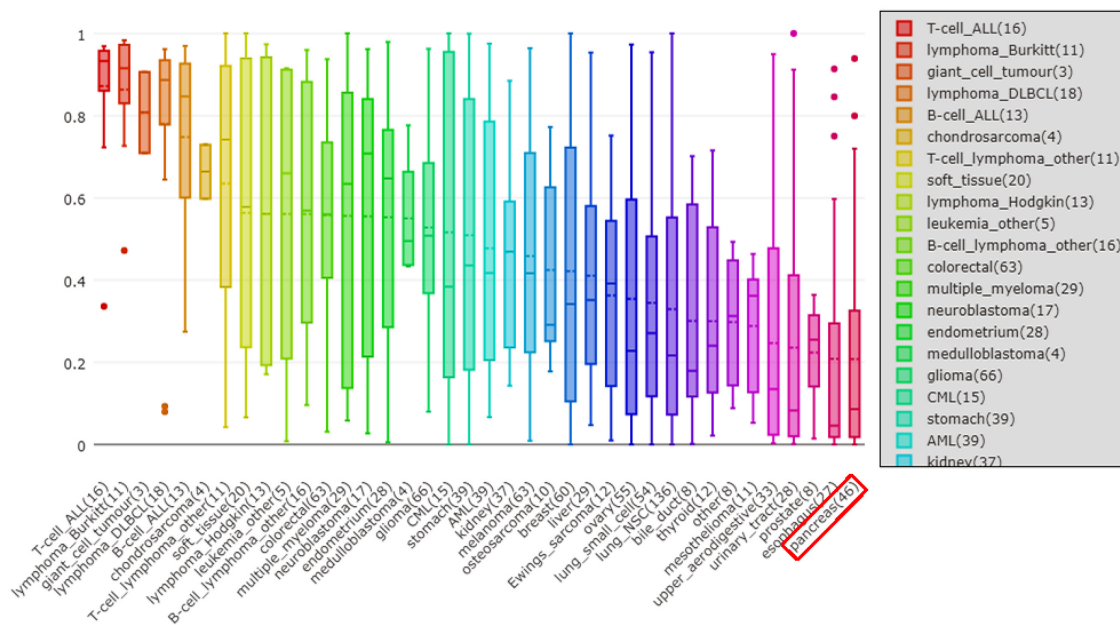


**Figure 4.** Pancreatic cancer cell lines exhibit the highest ALDH1A3 mRNA expression (A) and the lowest DNA methylation (B) of ALDH1A3 among all accessible human malignancy cell lines.

## 4.2 Aldh1a3 is also expressed in primary and metastatic murine PDAC

In consistence with the feature that ALDH1A3 underlines a subtype of aggressiveness, our data showed that Aldh1a3 was found to be expressed in metastatic PDAC derived from LSL-Kras<sup>G12D/+</sup>; Trp53<sup>flox/+</sup>; Ptf1a<sup>Cre/+</sup> (KPC) mouse model. The primary tumours of KPC mice had elevated Aldh1a3 expression. Notably, PDAC cells of metastases were found to often contain Aldh1a3 positive tumour cells, especially along the border line between metastatic tumours and normal tissues (*Figure 5*), indicating the active capability of proliferation and invasion of those cells.

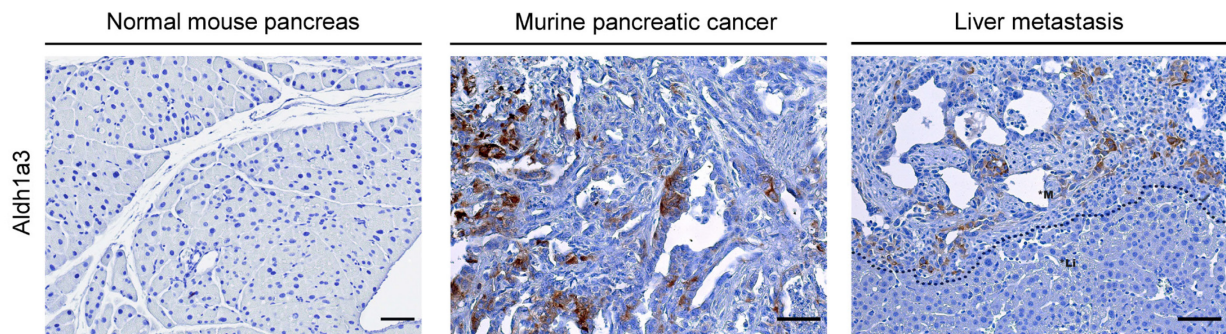


**Figure 5.** Aldh1a3 in epithelial cells were positively detected in pancreatic cancer (middle) and liver metastasis (right) in the KPC mouse model. Aldh1a3 accumulated notably more near the border line between metastatic and normal tissue. Scale bar: 50 $\mu$ m.



### 4.3 Aldh1a3 was expressed in pre-neoplastic lesions driven by oncogenic Kras<sup>G12D</sup>

In caerulein-induced acute pancreatitis, three characteristic phases appear in sequential order, termed inflammation, regeneration, and refinement. While in mice carrying Kras<sup>G12D</sup> mutation, an extended inflammatory phase takes place instead, along with a proliferation of mesenchymal, progenitor-like cells (Kong et al., 2018).

Firstly, we investigated the expression of Aldh1a3 using IHC analysis in different phases of acute pancreatitis. A set of wild-type mice or p48<sup>Cre</sup>; Kras<sup>G12D</sup> (KC) mice were sacrificed between 3 hours and 14 days after intraperitoneal caerulein injections for 2 days consecutively. The expression of Aldh1a3 in epithelial cells was induced after caerulein injection and gradually increased in KC mice; however, its expression in wild-type mice was barely detectable (*Figure 6A*). Immunoblot analysis helped to confirm this increased Aldh1a3 expression in KC mouse pancreata at different time points after caerulein injection. (*Figure 6B, C*)

Furthermore, we performed immunofluorescence analysis to investigate which cell types acquire Aldh1a3 expression during early carcinogenesis. As acini undergo acinar-ductal metaplasia (ADM) during acute pancreatitis, they lose acinar marker (e.g. alpha-Amylase) character gradually and acquire ductal cell marker (e.g. cytokeratin 19 (Krt19)). Here, we observed that Aldh1a3 expression is not detectable in alpha-amylase-expressing cells, but in ductal cells (Krt-19 positive) (*Figure 6D*). Thus, it implies that Aldh1a3 expression was induced as ductal properties were obtained. The partial overlap of Aldh1a3 and Muc5ac (Mucin 5 subtype A and C, a marker for PanIN lesions) confirmed the accumulation of Aldh1a3 in more advanced precancerous lesions. Nonetheless, proliferating cells, labelled by BrdU, can be observed in both Aldh1a3-positive and negative lesions (*Figure 6D*).

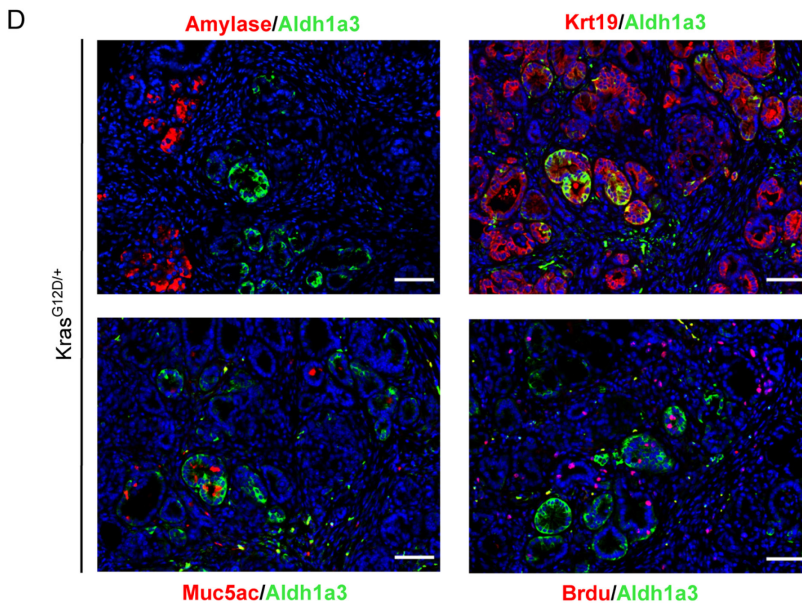
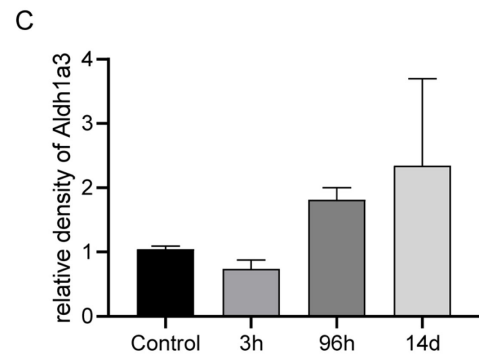
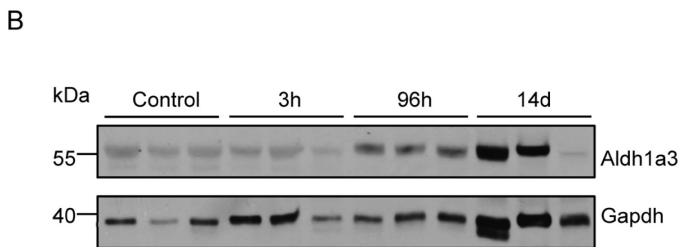
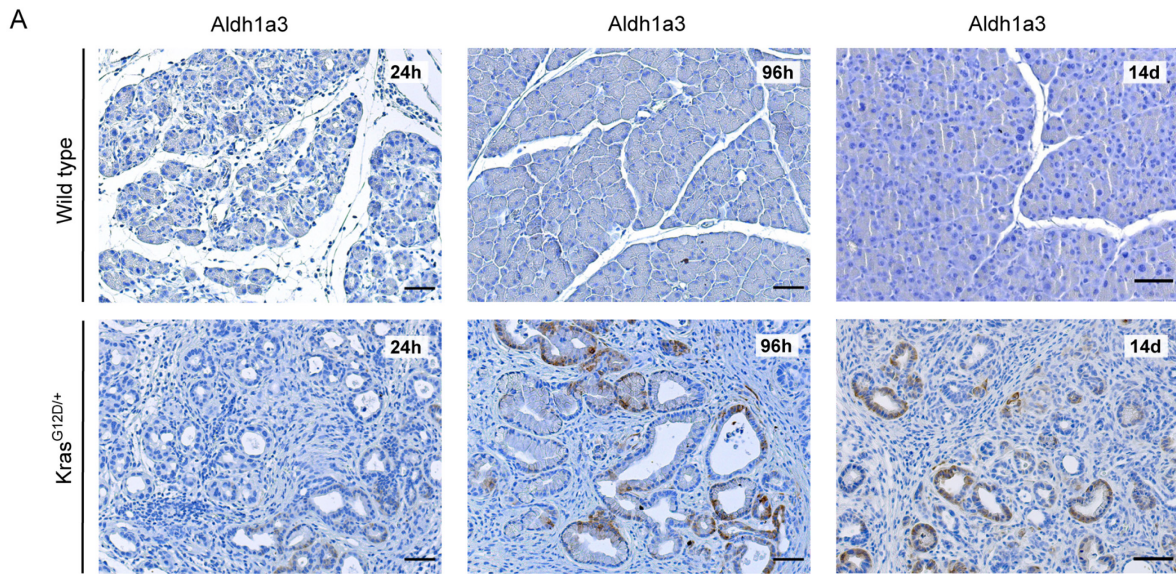


**Figure 6.** (A) Aldh1a3 expression in wild-type (upper panel) and KC mice (lower panel) after caerulein injection. Scale bar: 50 $\mu$ m. (B, C) Immunoblot analysis of Aldh1a3 in KC mouse at different time points after caerulein. (D) Representative IF analysis of KC mouse pancreas at 14d after caerulein injection. Scale bar: 50 $\mu$ m.

#### 4.4 Aldh1a3 ablation does not affect pancreatic physiology

As acute pancreatitis induces a non-resolving process in KC mice and further leads to early carcinogenesis, and Aldh1a3 expression is induced during this process, we continued to explore the role of Aldh1a3 in the development of early carcinogenesis.

Therefore, we generated transgenic Aldh1a3<sup>KO</sup> mice with exon 8-9 of the Aldh1a3 gene flanked by Loxp sites, and afterwards, p48<sup>Cre/+</sup>; Kras<sup>G12D/+</sup>; Aldh1a3<sup>KO</sup> mouse line (hereafter Kras<sup>G12D</sup>Aldh1a3<sup>KO</sup> or KC-Aldh1a3<sup>KO</sup>), in which both two alleles of Aldh1a3 were specifically deleted in pancreas, was generated by crossing the Aldh1a3<sup>KO</sup> line with p48<sup>Cre/+</sup> line and Kras<sup>G12D/+</sup> line (*Figure 7A*).

All transgenic mice with pancreas-specific Aldh1a3 ablation gave birth at the expected rates. Basal levels of Aldh1a3 expression was downregulated in Aldh1a3<sup>KO</sup> mice by qRT-PCR analysis (*Figure 7C*). After following up for one year, mice with pancreas-specific Aldh1a3 deficiency stayed healthy. Histological examination of the pancreas from Aldh1a3<sup>KO</sup> mice did not show any abnormal lesions at a half-year time point (*Figure 7B*). Thus, Aldh1a3 ablation does not affect pancreatic physiology.

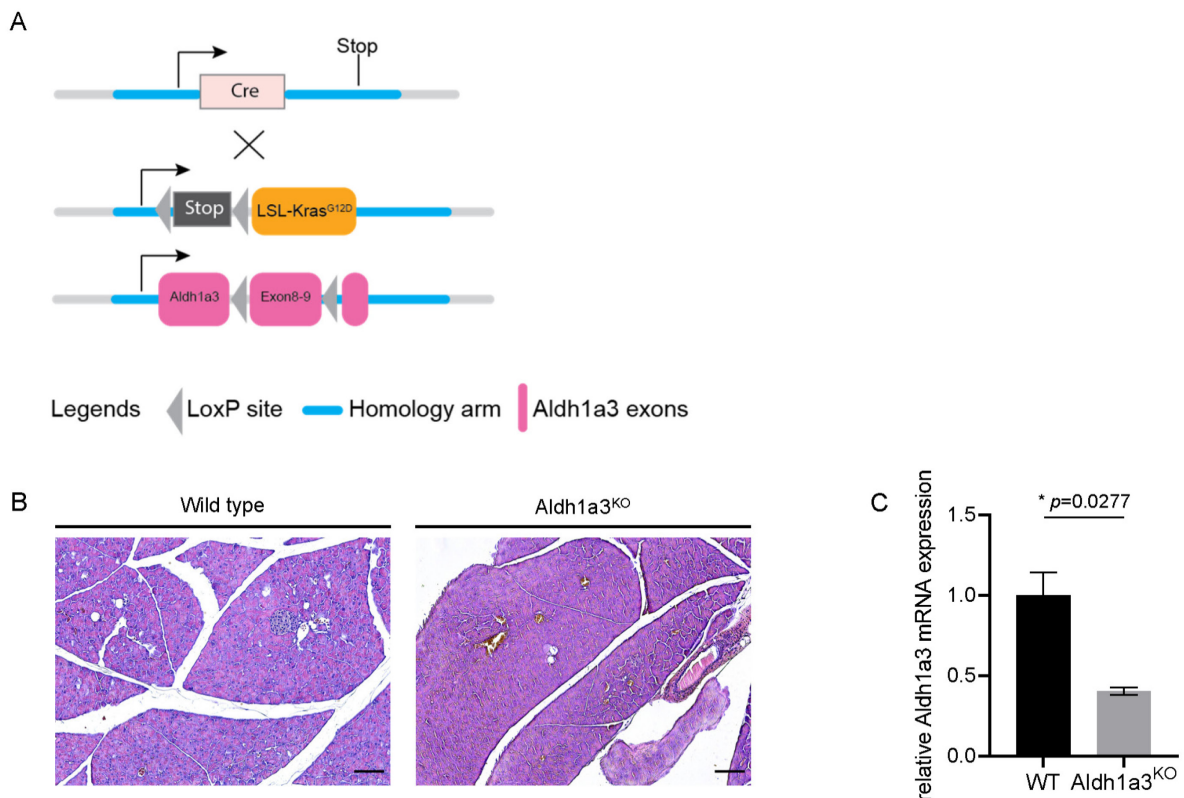


**Figure 7.** (A) Ablation of mouse Aldh1a3 with LoxP system. (B) HE stains analysis showed no visible lesion in Aldh1a3-deficient mouse pancreas as in wild type mouse pancreas at six months. Scale bar: 100  $\mu$ m. (C) Relative mRNA expression of Aldh1a3 in Aldh1a3<sup>KO</sup> in the pancreata of WT and Aldh1a3<sup>KO</sup> mice.

#### 4.5 Aldh1a3 deletion in pancreatic epithelial cells slightly promotes PanIN lesions in KC mice with acute pancreatitis

As Aldh1a3 was detected in pre-neoplastic lesions including ADMs and PanINs, it, therefore, was hypothesized that Aldh1a3 ablation in pancreatic epithelial cells influences ADM and PanIN formation. Thus, we investigated the functional role of Aldh1a3 in early pancreatic carcinogenesis by inducing acute pancreatitis in KC and KC-Aldh1a3<sup>KO</sup> mice.

The IHC analysis revealed that no positive Aldh1a3 staining could be detected in pancreatic acinar cells or ADM lesions in KC Aldh1a3<sup>KO</sup> mice (Figure 8A, B). Western Blot and qPCR analysis confirmed these results on both protein levels and mRNA levels (Figure 8C, D, E).

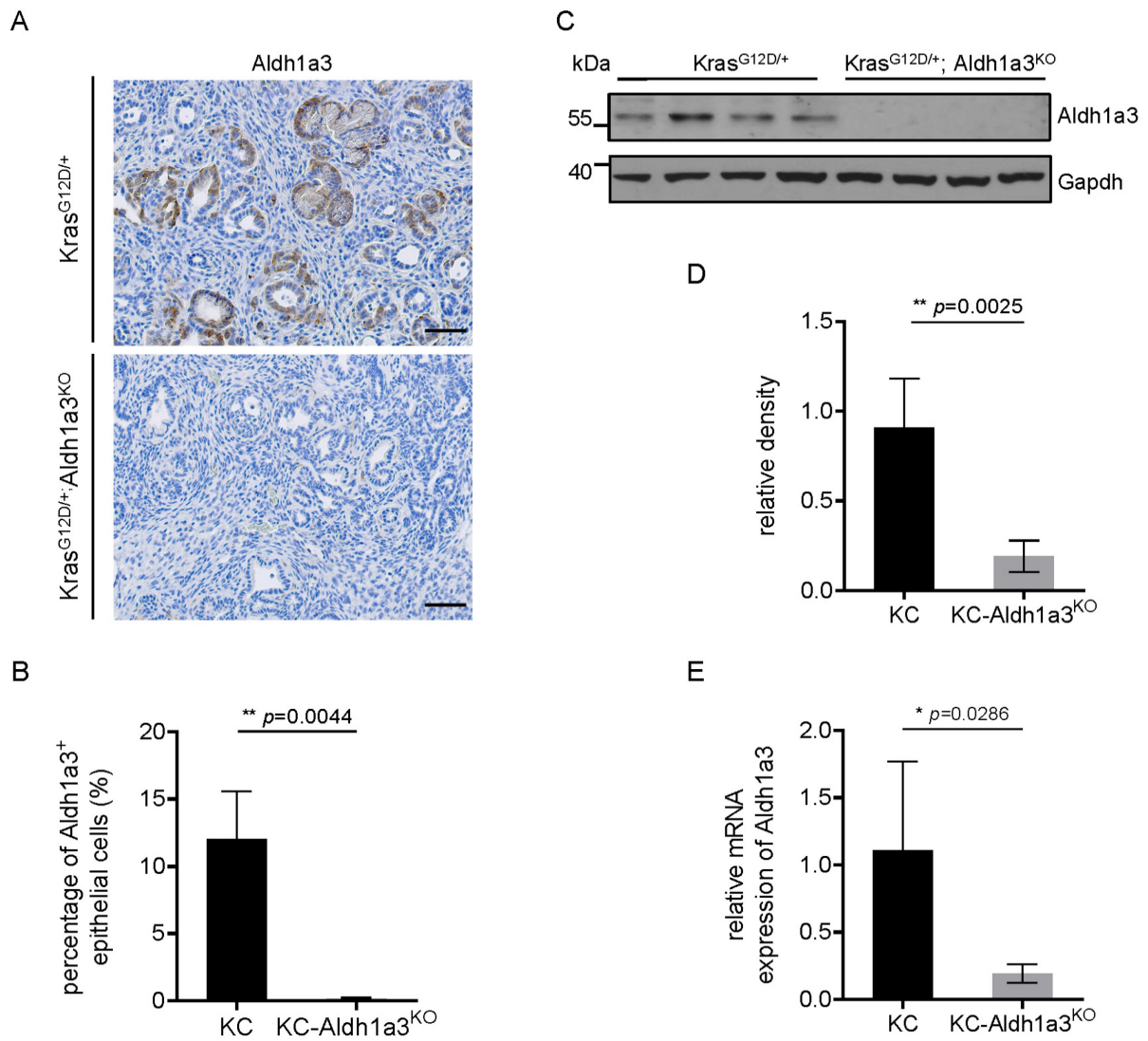


**Figure 8.** (A, B) IHC analysis and quantification of Aldh1a3 in mouse pancreas. Scale bar: 50  $\mu$ m. (C, D) Western Blot and quantification confirmed the deletion of Aldh1a3 expression in Aldh1a3<sup>KO</sup> mice. (E) Relative mRNA expression of Aldh1a3 in mouse pancreas of KC and KC-Aldh1a3<sup>KO</sup> mice.

Acute pancreatitis model was set up in KC and KC-Aldh1a3<sup>KO</sup> mice (Figure 9A). On day 14, after caerulein injection, no overt difference was observed regarding gross pathology or HE staining between two mice strains (Figure 9B, C). Mice from both groups presented histologically atrophic pancreas with ductal-like structure. Moreover, the weight change or pancreas/body weight ratio between the two groups was comparable (Figure 9D, E).

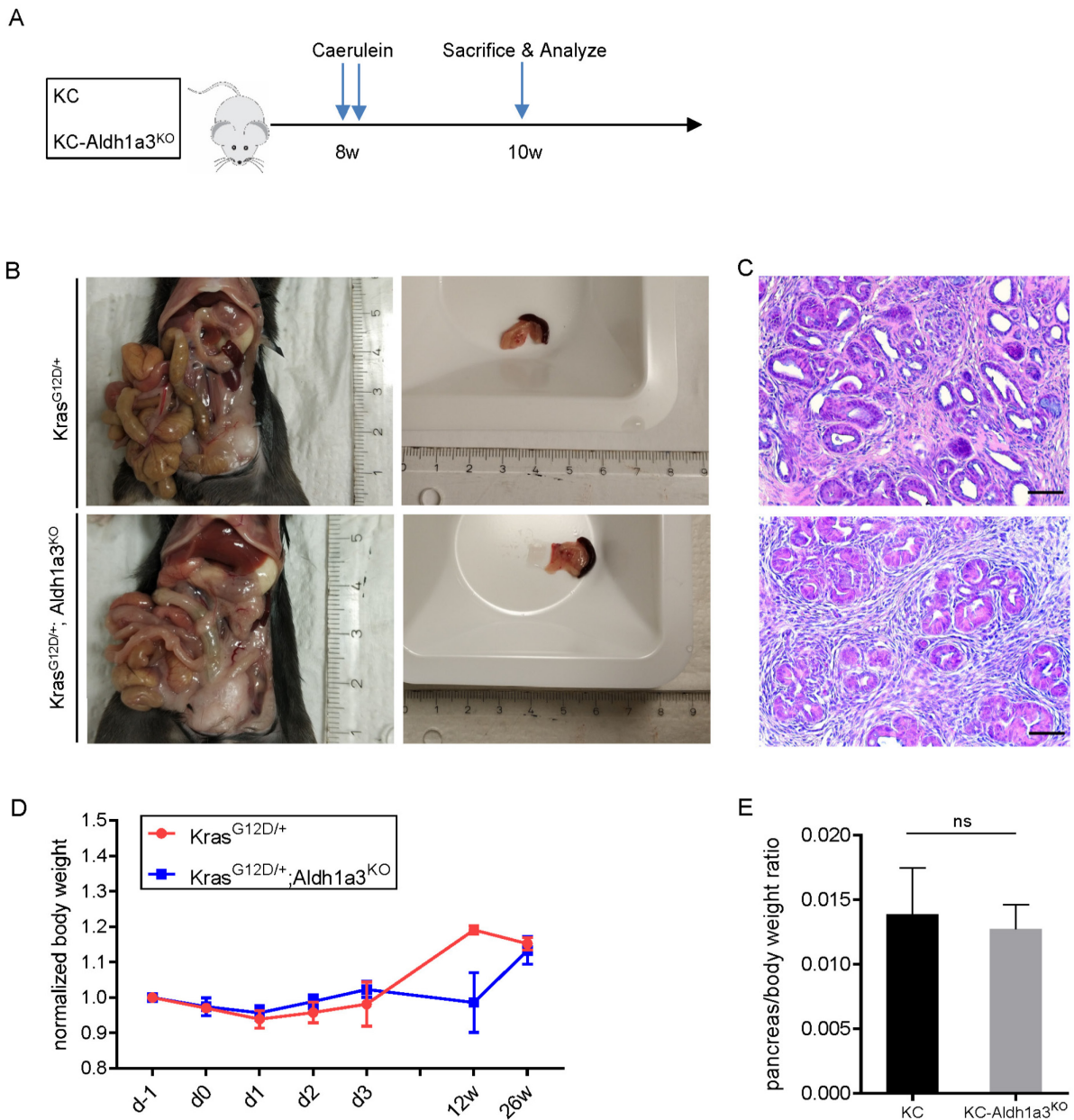


**Figure 9.** (A) Procedure of caerulein treatment and time point of sacrifice in schematic diagrams. (B, C) Both mouse models presented atrophic pancreas with ADM formation at day 14 after caerulein, no distinguishable difference was detected. Scale bar: 100  $\mu$ m. (D, E) Weight changes or pancreas/body weight ratio showed no significant difference between the two strains.

To further explore histological alteration upon the deletion of Aldh1a3 in pancreatic epithelial cells, we performed IHC analysis for several biological markers including alpha-amylase (acinar cells), Krt19 (ductal cells), Claudin 18 and Muc5ac (PanIN markers). Alpha-Amylase and Krt19 stainings did not show any significant difference (*Figure 10 A, B*) between these two strains, indicating the ablation of Aldh1a3 did not affect ADM formation in the context of acute pancreatitis. Interestingly, PanIN lesions (labelled by Claudin 18) were more frequently observed in KC-Aldh1a3<sup>KO</sup> than in KC mice. Notably, a similar trend was observed when another PanIN marker (Muc5ac) was used (*Figure 10 A, B*).

However, although an elevated PanIN formation displayed at day 14 after caerulein treatment, no accelerated tumour formation was observed in long-term (26 weeks) analysis upon Aldh1a3 deletion after acute pancreatitis. KC-Aldh1a3<sup>KO</sup> mice presented similar weight changes as KC mice by the time of 26 weeks, though a slight decline in body weight was noticed by the time of 12 weeks (*Figure 9D*). Comparable PanIN lesions are shown from HE analysis for KC mice with or without knockout of Aldh1a3 in pancreatic epithelial cells by the time of 26 weeks (*Figure 10C*)

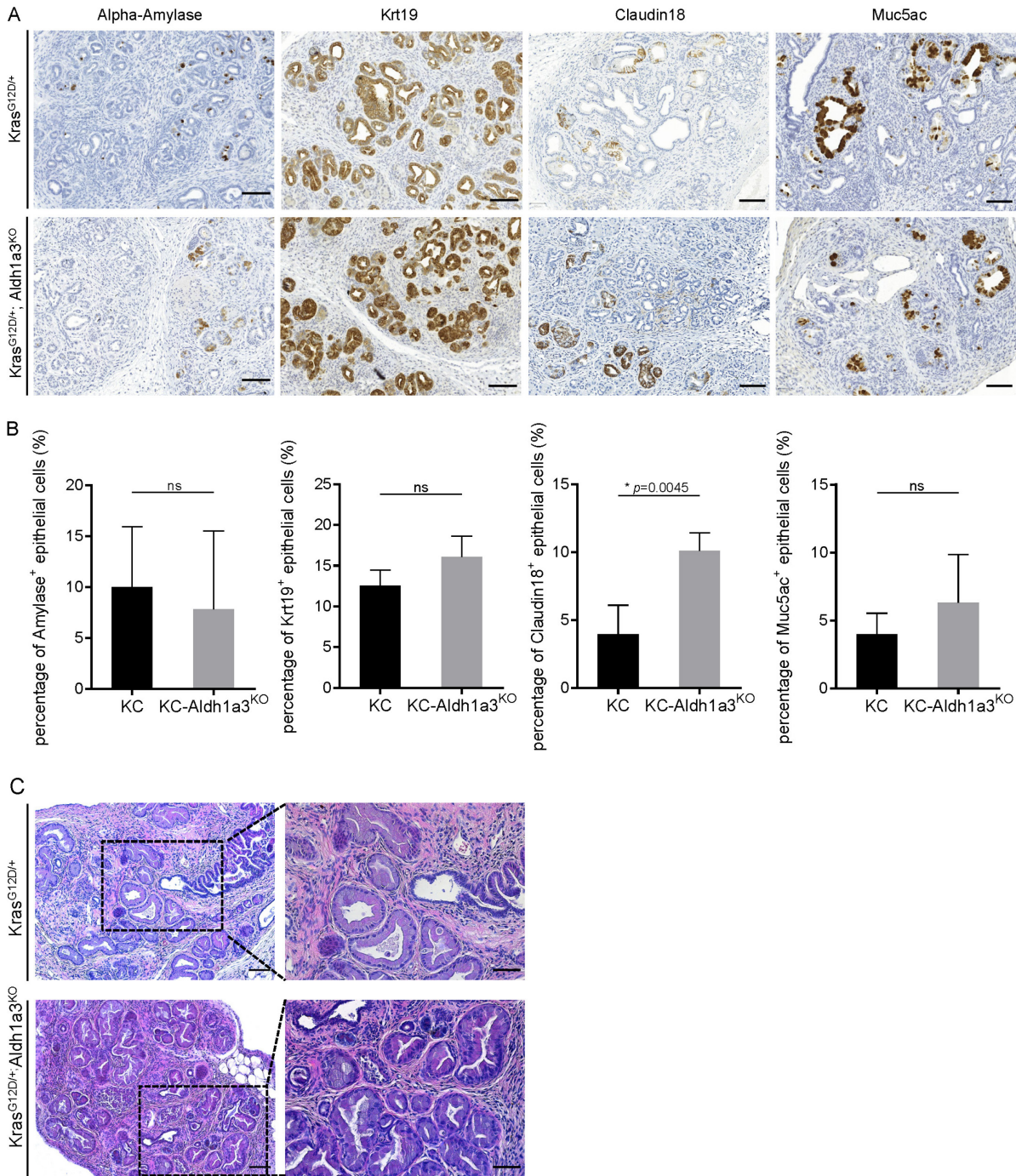


**Figure 10.** (A, B) IHC analysis revealed no difference in alpha-Amylase or Krt19, but more Claudin 18 and Muc5ac upon loss of Aldh1a3 in the pancreatic epithelium. (C) HE staining analysis for KC mice and KC-Aldh1a3<sup>KO</sup> mice by the time 26 weeks after caerulein injection. Scale bar: 100  $\mu$ m (left), 50  $\mu$ m (right).



#### 4.6 Aldh1a3 ablation promotes PanIN formation via suppressing p53 in the context of acute pancreatitis

Though depletion of Aldh1a3 led to an increased PanIN formation on KC mouse model in the context of acute pancreatitis, we observed that pre-neoplastic lesions from KC-Aldh1a3<sup>KO</sup> mice did not harbour more proliferating cells (BrdU-positive cells, *Figure 11A, B*) than those from KC mice. Since p53 is involved in early pancreatic carcinogenesis, we firstly assessed p53 expression using various analysis upon Aldh1a3 deletion. The IHC analysis of p53 exhibited no evident tendency in pancreatic epithelial cells (*Figure 11A, B*). No significant difference was found on mRNA level as well (*Figure 11C*). However, the immunoblotting analysis revealed that p53 was significantly downregulated at the protein level (*Figure 12A, B*). Besides, downstream molecules of the p53 pathway such as p21 and p27 were also investigated. p21 was also decreased at protein level upon Aldh1a3 knockout in immunoblotting and IHC assay (*Figure 11A, B, 12B*).

Moreover, at day 14 after caerulein injection, an elevation in SQSTM1 (p62) on mRNA level was observed in KC-Aldh1a3<sup>KO</sup> group (*Figure 11C*), which implied impaired autophagy resulting from pancreatic-specific Aldh1a3 ablation. This alteration was in line with the increased expression of Light Chain 3b (Lc3b, autophagy marker) in Aldh1a3-deficient murine pancreas (*Figure 12A, B*). These data suggested that the autophagy process might be potentially affected by loss of Aldh1a3.

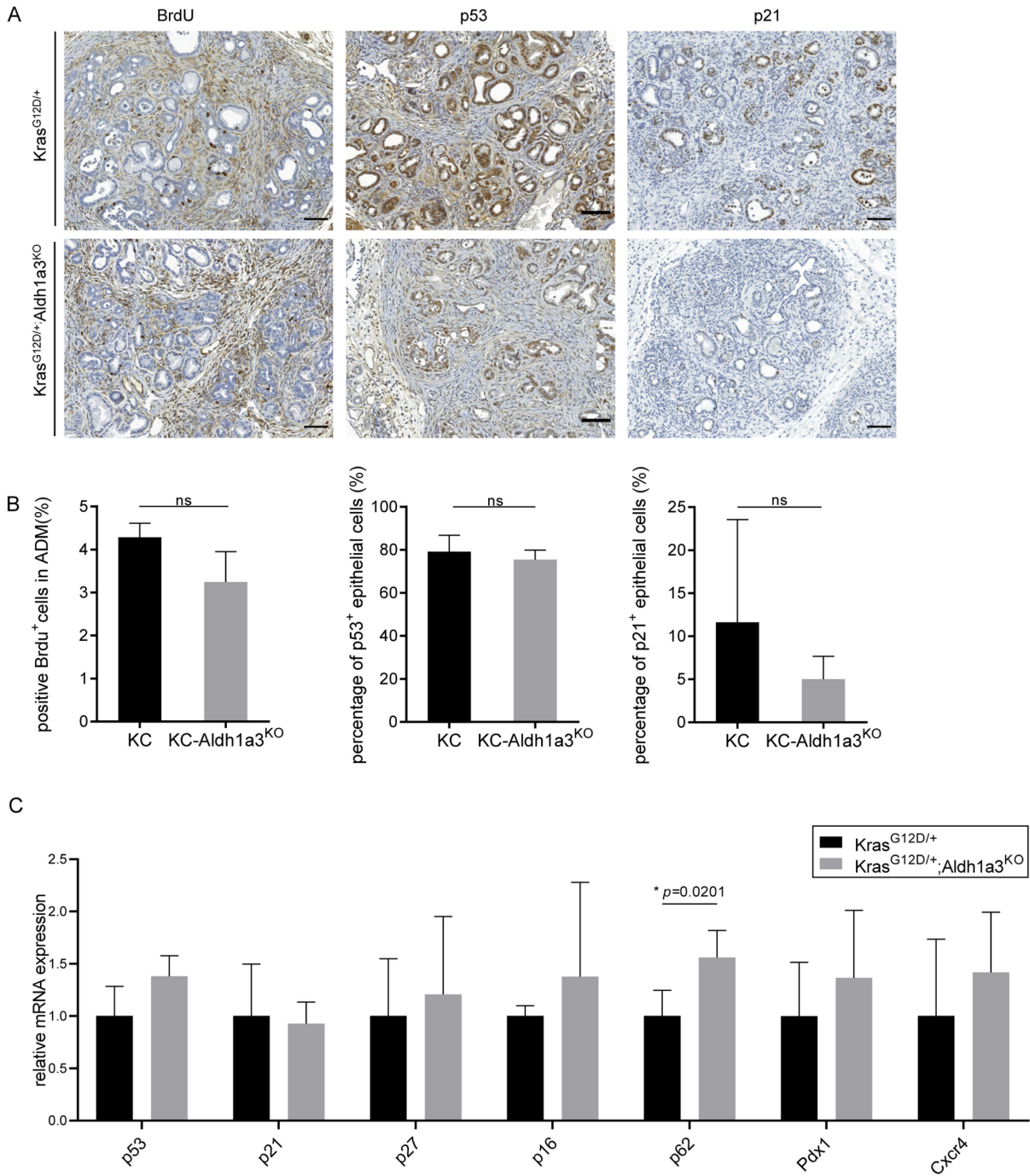


**Figure 11.** (A, B) IHC revealed no significant alteration in the pancreas acinar-derived cells on BrdU, p53 or p21. scale bar: 50  $\mu$ m. (C) qRT-PCR analysis of relative mRNA expression of signals of interest.

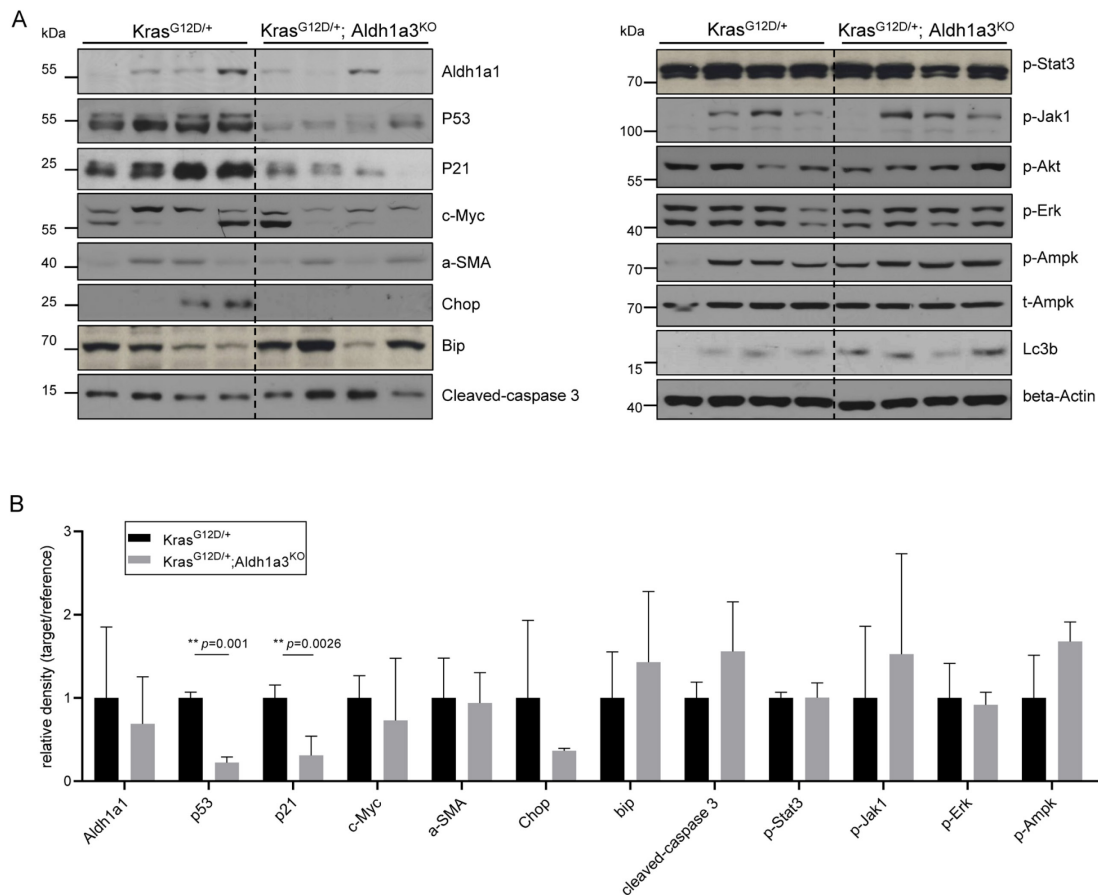


**Figure 12.** (A, B) Immunoblot analysis and quantification by screening signals on protein levels.

Next, we performed immunofluorescence assay to test whether this suppressed p53 function led to increased proliferation potential in pre-neoplastic lesions. Notably, more BrdU/Krt19-positive proliferating cells (proliferative ADM cells), but less p53/Krt19-positive cells were detected in KC-Aldh1a3<sup>KO</sup> compared to KC mice (*Figure 13A, B*). However, the number of BrdU/Claudin18-positive cells was comparable between KC and KC-Aldh1a3<sup>KO</sup> pancreata (*Figure 13B*). These data suggested that, upon Aldh1a3 ablation, the ADM lesions tended to have a higher capability of proliferation due to p53 suppression in the context of acute pancreatitis. This may contribute to accelerated PanIN formation in KC-Aldh1a3<sup>KO</sup> mice.

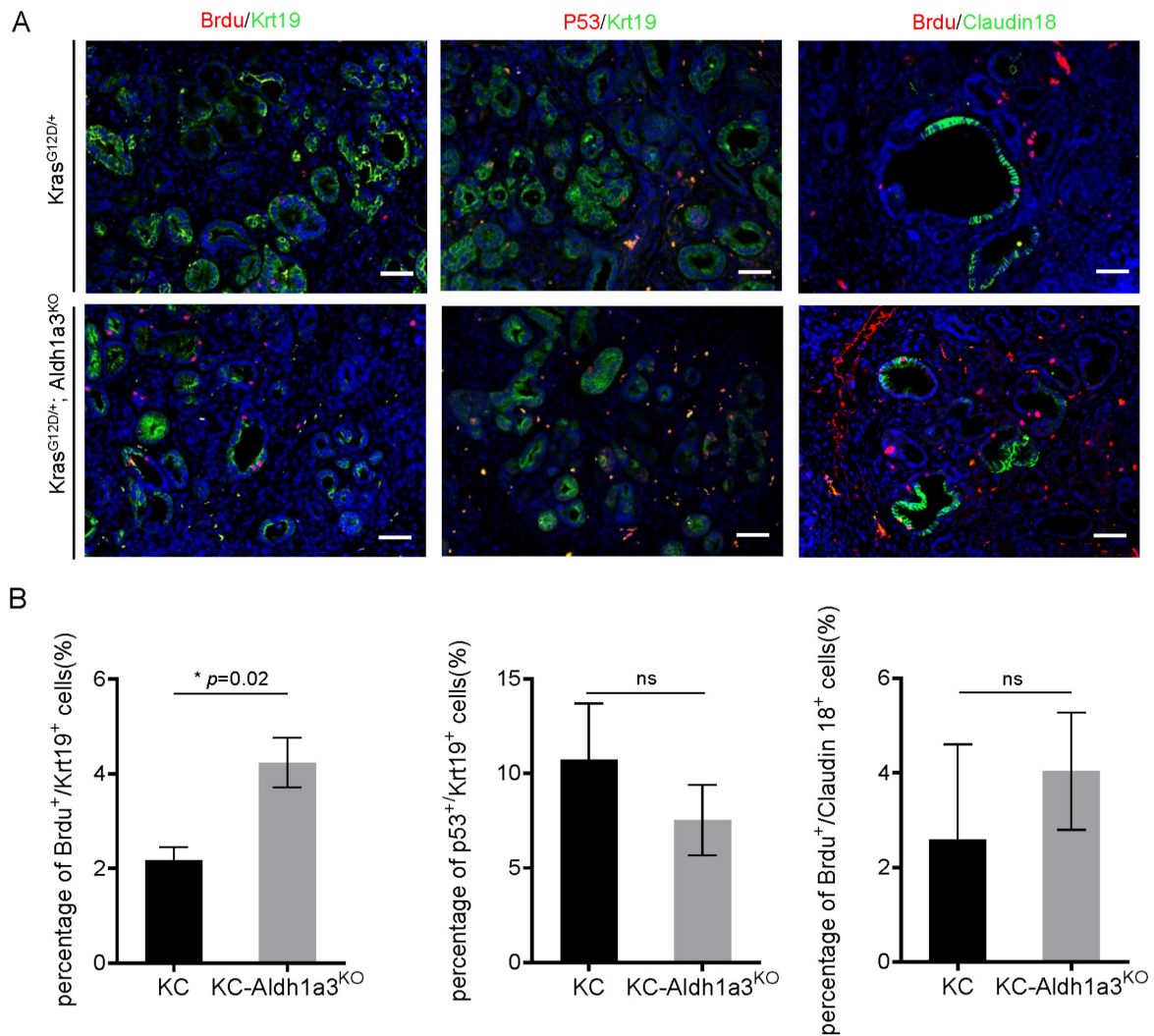


**Figure 13.** (A, B) Immunofluorescence analysis and quantification in KC and KC-Aldh1a3<sup>KO</sup> mice at day14 after caerulein injection. BrdU/Krt19/DAPI (left panel), p53/Krt19/DAPI (middle panel), BrdU/Claudin18/DAPI (right panel), scale bar: 50  $\mu$ m.

#### 4.7 Loss of Aldh1a3 reduced the “stemness” of pre-neoplastic lesions

As a member of the Aldh1a family, Aldh1a3 is known as a stemness marker in different biological contexts. Firstly, we compared the expression of putative normal stem cell markers, including Aldh1a1, Nanog, Oct4, and Sox2 between KC-Aldh1a3<sup>KO</sup> and KC mice. A significant downregulation in Aldh1a1 and Oct4 was observed at day 14 after caerulein treatment. No difference in the expression of Sox2 and Nanog was detected (*Figure 14A*). Interestingly, no significant change in the expression of classic CSC markers (Cd24, Cd44, Cd133 and Epcam) was observed upon Aldh1a3 deletion (*Figure 14B*). These results suggested that loss of

Aldh1a3 impaired the “stemness” of pre-neoplastic cells (or ADM cells), resulting in PanIN formation in the context of acute pancreatitis. These data are in line with increased proliferative potential upon Aldh1a3 ablation in these cells.

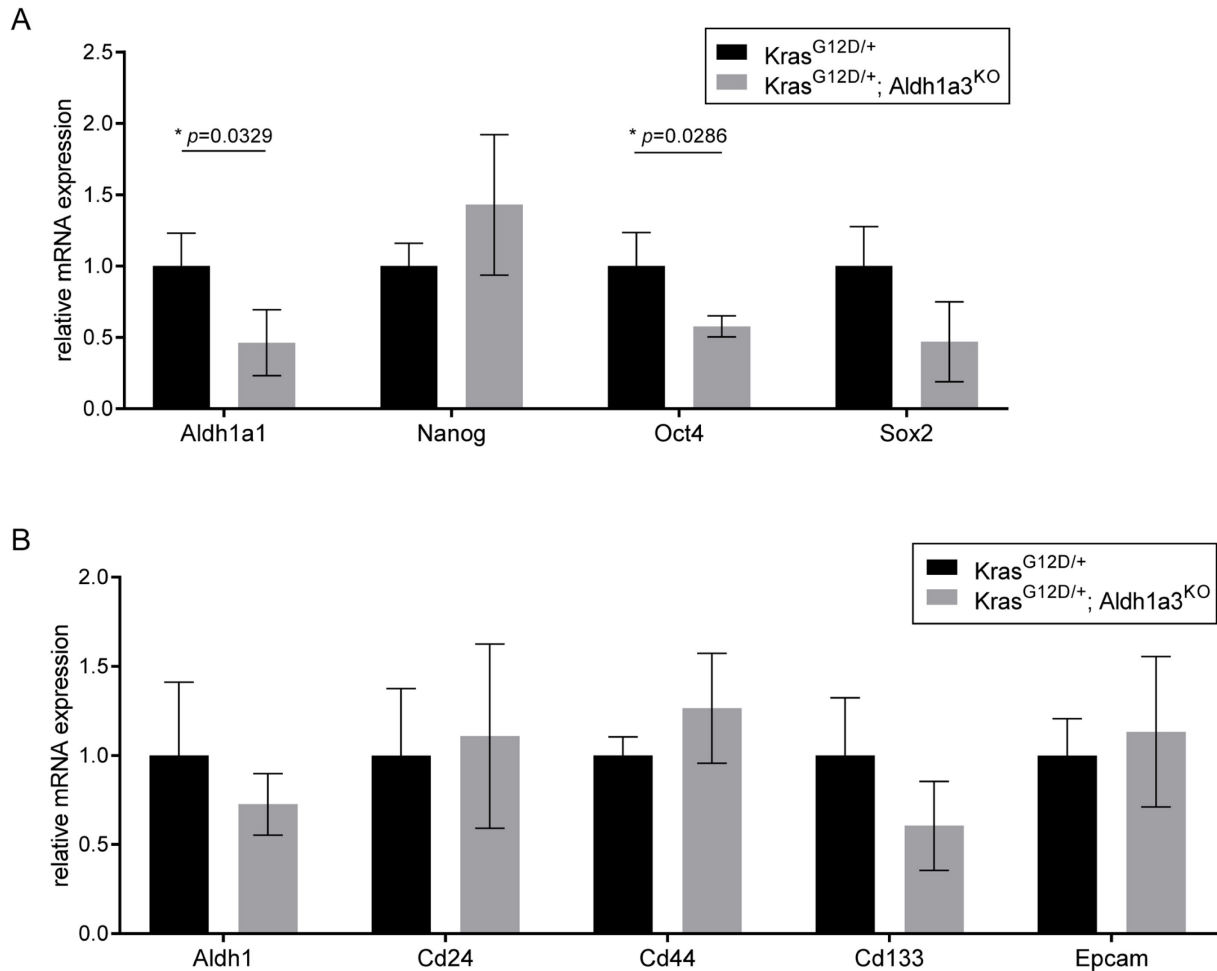


**Figure 14.** (A) Relative mRNA expression regarding CSC marker upon Aldh1a3 deletion. (B) Relative mRNA expression regarding normal cell stemness upon knockdown of Aldh1a3.

#### 4.8 Aldh1a3 promotes early pancreatic carcinogenesis in the absence of acute inflammation

Since the expression of Aldh1a3 in ADM/PanIN lesions was significantly lower than that in established PDACs, we speculate that the expression level of Aldh1a3 needs to reach a certain threshold to exert its oncogenic function. To this end, we generated a Rosa26 conditional knock-in line to overexpress Aldh1a3 (hereafter as Aldh1a3<sup>OE</sup>), by inserting a targeting vector between exon 1 and exon 2 of Rosa26 locus to generate Rosa26-Aldh1a3, led by CAG promoter. The vector contained a polyA cassette flanked by inward-facing loxP sites (*Figure 15A*). This Aldh1a3-knockin line was further crossed with pancreas-specific Cre recombinase line Ptf1a<sup>Cre/+</sup>. After the mouse line was established and stably passaged, an overexpression of Aldh1a3 in pancreatic tissues was confirmed by both IHC and qRT-PCR analysis (*Figure 15B, C*).

Among breeding pairs from p48<sup>Cre/+</sup>; Aldh1a3<sup>OE</sup> and Kras<sup>G12D/+</sup>; Aldh1a3<sup>OE</sup> as well as from p48<sup>Cre/+</sup> and Kras<sup>G12D/+</sup>; Aldh1a3<sup>OE</sup>, we generated 68 offsprings in total. Only two mice of p48<sup>Cre/+</sup>; Kras<sup>G12D/+</sup>; Aldh1a3<sup>OE</sup> were yielded whereas the regular amount mice of p48<sup>Cre/+</sup>; Aldh1a3<sup>OE</sup> and Kras<sup>G12D/+</sup>; Aldh1a3<sup>OE</sup> were produced. The amount of each labour was 4.857 mice on average with similar gender distribution. The expected rate of generating p48<sup>Cre/+</sup>; Kras<sup>G12D/+</sup>; Aldh1a3<sup>OE</sup> was estimated to be around 6.25% ~18.75%. The birth rate (2.94%) of these mice was lower in our hands. The p48<sup>Cre/+</sup>; Aldh1a3<sup>OE</sup> mice presented no abnormalities, and their pancreata showed no dysplasia until week 35. Interestingly, in the absence of acute inflammation, KC-Aldh1a3<sup>OE</sup> mice contained more spontaneous pre-neoplastic lesions at week 20, compared to KC mice. In line, significantly less amount of spontaneous pre-neoplastic lesions was observed in KC-Aldh1a3<sup>KO</sup> mice, compared to KC mice (*Figure 15D*). This data suggested that Aldh1a3 was oncogenic in the absence of acute inflammation.

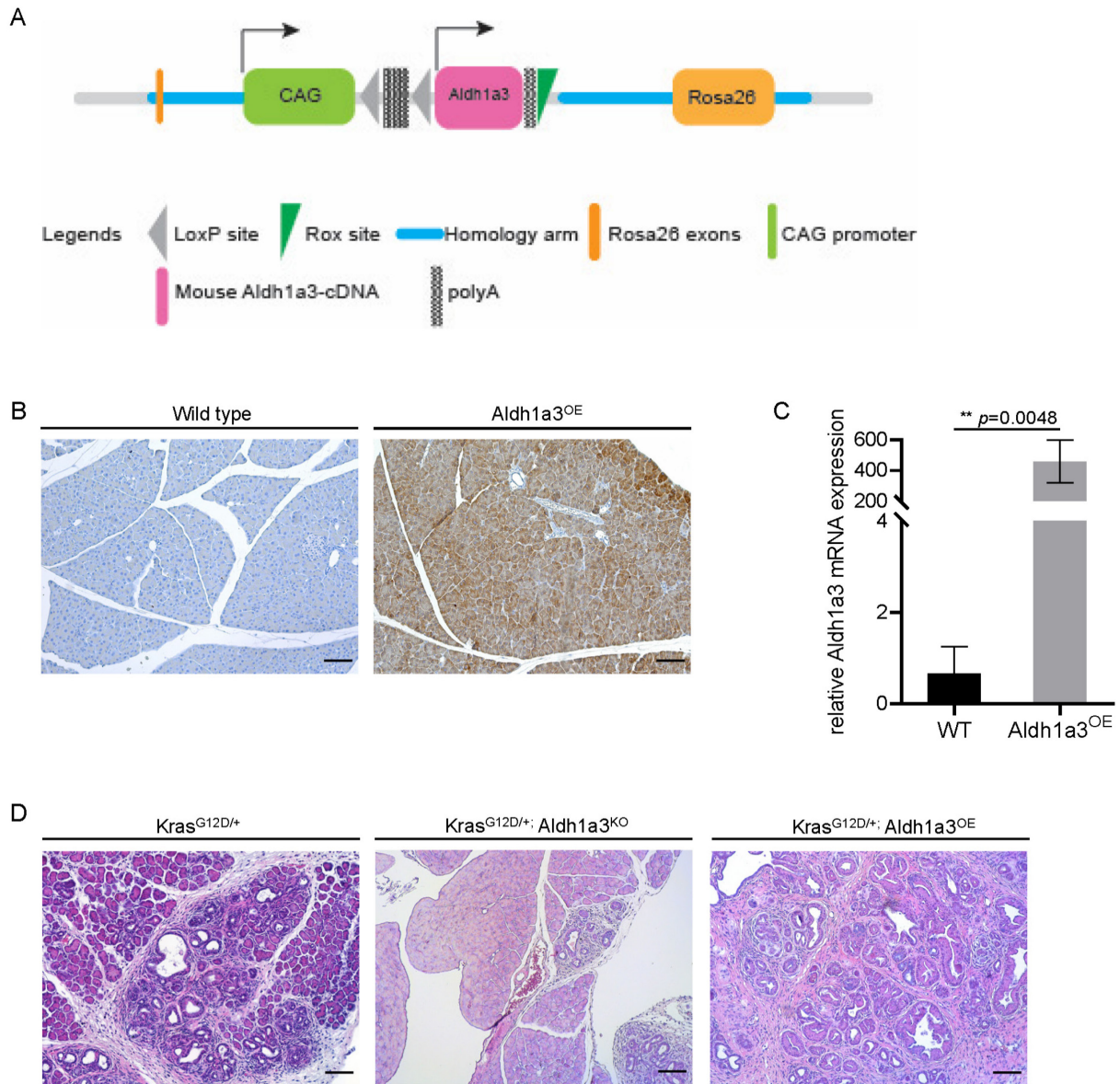


**Figure 15.** (A) Schematic diagram of generating conditional knock-in line of Aldh1a3<sup>OE</sup>; (B, C) Overexpression of Aldh1a3 was successfully induced in pancreatic epithelial cells confirmed by Aldh1a3 IHC staining and qRT-PCR analysis. scale bar: 100  $\mu$ m. (D) KC-Aldh1a3<sup>OE</sup> mice contained more pre-neoplastic lesions at 20 weeks, compared to KC mice; however, less pre-neoplastic lesions were observed in KC-Aldh1a3<sup>KO</sup>, scale bar: 100  $\mu$ m.

#### 4.9 ALDH1A3 labels a subgroup of mesenchymal cells.

Despite the expression in tumour cells, ALDH1A3 expression was also detected in the stroma in human PDAC samples, as well as in remodelled intrapancreatic nerve epineurium (*Figure 16A*). ALDH1A3 was also detectable in the stroma of human chronic pancreatitis samples (*Figure 16A*). Furthermore, patients with ALDH1A3 positive cells in mesenchyme tended to have worse survival (*Figure 16B*). Also, we observed that the area with ALDH1A3-enriched stroma was often infiltrated with immune cells.

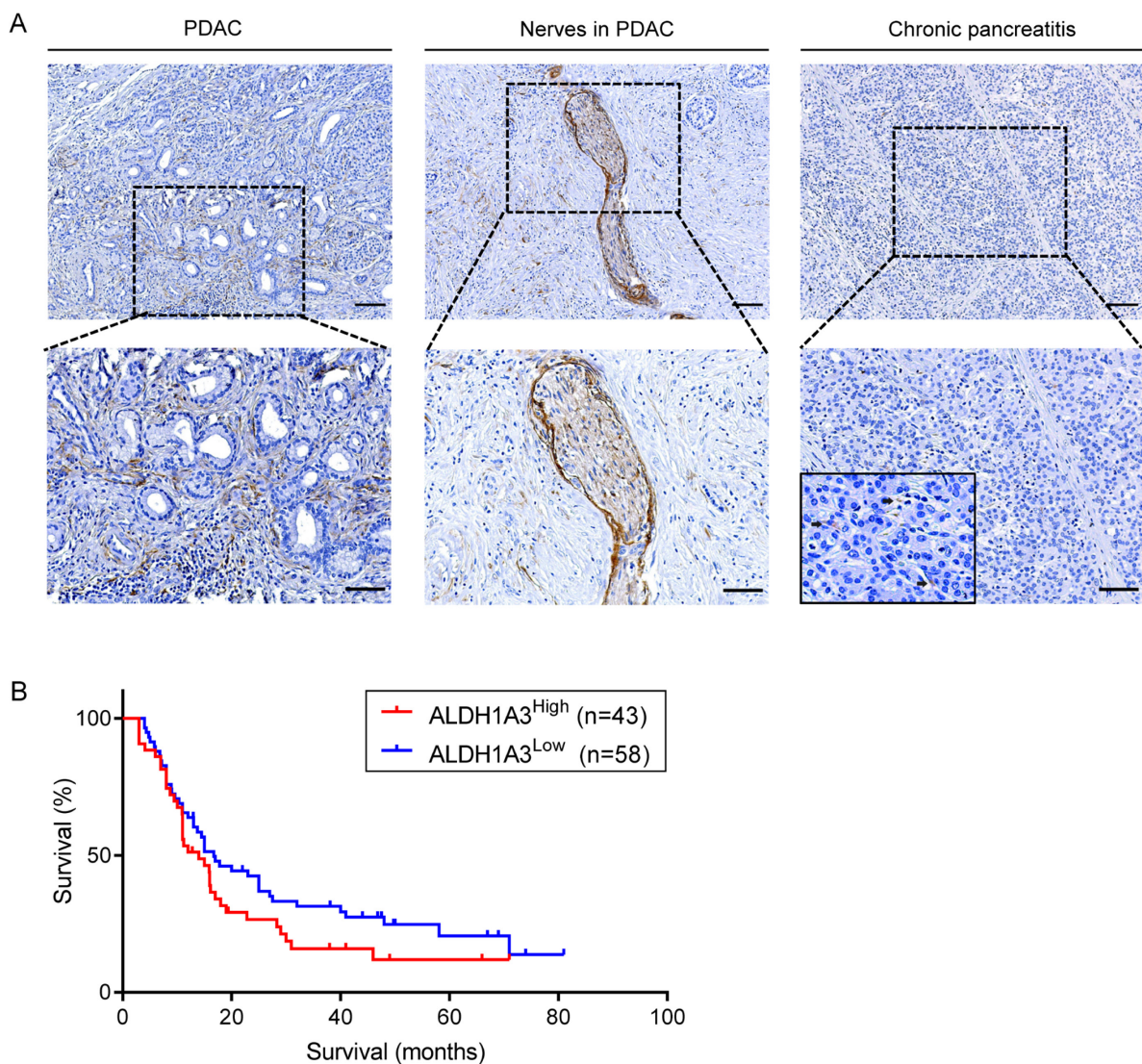


**Figure 16.** (A) ALDH1A3 expression was detected in the stroma in human PDAC samples, intrapancreatic nerve and epineurium, and in pancreatitis (arrow). Scale bar: 100  $\mu$ m (upper panel), 50  $\mu$ m (lower panel). (B) Patients with ALDH1A3 positive cells in mesenchyme tended to have an unfavourable prognosis.



In line with results from human samples, mouse pancreatic cancer, precursor lesions, and liver metastases showed detectable Aldh1a3 expression in the mesenchyme (*Figure 17*). Moreover, KC-Aldh1a3<sup>KO</sup>, although expressed no Aldh1a3 in pancreatic epithelium-derived precursor lesions, still harboured Aldh1a3 positive cells in stroma (*Figure 17, right*).

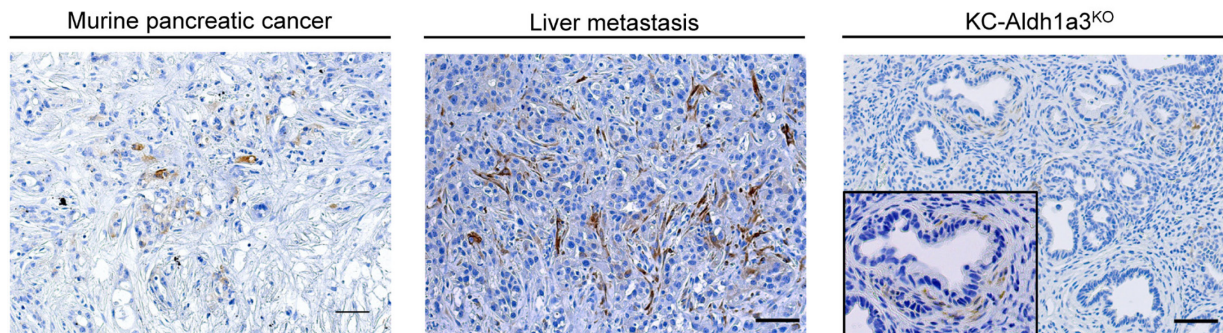


**Figure 17.** Aldh1a3-positive stroma cells were detected in mouse pancreatic cancer, metastasis, and in KC-Aldh1a3<sup>KO</sup>. Scale bar: 50  $\mu$ m.

To further explore whether these Aldh1a3-positive mesenchymal cells played a role in PDAC development, we generated Aldh1a3<sup>CreERT2</sup> mouse line and crossed them with Rosa26/tdTomato line (as a reporter gene). With this strategy, we were able to trace the Aldh1a3-positive cells after tamoxifen treatment (*Figure 18A*).

As expected, Aldh1a3 expression was not detectable in normal pancreatic epithelial cells. Compellingly, Aldh1a3-positive cells were detected in the mesenchyme (*Figure 18B*). As tamoxifen administration was performed by oral gavage, another effectively detectable field through the digestive system was found in the ileum with positive cells in lamina propria (*Figure 18B*). Immunofluorescence analysis showed that those Aldh1a3-positive cells were negative for Epcam, a marker for epithelial cells, ruling out the possibility that these cells derived from epithelial cells.

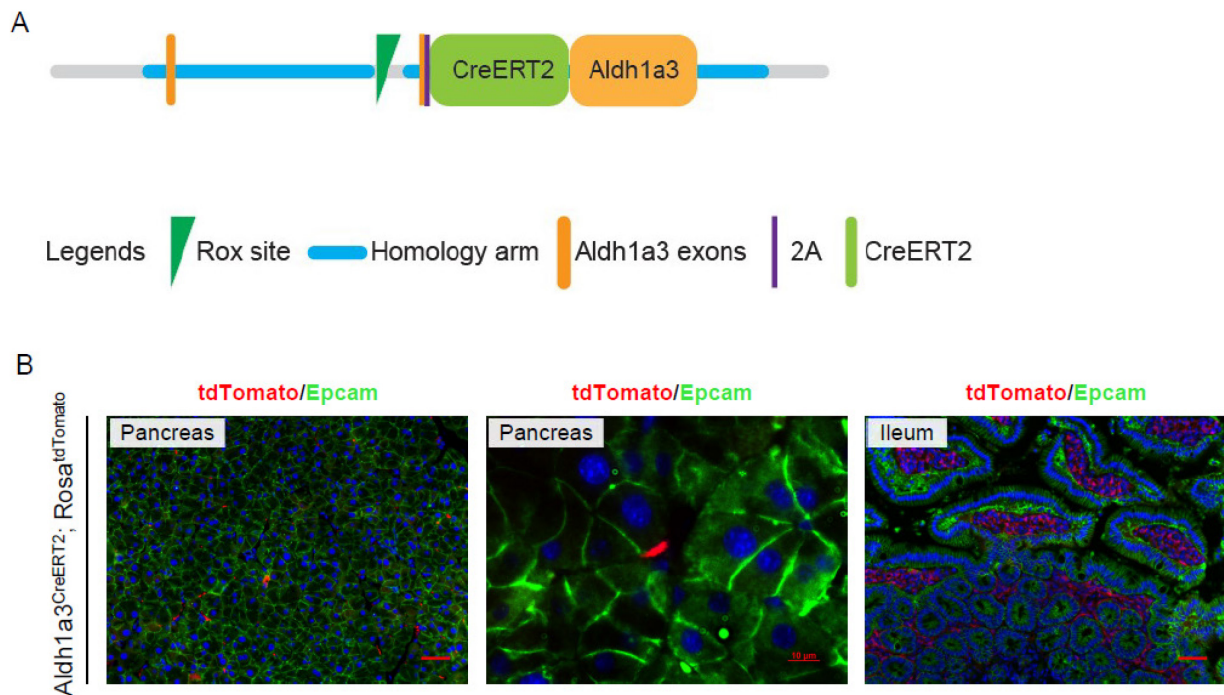


**Figure 18.** (A) Generation of Aldh1a3<sup>CreERT2</sup> mouse line. (B) Representative IF of tdTomato/Epcam/DAPI in pancreatic tissue and lamina propria of ileum, scale bar: left and right 50  $\mu$ m, middle 10  $\mu$ m.

Next, we performed fluorescence-activated cell sorter (FACS) analysis to further characterize Aldh1a3-positive mesenchymal cells. After tamoxifen administration, mice were sacrificed at the age of 8 weeks, and primary pancreatic cells were isolated and subjected to FACS analysis. This analysis revealed that Aldh1a3-positive cells accounted for around 0.8% of pancreatic cells. These Aldh1a3-positive cells were sorted out by FACS and cultured in advanced DMEM/F12 (with 10% FBS, 1% P/S). Aldh1a3-positive cells were closely observed and followed afterwards. On the first day after seeding, cells attached to the plate exhibited the morphology of quiescent pancreatic stellate cells, harbouring the lipid droplets inside (*Figure 19A*). On the second day, the cells started to proliferate. Meanwhile, a loss of the storage of lipid droplets and stretched fibroblastic morphology were observed over time (*Figure 19B*), indicating their activated status and their capability of desmoplasia. This process was comparable to that of pancreatic stellate cells (*Figure 19B*).

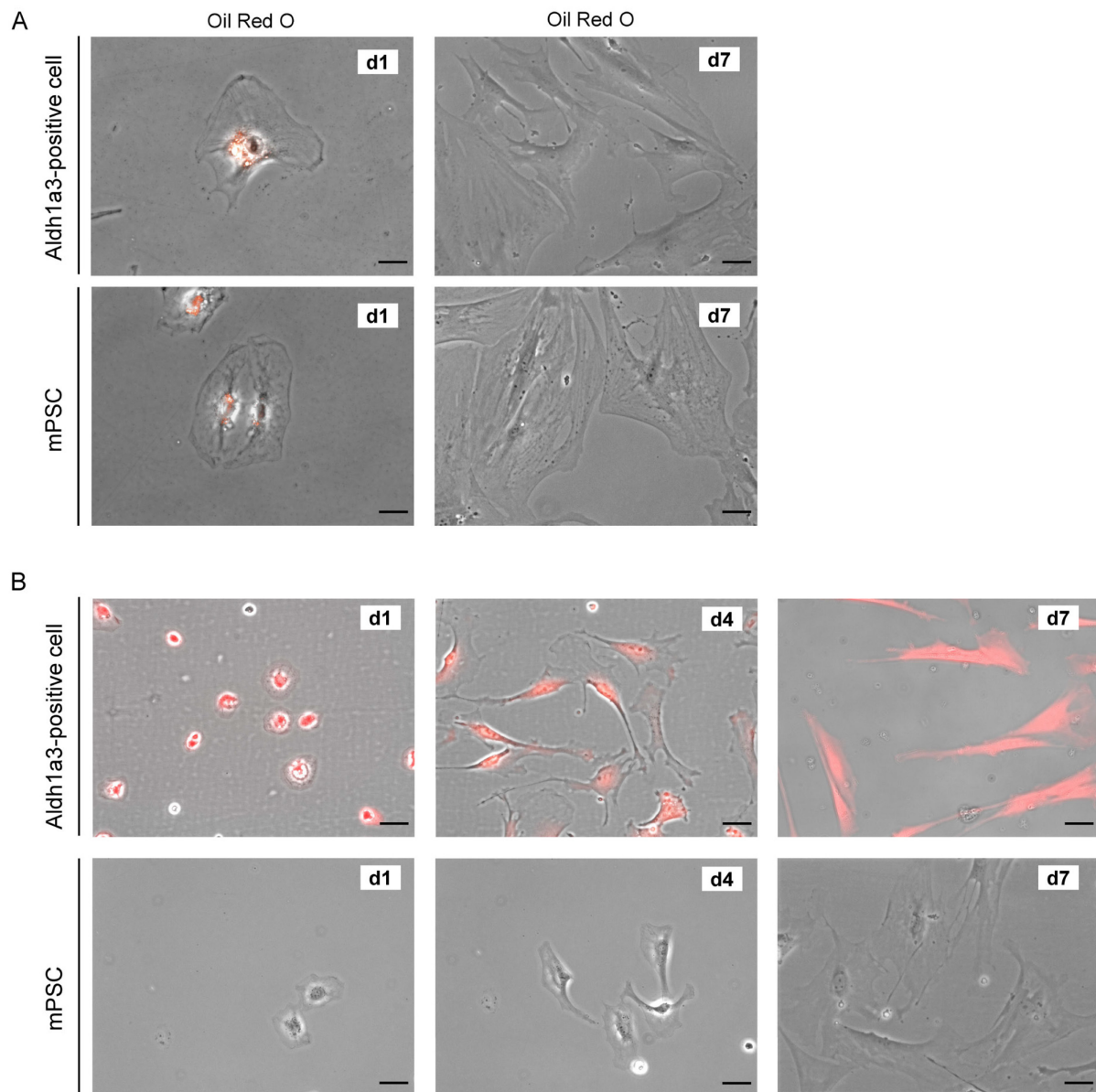


**Figure 19.** (A) Oil Red O staining of Aldh1a3-positive cells (upper panel) and pancreatic stellate cells (lower panel). Scale bar: 25  $\mu$ m. (B) Representative morphological changes of Aldh1a3-positive cells after sorting (upper panel) and primary isolated mouse pancreatic stellate cells (lower panel), scale bar: 50  $\mu$ m.

## 5. DISCUSSION

Pancreatic ductal adenocarcinoma is the fourth leading cause of cancer-related disease with poor prognosis. Thus, effective biomarkers for early diagnosis and targeted treatment would play an essential role in clinical prevention and intervention for PDAC.

Previous research of our group has identified an aggressive subtype of PDAC labelled by ALDH1A3 (Kong et al., 2016). Hereby, we focused on the exact role of Aldh1a3 in early carcinogenesis.

Transcriptomic and epigenetic data described that, compared to normal derived tissues, ALDH1A3 was abundantly expressed in pancreatic cancer cell lines and tumor tissues (1,630 fold and 78.5 fold on mRNA level, respectively) (Jia et al., 2013). Cancer Cell Line Encyclopedia (CCLE) unravelled accordantly the highest ALDH1A3 mRNA expression and the lowest DNA methylation of ALDH1A3 compared to normal derived tissue in pancreatic cancer cell lines, among all accessible human malignancy cell lines (Barretina et al., 2012).

In line with the previous data, it was confirmed that human PDAC patients with positive ALDH1A3 expression in tumor cells showed worse survival. Experiments *in vivo* also illustrated that KPC mice with liver metastases presented positive Aldh1a3 expression in both local tumors and metastases. It was thereby rational to hypothesize that modulation of Aldh1a3 in pancreatic epithelial cells could influence carcinogenesis and prognosis of pancreatic cancer.

Activation of oncogenic Kras in mouse pancreatic acinar cells alters gene expression profiles in two parallel clusters: silencing acinar genes such as amylase encoding genes, elastase encoding genes such as Muscle Intestine and Stomach Expression 1 (Mist1) and Carboxypeptidase A1 (Cpa1); inducing ductal genes including Krt19, Mucin 1 Cell Surface

Associated (Muc1) (Shi et al., 2013). Pancreatic progenitor related genes, like pancreatic and duodenal homeobox 1 (Pdx1) and Sry-related high-mobility group box 9 (Sox9), are also upregulated upon oncogene Kras expression.

Here, this study revealed that Aldh1a3 expression was acquired in the formation of pre-neoplastic lesions. The acquisition of Aldh1a3 was found to take place in parallel with the loss of amylase expression and the gain of expression of Krt19 in the context of acute pancreatitis. However, such acquired Aldh1a3 expression can only be observed in KC mice. Mice of wild type, which also presented ductal-like structures during acute inflammation phase, showed no Aldh1a3 expression.

As Claudin-18 is found to be present in almost all stages of PanIN (Tanaka et al., 2011) and Muc5ac represents the enhanced mucin production, the finding of co-localization between Aldh1a3 and Claudin-18, as well as the increased Muc5ac presence in Aldh1a3-positive epithelial cells, supported that Aldh1a3 was induced in pancreatic ductal metaplasia and accumulated as lesions progressed. Thereby, Aldh1a3 expression in pancreatic epithelial cells was indicated to be relevant to the Kras<sup>G12D</sup>-driving progenitor cell features and proliferating properties.

Although global Aldh1a3 knockout mice die shortly after birth as reported (Dupe et al., 2003), our study observed that pancreas-specific Aldh1a3-ablated mice were as healthy as wild-type mice, indicating that ablation of Aldh1a3 in pancreatic epithelium had no impact on the development of the murine pancreas. Meanwhile, overexpression of Aldh1a3 in pancreas did not impact pancreatic development. Conclusively, Aldh1a3, though contributes substantially to murine embryogenesis, does not influence the development of pancreas in mice.

It has been noticed that silencing ALDH1A3 gene by shRNA in human melanoma cells could result in an arrest in cell cycle and induce apoptosis of ALDH1A3+ cells, and further inhibit

tumor growth in xenograft in mouse (Luo et al., 2012). The similar function of ALDH1A3 in promoting tumor progression was also reported in breast cancer cells, although they demonstrated a divergent effect of ALDH1A3 on tumor progression in one breast cell line (MDA-MB-435) (Marcato et al., 2015). Interestingly, our data demonstrated that an ablation of *Aldh1a3* specifically in murine pancreatic epithelial cells showed similar phenotypes in precursor lesions compared to KC mice in the context of acute inflammation. However, we observed transiently an increased PanIN formation after *Aldh1a3* deletion. Meanwhile, more proliferating pre-neoplastic cells were detected upon deletion of *Aldh1a3*. The early stage of pancreatic precursor lesions, such as ADM lesions, were therefore suggested to gain higher capability of differentiation and proliferation upon *Aldh1a3* deletion in the context of acute inflammation, which could partially explain why more PanIN lesions were observed in KC-*Aldh1a3*<sup>KO</sup> mice.

Interestingly, *Aldh1a3*-deletion in pancreatic epithelial cells elicited a negative regulation of p53 in ADM and PanIN lesions in the context of acute inflammation. The loss of p53 and its downstream target p21, could explain the increasing proliferation ability of precursor cells and the abundant PanIN formation after that. Also, impaired autophagy, marked by increased Lc3ii and p62/Sqstm1, was also observed in KC-*Aldh1a3*<sup>KO</sup> mice after the induction of acute pancreatitis. As reported by *Todoric et al.* (*Todoric et al., 2017*), defective autophagy led to the accumulation of autophagy substrate p62/SQSTM1, which further could promote pancreatic neoplastic progression by controlling NRF2/MDM2/p53 axis. They showed that accumulated SQSTM1 could activate NRF2, which blocks p53 and therefore accelerates precursor lesion progression. This data provided a presumed explanation for the downregulation of p53 and enhanced PanIN formation. However, they also demonstrated that accumulated autophagy substrate would induce upregulation of stem/progenitor marker genes, which contradicts our data.

In conclusion, our study demonstrated that Aldh1a3 ablation transiently promoted cell proliferation in ADM lesions, and further led to a faster formation of PanINs in the context of acute pancreatitis. However, no long-term effect was observed.

Aldefluor-positive centroacinar and terminal ductal epithelial cells were reported with high expressional level of Aldh1a1 and Aldh1a7, but low expressional level of Aldh1a2, Aldh1a3, and Aldh8a1 (Rovira et al., 2010), suggesting Aldh1a1 (rather than Aldh1a3) is more likely to be responsible for aldehyde activity and stemness in pancreas. However, the role of Adh1a1 in PDAC is still under debate as divergent influences of Aldh1a1 on PDAC were observed (Kahlert et al., 2011; Oria et al., 2018; Rasheed et al., 2010). As for Aldh1a3, our data revealed that depletion of Aldh1a3 reduced the expression of stemness markers in pre-neoplastic lesions.

Accordingly, our data demonstrated that the basal level of Aldh1a3 expression was low in mouse pancreas. Thus, it was rational that Aldh1a3 ablation in early pancreatic precursor lesion could not lead to distinguishable phenotypes. Similar results were published for human breast cancer cells with knockdown of ALDH1A3 on MDA-MB-231 (Marcato et al., 2015), which expresses a low level ALDH1A3, did not affect the malignant behaviors of these cells.

Our study investigated the role of Aldh1a3 not only with conditional knockout strategy but also with the conditional knockin/overexpression system. Though the overexpression of Aldh1a3 was successfully confirmed in mouse pancreatic epithelial cells, the co-existence of overexpression of Aldh1a3 and activated Kras<sup>G12D</sup> seemed to be less productive while breeding. An average amount of 4.857 progenies were obtained from each labor, compared to the common 6~9 baby mice in normal breeding on the background of C57BL/6. More notably, only 2.94% of descendants displayed the ideal genotypes, which is significantly less than the estimated 6.25~18.75%. As mus musculus Rosa26 gene, where overexpression Aldh1a3 vector was inserted, and Kras gene locates at mouse chromosome 6 (113,067,428 –

13,077,333 and 145,216,699 – 145,250,239, respectively), they should not interfere with each other concerning transcription process. Ptf1 $\alpha$  is firstly expressed in the pancreas at E9.5 (Chiang & Melton, 2003; Kawaguchi et al., 2002), and pancreatic multipotent progenitor cells (MPCs) maintained until E12.5 (Zhou et al., 2007). After pancreatic MPCs are allocated, the expression of Ptf1 $\alpha$  is only sustained in pancreatic acinar cell. Hereby, co-expression of high level of Aldh1a3 and activated Kras<sup>G12D</sup> mutation in pancreatic MPCs or in premature acinar cells might interfere with pancreatic organogenesis.

Intriguingly, our study observed that a subset of mesenchymal cells was positive for ALDH1A3 expression in the stroma from both human PDAC samples and KPC mouse models. Moreover, we identified a subgroup of mesenchymal cells in mouse, which had intrinsic high expression of Aldh1a3. In adult organ, these cells can only be detected at a small population with quiescent status; however, they can be presumably activated and further proliferated upon the onset of early carcinogenesis. Once isolated and cultured in 2-dimensional condition, these cells displayed similar biological features as pancreatic stellate cells, indicating that they could be categorized into a subgroup of pancreatic stellate cells. Furthermore, ALDH1A3-positive fibroblasts were often noticed with accumulated immune cells in human samples, implying the interaction between those fibroblasts and immune response.

Lately, two distinct subtypes of PSCs-derived CAFs have been identified, myofibroblastic type (myCAF) and inflammatory type (iCAF) (Ohlund et al., 2017). Myofibroblastic CAFs are characterized by elevated expression in  $\alpha$ -SMA and its adjacent location to neoplastic cell. On the contrary, inflammatory CAFs, staying relatively distant from neoplastic cells, lack the expression of  $\alpha$ -SMA and harbor elevated IL6 expression and other inflammatory cytokines. The secretory iCAFs were suggested to promote tumor progression and suppress immune response by secreting specific cytokines, while myCAFs were suggested to restrain cancer progression (Ozdemir et al., 2015). Recently, another distinctive subtype of CAFs with low



expression of both  $\alpha$ -SMA and IL-6 was identified. It has been demonstrated IL1/LIF/JAK/STAT signaling and TGF $\beta$  signaling underlie the mechanism of the diverse differentiations and suggested that iCAFs and myCAFs were interconvertible states of CAFs (Biffi et al., 2019). Here, the function of Aldh1a3-positive mesenchymal cells needs to be further investigated. Prospective studies to examine the interaction between the specific subgroup and neoplastic cells may ultimately confirm their exact function.

## 6. SUMMARY

In this study, we explored the role of ALDH1A3 in the development of PDAC using transgenic mouse models driven by oncogenic Kras<sup>G12D</sup> mutation. In line with the clinical correlation between the high expression of ALDH1A3 and worse prognosis, an enhanced Aldh1a3 level was observed in mouse PDAC and its corresponding metastases. Additionally, such increased Aldh1a3 expression was also detectable in so-called pre-neoplastic lesions such as acinar-to-ductal metaplasia (ADM) and pancreatic intraepithelial neoplasia (PanIN) lesions. Interestingly, the specific Aldh1a3 ablation in pancreatic epithelial cells did not affect ADM and PanIN development, but rather slightly promoted PanIN formation in a well-established mouse model of acute pancreatitis-accelerated PDAC driven by Kras<sup>G12D</sup>. However, such alteration was insufficient to lead to a sustained impact on PDAC progression in long term. The promoted PanIN formation was suggested to result from higher capacity of proliferation due to p53 suppression, reduction of stemness, and impaired autophagy. On the contrary, in the absence of acute pancreatitis, the Aldh1a3 ablation significantly compromised Kras<sup>G12D</sup>-driven PDAC development. In line, overexpression of Aldh1a3 in pancreatic epithelial cells significantly promoted Kras<sup>G12D</sup>-driven pancreatic carcinogenesis. These data argue for a context-dependent function of Aldh1a3 in PDAC development, which is likely to be variable depending on the inflammatory status of organ. Finally, we defined a subtype of mesenchymal cells with enhanced ALDH1A3 expression in both human and mouse pancreatic cancers. The exact function of these mesenchymal cells needs to be further investigated.

Thereby, the questions raised as “AIMS OF THIS STUDY” have been demonstrated as followed:

Q1: What is the effect of knockout or overexpression of Aldh1a3 in murine pancreas development?

Conclusion 1 (C1): The Aldh1a3 ablation or overexpression in pancreatic epithelial cells presented no impact on pancreatic physiology.

Q2: What is the role of Aldh1a3 in Kras<sup>G12D</sup>-driven pancreatic carcinogenesis?

Conclusion 2 (C2): The Aldh1a3 expression was also detectable in pre-neoplastic lesions such as ADM and PanIN lesions. In the context of acute pancreatitis, ADM formation was not affected, however, we observed a transiently accelerated PanIN formation in these models after pancreas-specific Aldh1a3 ablation. In the absence of acute pancreatitis, Aldh1a3 ablation compromised the formation of pre-neoplastic lesions driven by oncogenic Kras<sup>G12D</sup> mutation. Meanwhile, Aldh1a3 overexpression promoted formation of these lesions.

Q3: what is the molecular mechanism responsible for potential function of Aldh1a3 in early pancreatic carcinogenesis?

Conclusion 3 (C3): Deletion of Aldh1a3 reduced the expression of stemness markers in pre-neoplastic lesions. It promotes cell proliferation with an impaired p53 and autophagy function in the context of acute pancreatitis. This temporary dysregulation may partially explain the PanIN-promoting phenotype upon Aldh1a3 ablation.

## 7. ABBREVIATION

ADM	Acinar-to-ductal metaplasia
AFLs	Atypical flat lesions
ALDH	Aldehyde dehydrogenases
ALDH1A1	Aldehyde dehydrogenase family 1, subfamily A1
ALDH1A3	Aldehyde dehydrogenase family 1, subfamily A1
Ampk	AMP-Activated Protein Kinase
$\alpha$ -SMA	Alpha-smooth muscle actin
atRA	<i>all-trans</i> Retinoic acid
Bip	Binding-Immunoglobulin Protein
BrdU	5-Bromo-2'-deoxyuridine
CAFs	Cancer-associated fibroblasts
CDKN2A	Cyclin Dependent Kinase Inhibitor 2A, p16
Chop	C/EBP-Homologous Protein 10
CSCs	Cancer stem cells
CTCs	Circulating tumour cells
Cxcr4	C-X-C Motif Chemokine Receptor 4
DAPI	4,6-diamidino-2-phenylindole
EGFR	Epidermal growth factor receptor
Epcam	Epithelial Cell Adhesion Molecule
Erk	Extracellular Signal-Regulated Kinase
ES	Embryonic stem
FACS	Fluorescence-activated cell sorter
GAPDH	Glyceraldehyde-3-Phosphate Dehydrogenase
HAs	Homology arms
iCAF	inflammatory type of cancer associated fibroblasts
IHC	Immunohistochemistry
IL1	Interleukin 1
ILR1	Interleukin 1 Receptor Type 1
IL6	Interleukin 6
IPMN	Intraductal papillary-mucinous neoplasm

JAK	Janus Kinase
Krt19	Cytokeratin 19
Lc3b	Light Chain 3b
LIF	Leukemia inhibitory factor
MCN	Mucinous cystic neoplasm
mTOR	Mammalian target of rapamycin
myCAFs	myofibroblastic type of cancer associated fibroblasts
MPC	Multipotent progenitor cells
Muc5ac	Mucin 5 subtype A and C
NSCLC	Non-small cell lung cancer
Oct4	Octamer-Binding Protein 4
P21	Cyclin Dependent Kinase Inhibitor 1A
P27	Cyclin Dependent Kinase Inhibitor 1B
PanIN	Pancreatic intraepithelial neoplasia
PDAC	Pancreatic ductal adenocarcinoma
Pdx1	Pancreatic And Duodenal Homeobox 1
PSCs	Pancreatic stellate cells
PTF1 $\alpha$	Pancreas transcription factor 1 subunit alpha
RA	Retinoic acid
SCLC	Small cell lung cancer
SOX2	SRY-Box 2
Sqstm1	Sequestosome 1, p62
STAT	Signal transducer and activator of transcription
TGF	Transforming growth factor
TP53	Tumor protein 53, p53

## 8. LIST OF FIGURES

- Figure 1.** (A) Schematic diagrams of the targeting strategy for conditional knock-in line to overexpress Aldh1a3. (B) Vector linearization with NotI for *Rosa*<sup>R26-CAG-Aldh1a3</sup> mouse line..... 17
- Figure 2.** (A) Schematic diagrams of the targeting strategy for Aldh1a3<sup>CreERT2</sup> mouse generation. (B) Vector linearization with NotI for Aldh1a3<sup>CreERT2</sup> mouse line..... 19
- Figure 3.** (A) Positive ALDH1A3 expression was detected in cancer cells in a subgroup of PDAC samples but not in normal pancreas or chronic pancreatitis tissues. (B) Patients with high ALDH1A3 expression in PDAC cells had shorter survival than those with low ALDH1A3 expression. (C) ALDH1A3 expression in HPDE and other 8 human PDAC cell lines..... 37
- Figure 4.** Pancreatic cancer cell lines exhibit the highest ALDH1A3 mRNA expression (A) and the lowest DNA methylation (B) of ALDH1A3 among all accessible human malignancy cell lines..... 38
- Figure 5.** Aldh1a3 in epithelial cells were positively detected in pancreatic cancer (middle) and liver metastasis (right) in the KPC mouse model. Aldh1a3 accumulated notably more near the border line between metastatic and normal tissue. .... 39
- Figure 6.** (A) Aldh1a3 expression in wild-type (upper panel) and KC mice (lower panel) after caerulein injection. (B, C) Immunoblot analysis of Aldh1a3 in KC mouse at different time points after caerulein. (D) Representative IF analysis of KC mouse pancreas at 14d after caerulein injection..... 41
- Figure 7.** (A) Ablation of mouse Aldh1a3 with LoxP system. (B) HE stains analysis showed no visible lesion in Aldh1a3-deficient mouse pancreas as in wild type mouse pancreas at six months. (C) Relative mRNA expression of Aldh1a3 in Aldh1a3<sup>KO</sup> in the pancreata of WT and Aldh1a3<sup>KO</sup> mice..... 43
- Figure 8.** (A, B) IHC analysis and quantification of Aldh1a3 in mouse pancreas. (C, D) Western Blot and quantification confirmed the deletion of Aldh1a3 in Aldh1a3<sup>KO</sup> mice. (E) Relative

mRNA expression of Aldh1a3 in murine pancreas of KC and KC-Aldh1a3<sup>KO</sup> mice.....44

**Figure 9.** (A) Procedure of caerulein treatment and sacrifice in schematic diagrams. (B, C) Both mouse models presented atrophic pancreas with ADM formation at day 14 after caerulein, no distinguishable difference was detected. (D, E) Weight changes or pancreas/body weight ratio showed no significant difference between the two strains.....45

**Figure 10.** (A, B) IHC analysis revealed no difference in alpha-Amylase or Krt19, but more Claudin 18 and Muc5ac upon loss of Aldh1a3 in the pancreatic epithelium. (C) HE staining for KC and KC-Aldh1a3<sup>KO</sup> mice by the time 26 weeks after caerulein injection.....47

**Figure 11.** (A, B) IHC revealed no significant alteration in the pancreas acinar-derived cells on BrdU, p53 or p21. (C) qRT-PCR analysis of mRNA expression of signals of interest.....49

**Figure 12.** (A, B) Immunoblot analysis and quantification by screening signals on protein levels.....50

**Figure 13.** (A, B) Immunofluorescence analysis and quantification in KC and KC-Aldh1a3<sup>KO</sup> mice at day14 after caerulein injection. BrdU/Krt19/DAPI (left panel), p53/Krt19/DAPI (middle panel), BrdU/Claudin18/DAPI (right panel) .....51

**Figure 14.** (A) Relative mRNA expression of CSC markers upon Aldh1a3 deletion. (B) Relative mRNA expression regarding normal cell stemness upon knockdown of Aldh1a3.....52

**Figure 15.** (A) Schematic diagram of generating conditional knock-in line of Aldh1a3<sup>OE</sup>; (B, C) Overexpression of Aldh1a3 was successfully induced in pancreatic epithelium confirmed by Aldh1a3 IHC and qRT-PCR analysis. (D) KC-Aldh1a3<sup>OE</sup> mice contained more preneoplastic lesions at 20 weeks, compared to KC mice; however, less pre-neoplastic lesions were observed in KC-Aldh1a3<sup>KO</sup> .....54

**Figure 16.** (A) ALDH1A3 expression was detected in the stroma in human PDAC samples, intrapancreatic nerve and epineurium, and in pancreatitis(arrow). (B) Patients with ALDH1A3 positive cells in mesenchyme tended to have an unfavourable prognosis.....55

**Figure 17.** Aldh1a3-positive stroma cells were detected in mouse pancreatic cancer, metastasis, and in acute pancreatitis of KC-Aldh1a3<sup>KO</sup> mouse.....56

**Figure 18.** (A) Generation of Aldh1a3<sup>CreERT2</sup> mouse line. (B) Representative IF pictures of tdTomato/Epcam/DAPI in pancreatic tissue and lamina propria of ileum.....57

**Figure 19.** (A) Oil Red O staining of Aldh1a3-positive cells (upper panel) and pancreatic stellate cells (lower panel). (B) Representative morphological changes of Aldh1a3-positive cells after sorting (upper panel) and primary isolated mouse pancreatic stellate cells (lower panel) .....58



## 9. REFERENCE

- Aichler, M., Seiler, C., Tost, M., Siveke, J., Mazur, P. K., Da Silva-Buttkus, P., Bartsch, D. K., Langer, P., Chiblak, S., Durr, A., Hofler, H., Kloppel, G., Muller-Decker, K., Brielmeier, M., & Esposito, I. (2012). Origin of pancreatic ductal adenocarcinoma from atypical flat lesions: a comparative study in transgenic mice and human tissues. *J Pathol*, *226*(5), 723-734. doi:10.1002/path.3017
- Almoguera, C., Shibata, D., Forrester, K., Martin, J., Arnheim, N., & Perucho, M. (1988). Most human carcinomas of the exocrine pancreas contain mutant c-K-ras genes. *Cell*, *53*(4), 549-554. Retrieved from <https://www.ncbi.nlm.nih.gov/pubmed/2453289>
- Bachem, M. G., Schunemann, M., Ramadani, M., Siech, M., Beger, H., Buck, A., Zhou, S., Schmid-Kotsas, A., & Adler, G. (2005). Pancreatic carcinoma cells induce fibrosis by stimulating proliferation and matrix synthesis of stellate cells. *Gastroenterology*, *128*(4), 907-921. Retrieved from <https://www.ncbi.nlm.nih.gov/pubmed/15825074>
- Barretina, J., Caponigro, G., Stransky, N., Venkatesan, K., Margolin, A. A., Kim, S., Wilson, C. J., Lehar, J., Kryukov, G. V., Sonkin, D., Reddy, A., Liu, M., Murray, L., Berger, M. F., Monahan, J. E., Morais, P., Meltzer, J., Korejwa, A., Jane-Valbuena, J., Mapa, F. A., Thibault, J., Bric-Furlong, E., Raman, P., Shipway, A., Engels, I. H., Cheng, J., Yu, G. K., Yu, J., Aspesi, P., Jr., de Silva, M., Jagtap, K., Jones, M. D., Wang, L., Hatton, C., Palesscandolo, E., Gupta, S., Mahan, S., Sougnez, C., Onofrio, R. C., Liefeld, T., MacConaill, L., Winckler, W., Reich, M., Li, N., Mesirov, J. P., Gabriel, S. B., Getz, G., Ardlie, K., Chan, V., Myer, V. E., Weber, B. L., Porter, J., Warmuth, M., Finan, P., Harris, J. L., Meyerson, M., Golub, T. R., Morrissey, M. P., Sellers, W. R., Schlegel, R., & Garraway, L. A. (2012). The Cancer Cell Line Encyclopedia enables predictive modelling of anticancer drug sensitivity. *Nature*, *483*(7391), 603-607. doi:10.1038/nature11003
- Biffi, G., Oni, T. E., Spielman, B., Hao, Y., Elyada, E., Park, Y., Preall, J., & Tuveson, D. A. (2019). IL1-Induced JAK/STAT Signaling Is Antagonized by TGFbeta to Shape CAF Heterogeneity in Pancreatic Ductal Adenocarcinoma. *Cancer Discov*, *9*(2), 282-301. doi:10.1158/2159-8290.CD-18-0710

- Blentic, A., Gale, E., & Maden, M. (2003). Retinoic acid signalling centres in the avian embryo identified by sites of expression of synthesising and catabolising enzymes. *Dev Dyn*, 227(1), 114-127. doi:10.1002/dvdy.10292
- Bonnet, D., & Dick, J. E. (1997). Human acute myeloid leukemia is organized as a hierarchy that originates from a primitive hematopoietic cell. *Nat Med*, 3(7), 730-737. Retrieved from <https://www.ncbi.nlm.nih.gov/pubmed/9212098>
- Burlison, J. S., Long, Q., Fujitani, Y., Wright, C. V., & Magnuson, M. A. (2008). Pdx-1 and Ptf1a concurrently determine fate specification of pancreatic multipotent progenitor cells. *Dev Biol*, 316(1), 74-86. doi:10.1016/j.ydbio.2008.01.011
- Cai, J., Cheng, A., Luo, Y., Lu, C., Mattson, M. P., Rao, M. S., & Furukawa, K. (2004). Membrane properties of rat embryonic multipotent neural stem cells. *J Neurochem*, 88(1), 212-226. Retrieved from <https://www.ncbi.nlm.nih.gov/pubmed/14675165>
- Cancer Genome Atlas Research Network. Electronic address, a. a. d. h. e., & Cancer Genome Atlas Research, N. (2017). Integrated Genomic Characterization of Pancreatic Ductal Adenocarcinoma. *Cancer Cell*, 32(2), 185-203 e113. doi:10.1016/j.ccell.2017.07.007
- Canino, C., Luo, Y., Marcato, P., Blandino, G., Pass, H. I., & Cioce, M. (2015). A STAT3-NFkB/DDIT3/CEBPbeta axis modulates ALDH1A3 expression in chemoresistant cell subpopulations. *Oncotarget*, 6(14), 12637-12653. doi:10.18632/oncotarget.3703
- Charafe-Jauffret, E., Ginestier, C., Bertucci, F., Cabaud, O., Wicinski, J., Finetti, P., Josselin, E., Adelaide, J., Nguyen, T. T., Monville, F., Jacquemier, J., Thomassin-Piana, J., Pinna, G., Jalaguier, A., Lambaudie, E., Houvenaeghel, G., Xerri, L., Harel-Bellan, A., Chaffanet, M., Viens, P., & Birnbaum, D. (2013). ALDH1-positive cancer stem cells predict engraftment of primary breast tumors and are governed by a common stem cell program. *Cancer Res*, 73(24), 7290-7300. doi:10.1158/0008-5472.CAN-12-4704
- Chari, S. T., Kelly, K., Hollingsworth, M. A., Thayer, S. P., Ahlquist, D. A., Andersen, D. K., Batra, S. K., Brentnall, T. A., Canto, M., Cleeter, D. F., Firpo, M. A., Gambhir, S. S., Go, V. L., Hines, O. J., Kenner, B. J., Klimstra, D. S., Lerch, M. M., Levy, M. J., Maitra, A., Mulvihill, S. J., Petersen, G. M., Rhim, A. D., Simeone, D. M., Srivastava, S., Tanaka, M., Vinik, A. I., & Wong, D. (2015). Early detection of sporadic pancreatic cancer:

- summative review. *Pancreas*, 44(5), 693-712. doi:10.1097/MPA.0000000000000368
- Chen, M. H., Weng, J. J., Cheng, C. T., Wu, R. C., Huang, S. C., Wu, C. E., Chung, Y. H., Liu, C. Y., Chang, M. H., Chen, M. H., Chiang, K. C., Yeh, T. S., Su, Y., & Yeh, C. N. (2016). ALDH1A3, the Major Aldehyde Dehydrogenase Isoform in Human Cholangiocarcinoma Cells, Affects Prognosis and Gemcitabine Resistance in Cholangiocarcinoma Patients. *Clin Cancer Res*, 22(16), 4225-4235. doi:10.1158/1078-0432.CCR-15-1800
- Cheung, A. M., Wan, T. S., Leung, J. C., Chan, L. Y., Huang, H., Kwong, Y. L., Liang, R., & Leung, A. Y. (2007). Aldehyde dehydrogenase activity in leukemic blasts defines a subgroup of acute myeloid leukemia with adverse prognosis and superior NOD/SCID engrafting potential. *Leukemia*, 21(7), 1423-1430. doi:10.1038/sj.leu.2404721
- Chiang, M. K., & Melton, D. A. (2003). Single-cell transcript analysis of pancreas development. *Dev Cell*, 4(3), 383-393. Retrieved from <https://www.ncbi.nlm.nih.gov/pubmed/12636919>
- Christ, O., Lucke, K., Imren, S., Leung, K., Hamilton, M., Eaves, A., Smith, C., & Eaves, C. (2007). Improved purification of hematopoietic stem cells based on their elevated aldehyde dehydrogenase activity. *Haematologica*, 92(9), 1165-1172. Retrieved from <https://www.ncbi.nlm.nih.gov/pubmed/17666374>
- Corti, S., Locatelli, F., Papadimitriou, D., Donadoni, C., Salani, S., Del Bo, R., Strazzer, S., Bresolin, N., & Comi, G. P. (2006). Identification of a primitive brain-derived neural stem cell population based on aldehyde dehydrogenase activity. *Stem Cells*, 24(4), 975-985. doi:10.1634/stemcells.2005-0217
- Ding, X. W., Wu, J. H., & Jiang, C. P. (2010). ABCG2: a potential marker of stem cells and novel target in stem cell and cancer therapy. *Life Sci*, 86(17-18), 631-637. doi:10.1016/j.lfs.2010.02.012
- Diop-Frimpong, B., Chauhan, V. P., Krane, S., Boucher, Y., & Jain, R. K. (2011). Losartan inhibits collagen I synthesis and improves the distribution and efficacy of nanotherapeutics in tumors. *Proc Natl Acad Sci U S A*, 108(7), 2909-2914. doi:10.1073/pnas.1018892108

- Dupe, V., Matt, N., Garnier, J. M., Chambon, P., Mark, M., & Ghyselinck, N. B. (2003). A newborn lethal defect due to inactivation of retinaldehyde dehydrogenase type 3 is prevented by maternal retinoic acid treatment. *Proc Natl Acad Sci U S A*, *100*(24), 14036-14041. doi:10.1073/pnas.2336223100
- Erkan, M., Adler, G., Apte, M. V., Bachem, M. G., Buchholz, M., Detlefsen, S., Esposito, I., Friess, H., Gress, T. M., Habisch, H. J., Hwang, R. F., Jaster, R., Kleeff, J., Kloppel, G., Kordes, C., Logsdon, C. D., Masamune, A., Michalski, C. W., Oh, J., Phillips, P. A., Pinzani, M., Reiser-Erkan, C., Tsukamoto, H., & Wilson, J. (2012). StellaTUM: current consensus and discussion on pancreatic stellate cell research. *Gut*, *61*(2), 172-178. doi:10.1136/gutjnl-2011-301220
- Everts, H. B., King, L. E., Jr., Sundberg, J. P., & Ong, D. E. (2004). Hair cycle-specific immunolocalization of retinoic acid synthesizing enzymes Aldh1a2 and Aldh1a3 indicate complex regulation. *J Invest Dermatol*, *123*(2), 258-263. doi:10.1111/j.0022-202X.2004.23223.x
- Fatima, S., Zhou, S., & Sorrentino, B. P. (2012). Abcg2 expression marks tissue-specific stem cells in multiple organs in a mouse progeny tracking model. *Stem Cells*, *30*(2), 210-221. doi:10.1002/stem.1002
- Feig, C., Jones, J. O., Kraman, M., Wells, R. J., Deonarine, A., Chan, D. S., Connell, C. M., Roberts, E. W., Zhao, Q., Caballero, O. L., Teichmann, S. A., Janowitz, T., Jodrell, D. I., Tuveson, D. A., & Fearon, D. T. (2013). Targeting CXCL12 from FAP-expressing carcinoma-associated fibroblasts synergizes with anti-PD-L1 immunotherapy in pancreatic cancer. *Proc Natl Acad Sci U S A*, *110*(50), 20212-20217. doi:10.1073/pnas.1320318110
- Fu, Z. D., Selwyn, F. P., Cui, J. Y., & Klaassen, C. D. (2016). RNA Sequencing Quantification of Xenobiotic-Processing Genes in Various Sections of the Intestine in Comparison to the Liver of Male Mice. *Drug Metab Dispos*, *44*(6), 842-856. doi:10.1124/dmd.115.068270
- Fukuda, A., Wang, S. C., Morris, J. P. t., Folias, A. E., Liou, A., Kim, G. E., Akira, S., Boucher, K. M., Firpo, M. A., Mulvihill, S. J., & Hebrok, M. (2011). Stat3 and MMP7 contribute to

- pancreatic ductal adenocarcinoma initiation and progression. *Cancer Cell*, 19(4), 441-455. doi:10.1016/j.ccr.2011.03.002
- Gangavarapu, K. J., Azabdaftari, G., Morrison, C. D., Miller, A., Foster, B. A., & Huss, W. J. (2013). Aldehyde dehydrogenase and ATP binding cassette transporter G2 (ABCG2) functional assays isolate different populations of prostate stem cells where ABCG2 function selects for cells with increased stem cell activity. *Stem Cell Res Ther*, 4(5), 132. doi:10.1186/scrt343
- Ginestier, C., Hur, M. H., Charafe-Jauffret, E., Monville, F., Dutcher, J., Brown, M., Jacquemier, J., Viens, P., Kleer, C. G., Liu, S., Schott, A., Hayes, D., Birnbaum, D., Wicha, M. S., & Dontu, G. (2007). ALDH1 is a marker of normal and malignant human mammary stem cells and a predictor of poor clinical outcome. *Cell Stem Cell*, 1(5), 555-567. doi:10.1016/j.stem.2007.08.014
- Grun, F., Hirose, Y., Kawauchi, S., Ogura, T., & Umesono, K. (2000). Aldehyde dehydrogenase 6, a cytosolic retinaldehyde dehydrogenase prominently expressed in sensory neuroepithelia during development. *J Biol Chem*, 275(52), 41210-41218. doi:10.1074/jbc.M007376200
- Guerra, C., Collado, M., Navas, C., Schuhmacher, A. J., Hernandez-Porras, I., Canamero, M., Rodriguez-Justo, M., Serrano, M., & Barbacid, M. (2011). Pancreatitis-induced inflammation contributes to pancreatic cancer by inhibiting oncogene-induced senescence. *Cancer Cell*, 19(6), 728-739. doi:10.1016/j.ccr.2011.05.011
- Hermann, P. C., Huber, S. L., Herrler, T., Aicher, A., Ellwart, J. W., Guba, M., Bruns, C. J., & Heeschen, C. (2007). Distinct populations of cancer stem cells determine tumor growth and metastatic activity in human pancreatic cancer. *Cell Stem Cell*, 1(3), 313-323. doi:10.1016/j.stem.2007.06.002
- Hosoda, W., Chianchiano, P., Griffin, J. F., Pittman, M. E., Brosens, L. A., Noe, M., Yu, J., Shindo, K., Suenaga, M., Rezaee, N., Yonescu, R., Ning, Y., Albores-Saavedra, J., Yoshizawa, N., Harada, K., Yoshizawa, A., Hanada, K., Yonehara, S., Shimizu, M., Uehara, T., Samra, J. S., Gill, A. J., Wolfgang, C. L., Goggins, M. G., Hruban, R. H., & Wood, L. D. (2017). Genetic analyses of isolated high-grade pancreatic intraepithelial

- neoplasia (HG-PanIN) reveal paucity of alterations in TP53 and SMAD4. *J Pathol*, 242(1), 16-23. doi:10.1002/path.4884
- Houbracken, I., de Waele, E., Lardon, J., Ling, Z., Heimberg, H., Rooman, I., & Bouwens, L. (2011). Lineage tracing evidence for transdifferentiation of acinar to duct cells and plasticity of human pancreas. *Gastroenterology*, 141(2), 731-741, 741 e731-734. doi:10.1053/j.gastro.2011.04.050
- Hsu, L. C., Chang, W. C., Hiraoka, L., & Hsieh, C. L. (1994). Molecular cloning, genomic organization, and chromosomal localization of an additional human aldehyde dehydrogenase gene, ALDH6. *Genomics*, 24(2), 333-341. doi:10.1006/geno.1994.1624
- Huang, E. H., Hynes, M. J., Zhang, T., Ginestier, C., Dontu, G., Appelman, H., Fields, J. Z., Wicha, M. S., & Boman, B. M. (2009). Aldehyde dehydrogenase 1 is a marker for normal and malignant human colonic stem cells (SC) and tracks SC overpopulation during colon tumorigenesis. *Cancer Res*, 69(8), 3382-3389. doi:10.1158/0008-5472.CAN-08-4418
- Hwang, R. F., Moore, T., Arumugam, T., Ramachandran, V., Amos, K. D., Rivera, A., Ji, B., Evans, D. B., & Logsdon, C. D. (2008). Cancer-associated stromal fibroblasts promote pancreatic tumor progression. *Cancer Res*, 68(3), 918-926. doi:10.1158/0008-5472.CAN-07-5714
- Ji, B., Tsou, L., Wang, H., Gaiser, S., Chang, D. Z., Daniluk, J., Bi, Y., Grote, T., Longnecker, D. S., & Logsdon, C. D. (2009). Ras activity levels control the development of pancreatic diseases. *Gastroenterology*, 137(3), 1072-1082, 1082 e1071-1076. doi:10.1053/j.gastro.2009.05.052
- Jia, J., Parikh, H., Xiao, W., Hoskins, J. W., Pflücke, H., Liu, X., Collins, I., Zhou, W., Wang, Z., Powell, J., Thorgeirsson, S. S., Rudloff, U., Petersen, G. M., & Amundadottir, L. T. (2013). An integrated transcriptome and epigenome analysis identifies a novel candidate gene for pancreatic cancer. *BMC Med Genomics*, 6, 33. doi:10.1186/1755-8794-6-33
- Jones, R. J., Gocke, C. D., Kasamon, Y. L., Miller, C. B., Perkins, B., Barber, J. P., Vala, M. S.,

- Gerber, J. M., Gellert, L. L., Siedner, M., Lemas, M. V., Brennan, S., Ambinder, R. F., & Matsui, W. (2009). Circulating clonotypic B cells in classic Hodgkin lymphoma. *Blood*, *113*(23), 5920-5926. doi:10.1182/blood-2008-11-189688
- Kahlert, C., Bergmann, F., Beck, J., Welsch, T., Mogler, C., Herpel, E., Dutta, S., Niemietz, T., Koch, M., & Weitz, J. (2011). Low expression of aldehyde dehydrogenase 1A1 (ALDH1A1) is a prognostic marker for poor survival in pancreatic cancer. *BMC Cancer*, *11*, 275. doi:10.1186/1471-2407-11-275
- Kamphorst, J. J., Nofal, M., Commisso, C., Hackett, S. R., Lu, W., Grabocka, E., Vander Heiden, M. G., Miller, G., Drebin, J. A., Bar-Sagi, D., Thompson, C. B., & Rabinowitz, J. D. (2015). Human pancreatic cancer tumors are nutrient poor and tumor cells actively scavenge extracellular protein. *Cancer Res*, *75*(3), 544-553. doi:10.1158/0008-5472.CAN-14-2211
- Kastan, M. B., Schlaffer, E., Russo, J. E., Colvin, O. M., Civin, C. I., & Hilton, J. (1990). Direct demonstration of elevated aldehyde dehydrogenase in human hematopoietic progenitor cells. *Blood*, *75*(10), 1947-1950. Retrieved from <https://www.ncbi.nlm.nih.gov/pubmed/2337669>
- Kawaguchi, Y., Cooper, B., Gannon, M., Ray, M., MacDonald, R. J., & Wright, C. V. (2002). The role of the transcriptional regulator Ptf1a in converting intestinal to pancreatic progenitors. *Nat Genet*, *32*(1), 128-134. doi:10.1038/ng959
- Kong, B., Bruns, P., Behler, N. A., Chang, L., Schlitter, A. M., Cao, J., Gewies, A., Ruland, J., Fritzsche, S., Valkovskaya, N., Jian, Z., Regel, I., Raulefs, S., Irmeler, M., Beckers, J., Friess, H., Erkan, M., Mueller, N. S., Roth, S., Hackert, T., Esposito, I., Theis, F. J., Kleeff, J., & Michalski, C. W. (2018). Dynamic landscape of pancreatic carcinogenesis reveals early molecular networks of malignancy. *Gut*, *67*(1), 146-156. doi:10.1136/gutjnl-2015-310913
- Kong, B., Wu, W., Cheng, T., Schlitter, A. M., Qian, C., Bruns, P., Jian, Z., Jager, C., Regel, I., Raulefs, S., Behler, N., Irmeler, M., Beckers, J., Friess, H., Erkan, M., Siveke, J. T., Tannapfel, A., Hahn, S. A., Theis, F. J., Esposito, I., Kleeff, J., & Michalski, C. W. (2016). A subset of metastatic pancreatic ductal adenocarcinomas depends quantitatively on

- oncogenic Kras/Mek/Erk-induced hyperactive mTOR signalling. *Gut*, 65(4), 647-657.  
doi:10.1136/gutjnl-2014-307616
- Lankadasari, M. B., Mukhopadhyay, P., Mohammed, S., & Harikumar, K. B. (2019). TAMing pancreatic cancer: combat with a double edged sword. *Mol Cancer*, 18(1), 48.  
doi:10.1186/s12943-019-0966-6
- Lapidot, T., Sirard, C., Vormoor, J., Murdoch, B., Hoang, T., Caceres-Cortes, J., Minden, M., Paterson, B., Caligiuri, M. A., & Dick, J. E. (1994). A cell initiating human acute myeloid leukaemia after transplantation into SCID mice. *Nature*, 367(6464), 645-648.  
doi:10.1038/367645a0
- Li, C., Heidt, D. G., Dalerba, P., Burant, C. F., Zhang, L., Adsay, V., Wicha, M., Clarke, M. F., & Simeone, D. M. (2007). Identification of pancreatic cancer stem cells. *Cancer Res*, 67(3), 1030-1037. doi:10.1158/0008-5472.CAN-06-2030
- Liou, G. Y., Doppler, H., Braun, U. B., Panayiotou, R., Scotti Buzhardt, M., Radisky, D. C., Crawford, H. C., Fields, A. P., Murray, N. R., Wang, Q. J., Leitges, M., & Storz, P. (2015). Protein kinase D1 drives pancreatic acinar cell reprogramming and progression to intraepithelial neoplasia. *Nat Commun*, 6, 6200. doi:10.1038/ncomms7200
- Liou, G. Y., Doppler, H., DelGiorno, K. E., Zhang, L., Leitges, M., Crawford, H. C., Murphy, M. P., & Storz, P. (2016). Mutant KRas-Induced Mitochondrial Oxidative Stress in Acinar Cells Upregulates EGFR Signaling to Drive Formation of Pancreatic Precancerous Lesions. *Cell Rep*, 14(10), 2325-2336. doi:10.1016/j.celrep.2016.02.029
- Logsdon, C. D., & Ji, B. (2009). Ras activity in acinar cells links chronic pancreatitis and pancreatic cancer. *Clin Gastroenterol Hepatol*, 7(11 Suppl), S40-43.  
doi:10.1016/j.cgh.2009.07.040
- Luo, Y., Dallaglio, K., Chen, Y., Robinson, W. A., Robinson, S. E., McCarter, M. D., Wang, J., Gonzalez, R., Thompson, D. C., Norris, D. A., Roop, D. R., Vasiliou, V., & Fujita, M. (2012). ALDH1A isozymes are markers of human melanoma stem cells and potential therapeutic targets. *Stem Cells*, 30(10), 2100-2113. doi:10.1002/stem.1193
- Luttges, J., Galehdari, H., Brocker, V., Schwarte-Waldhoff, I., Henne-Bruns, D., Kloppel, G., Schmiegel, W., & Hahn, S. A. (2001). Allelic loss is often the first hit in the biallelic



- inactivation of the p53 and DPC4 genes during pancreatic carcinogenesis. *Am J Pathol*, 158(5), 1677-1683. doi:10.1016/S0002-9440(10)64123-5
- Ma, S., Chan, K. W., Lee, T. K., Tang, K. H., Wo, J. Y., Zheng, B. J., & Guan, X. Y. (2008). Aldehyde dehydrogenase discriminates the CD133 liver cancer stem cell populations. *Mol Cancer Res*, 6(7), 1146-1153. doi:10.1158/1541-7786.MCR-08-0035
- Mace, T. A., Ameen, Z., Collins, A., Wojcik, S., Mair, M., Young, G. S., Fuchs, J. R., Eubank, T. D., Frankel, W. L., Bekaii-Saab, T., Bloomston, M., & Lesinski, G. B. (2013). Pancreatic cancer-associated stellate cells promote differentiation of myeloid-derived suppressor cells in a STAT3-dependent manner. *Cancer Res*, 73(10), 3007-3018. doi:10.1158/0008-5472.CAN-12-4601
- Magnuson, M. A., & Osipovich, A. B. (2013). Pancreas-specific Cre driver lines and considerations for their prudent use. *Cell Metab*, 18(1), 9-20. doi:10.1016/j.cmet.2013.06.011
- Marcato, P., Dean, C. A., Liu, R. Z., Coyle, K. M., Bydoun, M., Wallace, M., Clements, D., Turner, C., Mathenge, E. G., Gujar, S. A., Giacomantonio, C. A., Mackey, J. R., Godbout, R., & Lee, P. W. (2015). Aldehyde dehydrogenase 1A3 influences breast cancer progression via differential retinoic acid signaling. *Mol Oncol*, 9(1), 17-31. doi:10.1016/j.molonc.2014.07.010
- Marcato, P., Dean, C. A., Pan, D., Araslanova, R., Gillis, M., Joshi, M., Helyer, L., Pan, L., Leidal, A., Gujar, S., Giacomantonio, C. A., & Lee, P. W. (2011). Aldehyde dehydrogenase activity of breast cancer stem cells is primarily due to isoform ALDH1A3 and its expression is predictive of metastasis. *Stem Cells*, 29(1), 32-45. doi:10.1002/stem.563
- Matt, N., Dupe, V., Garnier, J. M., Dennefeld, C., Chambon, P., Mark, M., & Ghyselinck, N. B. (2005). Retinoic acid-dependent eye morphogenesis is orchestrated by neural crest cells. *Development*, 132(21), 4789-4800. doi:10.1242/dev.02031
- Moir, J. A., Mann, J., & White, S. A. (2015). The role of pancreatic stellate cells in pancreatic cancer. *Surg Oncol*, 24(3), 232-238. doi:10.1016/j.suronc.2015.05.002
- Moskaluk, C. A., Hruban, R. H., & Kern, S. E. (1997). p16 and K-ras gene mutations in the

- intraductal precursors of human pancreatic adenocarcinoma. *Cancer Res*, 57(11), 2140-2143. Retrieved from <https://www.ncbi.nlm.nih.gov/pubmed/9187111>
- Murphy, S. J., Hart, S. N., Lima, J. F., Kipp, B. R., Klebig, M., Winters, J. L., Szabo, C., Zhang, L., Eckloff, B. W., Petersen, G. M., Scherer, S. E., Gibbs, R. A., McWilliams, R. R., Vasmatazis, G., & Couch, F. J. (2013). Genetic alterations associated with progression from pancreatic intraepithelial neoplasia to invasive pancreatic tumor. *Gastroenterology*, 145(5), 1098-1109 e1091. doi:10.1053/j.gastro.2013.07.049
- Navas, C., Hernandez-Porras, I., Schuhmacher, A. J., Sibilia, M., Guerra, C., & Barbacid, M. (2012). EGF receptor signaling is essential for k-ras oncogene-driven pancreatic ductal adenocarcinoma. *Cancer Cell*, 22(3), 318-330. doi:10.1016/j.ccr.2012.08.001
- Notta, F., Chan-Seng-Yue, M., Lemire, M., Li, Y., Wilson, G. W., Connor, A. A., Denroche, R. E., Liang, S. B., Brown, A. M., Kim, J. C., Wang, T., Simpson, J. T., Beck, T., Borgida, A., Buchner, N., Chadwick, D., Hafezi-Bakhtiari, S., Dick, J. E., Heisler, L., Hollingsworth, M. A., Ibrahimov, E., Jang, G. H., Johns, J., Jorgensen, L. G., Law, C., Ludkovski, O., Lungu, I., Ng, K., Pasternack, D., Petersen, G. M., Shlush, L. I., Timms, L., Tsao, M. S., Wilson, J. M., Yung, C. K., Zogopoulos, G., Bartlett, J. M., Alexandrov, L. B., Real, F. X., Cleary, S. P., Roehrl, M. H., McPherson, J. D., Stein, L. D., Hudson, T. J., Campbell, P. J., & Gallinger, S. (2016). A renewed model of pancreatic cancer evolution based on genomic rearrangement patterns. *Nature*, 538(7625), 378-382. doi:10.1038/nature19823
- Ohlund, D., Handly-Santana, A., Biffi, G., Elyada, E., Almeida, A. S., Ponz-Sarvisé, M., Corbo, V., Oni, T. E., Hearn, S. A., Lee, E. J., Chio, I., Hwang, C. I., Tiriác, H., Baker, L. A., Engle, D. D., Feig, C., Kultti, A., Egeblad, M., Fearon, D. T., Crawford, J. M., Clevers, H., Park, Y., & Tuveson, D. A. (2017). Distinct populations of inflammatory fibroblasts and myofibroblasts in pancreatic cancer. *J Exp Med*, 214(3), 579-596. doi:10.1084/jem.20162024
- Oria, V. O., Bronsert, P., Thomsen, A. R., Foll, M. C., Zamboglou, C., Hannibal, L., Behringer, S., Biniossek, M. L., Schreiber, C., Grosu, A. L., Bolm, L., Rades, D., Keck, T., Werner, M., Wellner, U. F., & Schilling, O. (2018). Proteome Profiling of Primary Pancreatic

- Ductal Adenocarcinomas Undergoing Additive Chemoradiation Link ALDH1A1 to Early Local Recurrence and Chemoradiation Resistance. *Transl Oncol*, 11(6), 1307-1322. doi:10.1016/j.tranon.2018.08.001
- Ozdemir, B. C., Pentcheva-Hoang, T., Carstens, J. L., Zheng, X., Wu, C. C., Simpson, T. R., Laklai, H., Sugimoto, H., Kahlert, C., Novitskiy, S. V., De Jesus-Acosta, A., Sharma, P., Heidari, P., Mahmood, U., Chin, L., Moses, H. L., Weaver, V. M., Maitra, A., Allison, J. P., LeBleu, V. S., & Kalluri, R. (2015). Depletion of Carcinoma-Associated Fibroblasts and Fibrosis Induces Immunosuppression and Accelerates Pancreas Cancer with Reduced Survival. *Cancer Cell*, 28(6), 831-833. doi:10.1016/j.ccell.2015.11.002
- Pearce, D. J., Taussig, D., Simpson, C., Allen, K., Rohatiner, A. Z., Lister, T. A., & Bonnet, D. (2005). Characterization of cells with a high aldehyde dehydrogenase activity from cord blood and acute myeloid leukemia samples. *Stem Cells*, 23(6), 752-760. doi:10.1634/stemcells.2004-0292
- Pinho, A. V., Rومان, I., Reichert, M., De Medts, N., Bouwens, L., Rustgi, A. K., & Real, F. X. (2011). Adult pancreatic acinar cells dedifferentiate to an embryonic progenitor phenotype with concomitant activation of a senescence programme that is present in chronic pancreatitis. *Gut*, 60(7), 958-966. doi:10.1136/gut.2010.225920
- Poruk, K. E., Valero, V., 3rd, Saunders, T., Blackford, A. L., Griffin, J. F., Poling, J., Hruban, R. H., Anders, R. A., Herman, J., Zheng, L., Rasheed, Z. A., Laheru, D. A., Ahuja, N., Weiss, M. J., Cameron, J. L., Goggins, M., Iacobuzio-Donahue, C. A., Wood, L. D., & Wolfgang, C. L. (2016). Circulating Tumor Cell Phenotype Predicts Recurrence and Survival in Pancreatic Adenocarcinoma. *Ann Surg*, 264(6), 1073-1081. doi:10.1097/SLA.0000000000001600
- Provenzano, P. P., Cuevas, C., Chang, A. E., Goel, V. K., Von Hoff, D. D., & Hingorani, S. R. (2012). Enzymatic targeting of the stroma ablates physical barriers to treatment of pancreatic ductal adenocarcinoma. *Cancer Cell*, 21(3), 418-429. doi:10.1016/j.ccr.2012.01.007
- Puttini, S., Plaisance, I., Barile, L., Cervio, E., Milano, G., Marcato, P., Pedrazzini, T., & Vassalli, G. (2018). ALDH1A3 Is the Key Isoform That Contributes to Aldehyde Dehydrogenase

Activity and Affects in Vitro Proliferation in Cardiac Atrial Appendage Progenitor Cells.  
*Front Cardiovasc Med*, 5, 90. doi:10.3389/fcvm.2018.00090

Rahib, L., Smith, B. D., Aizenberg, R., Rosenzweig, A. B., Fleshman, J. M., & Matrisian, L. M. (2014). Projecting cancer incidence and deaths to 2030: the unexpected burden of thyroid, liver, and pancreas cancers in the United States. *Cancer Res*, 74(11), 2913-2921. doi:10.1158/0008-5472.CAN-14-0155

Rasheed, Z. A., Yang, J., Wang, Q., Kowalski, J., Freed, I., Murter, C., Hong, S. M., Koorstra, J. B., Rajeshkumar, N. V., He, X., Goggins, M., Iacobuzio-Donahue, C., Berman, D. M., Laheru, D., Jimeno, A., Hidalgo, M., Maitra, A., & Matsui, W. (2010). Prognostic significance of tumorigenic cells with mesenchymal features in pancreatic adenocarcinoma. *J Natl Cancer Inst*, 102(5), 340-351. doi:10.1093/jnci/djp535

Rovira, M., Scott, S. G., Liss, A. S., Jensen, J., Thayer, S. P., & Leach, S. D. (2010). Isolation and characterization of centroacinar/terminal ductal progenitor cells in adult mouse pancreas. *Proc Natl Acad Sci U S A*, 107(1), 75-80. doi:10.1073/pnas.0912589107

Sandgren, E. P., Luetkeke, N. C., Palmiter, R. D., Brinster, R. L., & Lee, D. C. (1990). Overexpression of TGF alpha in transgenic mice: induction of epithelial hyperplasia, pancreatic metaplasia, and carcinoma of the breast. *Cell*, 61(6), 1121-1135. Retrieved from <https://www.ncbi.nlm.nih.gov/pubmed/1693546>

Schneider, G., Siveke, J. T., Eckel, F., & Schmid, R. M. (2005). Pancreatic cancer: basic and clinical aspects. *Gastroenterology*, 128(6), 1606-1625. Retrieved from <https://www.ncbi.nlm.nih.gov/pubmed/15887154>

Shao, C., Sullivan, J. P., Girard, L., Augustyn, A., Yenerall, P., Rodriguez-Canales, J., Liu, H., Behrens, C., Shay, J. W., Wistuba, II, & Minna, J. D. (2014). Essential role of aldehyde dehydrogenase 1A3 for the maintenance of non-small cell lung cancer stem cells is associated with the STAT3 pathway. *Clin Cancer Res*, 20(15), 4154-4166. doi:10.1158/1078-0432.CCR-13-3292

Sherman, M. H., Yu, R. T., Engle, D. D., Ding, N., Atkins, A. R., Tiriach, H., Collisson, E. A., Connor, F., Van Dyke, T., Kozlov, S., Martin, P., Tseng, T. W., Dawson, D. W., Donahue, T. R., Masamune, A., Shimosegawa, T., Apte, M. V., Wilson, J. S., Ng, B., Lau, S. L.,

- Gunton, J. E., Wahl, G. M., Hunter, T., Drebin, J. A., O'Dwyer, P. J., Liddle, C., Tuveson, D. A., Downes, M., & Evans, R. M. (2014). Vitamin D receptor-mediated stromal reprogramming suppresses pancreatitis and enhances pancreatic cancer therapy. *Cell*, 159(1), 80-93. doi:10.1016/j.cell.2014.08.007
- Shi, G., DiRenzo, D., Qu, C., Barney, D., Miley, D., & Konieczny, S. F. (2013). Maintenance of acinar cell organization is critical to preventing Kras-induced acinar-ductal metaplasia. *Oncogene*, 32(15), 1950-1958. doi:10.1038/onc.2012.210
- Sophos, N. A., Pappa, A., Ziegler, T. L., & Vasiliou, V. (2001). Aldehyde dehydrogenase gene superfamily: the 2000 update. *Chem Biol Interact*, 130-132(1-3), 323-337. Retrieved from <https://www.ncbi.nlm.nih.gov/pubmed/11306055>
- Sophos, N. A., & Vasiliou, V. (2003). Aldehyde dehydrogenase gene superfamily: the 2002 update. *Chem Biol Interact*, 143-144, 5-22. Retrieved from <https://www.ncbi.nlm.nih.gov/pubmed/12604184>
- Sousa, C. M., Biancur, D. E., Wang, X., Halbrook, C. J., Sherman, M. H., Zhang, L., Kremer, D., Hwang, R. F., Witkiewicz, A. K., Ying, H., Asara, J. M., Evans, R. M., Cantley, L. C., Lyssiotis, C. A., & Kimmelman, A. C. (2016). Pancreatic stellate cells support tumour metabolism through autophagic alanine secretion. *Nature*, 536(7617), 479-483. doi:10.1038/nature19084
- Storms, R. W., Trujillo, A. P., Springer, J. B., Shah, L., Colvin, O. M., Ludeman, S. M., & Smith, C. (1999). Isolation of primitive human hematopoietic progenitors on the basis of aldehyde dehydrogenase activity. *Proc Natl Acad Sci U S A*, 96(16), 9118-9123. Retrieved from <https://www.ncbi.nlm.nih.gov/pubmed/10430905>
- Storz, P. (2017). Acinar cell plasticity and development of pancreatic ductal adenocarcinoma. *Nat Rev Gastroenterol Hepatol*, 14(5), 296-304. doi:10.1038/nrgastro.2017.12
- Tanaka, M., Shibahara, J., Fukushima, N., Shinozaki, A., Umeda, M., Ishikawa, S., Kokudo, N., & Fukayama, M. (2011). Claudin-18 is an early-stage marker of pancreatic carcinogenesis. *J Histochem Cytochem*, 59(10), 942-952. doi:10.1369/0022155411420569
- Tanei, T., Morimoto, K., Shimazu, K., Kim, S. J., Tanji, Y., Taguchi, T., Tamaki, Y., & Noguchi,

- S. (2009). Association of breast cancer stem cells identified by aldehyde dehydrogenase 1 expression with resistance to sequential Paclitaxel and epirubicin-based chemotherapy for breast cancers. *Clin Cancer Res*, *15*(12), 4234-4241. doi:10.1158/1078-0432.CCR-08-1479
- Tang, D. G. (2012). Understanding cancer stem cell heterogeneity and plasticity. *Cell Res*, *22*(3), 457-472. doi:10.1038/cr.2012.13
- Ting, D. T., Wittner, B. S., Ligorio, M., Vincent Jordan, N., Shah, A. M., Miyamoto, D. T., Aceto, N., Bersani, F., Brannigan, B. W., Xega, K., Ciciliano, J. C., Zhu, H., MacKenzie, O. C., Trautwein, J., Arora, K. S., Shahid, M., Ellis, H. L., Qu, N., Bardeesy, N., Rivera, M. N., Deshpande, V., Ferrone, C. R., Kapur, R., Ramaswamy, S., Shioda, T., Toner, M., Maheswaran, S., & Haber, D. A. (2014). Single-cell RNA sequencing identifies extracellular matrix gene expression by pancreatic circulating tumor cells. *Cell Rep*, *8*(6), 1905-1918. doi:10.1016/j.celrep.2014.08.029
- Tjensvoll, K., Nordgard, O., & Smaaland, R. (2014). Circulating tumor cells in pancreatic cancer patients: methods of detection and clinical implications. *Int J Cancer*, *134*(1), 1-8. doi:10.1002/ijc.28134
- Todoric, J., Antonucci, L., Di Caro, G., Li, N., Wu, X., Lytle, N. K., Dhar, D., Banerjee, S., Fagman, J. B., Browne, C. D., Umemura, A., Valasek, M. A., Kessler, H., Tarin, D., Goggins, M., Reya, T., Diaz-Meco, M., Moscat, J., & Karin, M. (2017). Stress-Activated NRF2-MDM2 Cascade Controls Neoplastic Progression in Pancreas. *Cancer Cell*, *32*(6), 824-839 e828. doi:10.1016/j.ccell.2017.10.011
- van den Hoogen, C., van der Horst, G., Cheung, H., Buijs, J. T., Lippitt, J. M., Guzman-Ramirez, N., Hamdy, F. C., Eaton, C. L., Thalmann, G. N., Cecchini, M. G., Pelger, R. C., & van der Pluijm, G. (2010). High aldehyde dehydrogenase activity identifies tumor-initiating and metastasis-initiating cells in human prostate cancer. *Cancer Res*, *70*(12), 5163-5173. doi:10.1158/0008-5472.CAN-09-3806
- Vasiliou, V., Bairoch, A., Tipton, K. F., & Nebert, D. W. (1999). Eukaryotic aldehyde dehydrogenase (ALDH) genes: human polymorphisms, and recommended nomenclature based on divergent evolution and chromosomal mapping.

- Pharmacogenetics*, 9(4), 421-434. Retrieved from <https://www.ncbi.nlm.nih.gov/pubmed/10780262>
- Vasiliou, V., & Pappa, A. (2000). Polymorphisms of human aldehyde dehydrogenases. Consequences for drug metabolism and disease. *Pharmacology*, 61(3), 192-198. doi:10.1159/000028400
- Vasiliou, V., Pappa, A., & Estey, T. (2004). Role of human aldehyde dehydrogenases in endobiotic and xenobiotic metabolism. *Drug Metab Rev*, 36(2), 279-299. doi:10.1081/DMR-120034001
- Vernet, N., Dennefeld, C., Rochette-Egly, C., Oulad-Abdelghani, M., Chambon, P., Ghyselinck, N. B., & Mark, M. (2006). Retinoic acid metabolism and signaling pathways in the adult and developing mouse testis. *Endocrinology*, 147(1), 96-110. doi:10.1210/en.2005-0953
- Vincent, A., Herman, J., Schulick, R., Hruban, R. H., & Goggins, M. (2011). Pancreatic cancer. *Lancet*, 378(9791), 607-620. doi:10.1016/S0140-6736(10)62307-0
- Visvader, J. E., & Lindeman, G. J. (2008). Cancer stem cells in solid tumours: accumulating evidence and unresolved questions. *Nat Rev Cancer*, 8(10), 755-768. doi:10.1038/nrc2499
- Visvader, J. E., & Lindeman, G. J. (2012). Cancer stem cells: current status and evolving complexities. *Cell Stem Cell*, 10(6), 717-728. doi:10.1016/j.stem.2012.05.007
- von Figura, G., Fahrenkrog-Petersen, L., Hidalgo-Sastre, A., Hartmann, D., Huser, N., Schmid, R. M., Hebrok, M., Roy, N., & Esposito, I. (2017). Atypical flat lesions derive from pancreatic acinar cells. *Pancreatology*, 17(3), 350-353. doi:10.1016/j.pan.2017.04.014
- Wagers, A. J., & Weissman, I. L. (2004). Plasticity of adult stem cells. *Cell*, 116(5), 639-648. Retrieved from <https://www.ncbi.nlm.nih.gov/pubmed/15006347>
- Wagner, M., Redaelli, C., Lietz, M., Seiler, C. A., Friess, H., & Buchler, M. W. (2004). Curative resection is the single most important factor determining outcome in patients with pancreatic adenocarcinoma. *Br J Surg*, 91(5), 586-594. doi:10.1002/bjs.4484
- Wilentz, R. E., Geradts, J., Maynard, R., Offerhaus, G. J., Kang, M., Goggins, M., Yeo, C. J., Kern, S. E., & Hruban, R. H. (1998). Inactivation of the p16 (INK4A) tumor-suppressor

- gene in pancreatic duct lesions: loss of intranuclear expression. *Cancer Res*, 58(20), 4740-4744. Retrieved from <https://www.ncbi.nlm.nih.gov/pubmed/9788631>
- Wilentz, R. E., Iacobuzio-Donahue, C. A., Argani, P., McCarthy, D. M., Parsons, J. L., Yeo, C. J., Kern, S. E., & Hruban, R. H. (2000). Loss of expression of Dpc4 in pancreatic intraepithelial neoplasia: evidence that DPC4 inactivation occurs late in neoplastic progression. *Cancer Res*, 60(7), 2002-2006. Retrieved from <https://www.ncbi.nlm.nih.gov/pubmed/10766191>
- Zhou, Q., Law, A. C., Rajagopal, J., Anderson, W. J., Gray, P. A., & Melton, D. A. (2007). A multipotent progenitor domain guides pancreatic organogenesis. *Dev Cell*, 13(1), 103-114. doi:10.1016/j.devcel.2007.06.001
- Ziegler, T. L., & Vasiliou, V. (1999). Aldehyde dehydrogenase gene superfamily. The 1998 update. *Adv Exp Med Biol*, 463, 255-263. Retrieved from <https://www.ncbi.nlm.nih.gov/pubmed/10352694>



## 10. CURRICULUM VITAE

**Familiennamen:** Cao

**Vorname:** Jing

**Geburtsdatum:** 10.12.1989

**Geschlecht:** weiblich

**Familienstatus:** ledig

**Nationalität:** chinesisch

**Adresse:** Katharina-Eberhard-Straße 14, 85540, Haar, München

**Tel:** +49 015141348313

**Email:** jing.v.cao@gmail.com

### **Ausbildung und beruflicher Werdegang:**

10/2015 - Stipendiat, Anfertigung der medizinischen Doktorarbeit

Technische Universität München

09/2013 - 06/2015 Master in Medizin, Southeast University, China

09/2008 - 06/2013 Bachelor in Medizin, Southeast University, China

### **Publikationen:**

**Jing Cao**, Zhiheng Zhang, Carsten Jäger, Helmut Friess and Bo Kong. Aldh1a3 labels a subtype of cancer-associated fibroblasts with inflammatory phenotype in pancreatic ductal adenocarcinoma. (Published in 51st Annual Meeting of the European Pancreatic Club. 2019.06)

Kong B\*, Bruns P\*, Behler NA\*, Chang L, Schlitter AM, **Cao J**, et al. Dynamic landscape of pancreatic carcinogenesis reveals early molecular networks of malignancy. *Gut*. 2018 Jan;67(1):146-156. doi: 10.1136/gutjnl-2015-310913.

Kong B\*, Cheng T\*, Qian C\*, Wu W, Steiger K, **Cao J**, et al. Pancreas-specific activation of mTOR and loss of p53 induce tumors reminiscent of acinar cell carcinoma. *Mol Cancer*. 2015 Dec 18;14:212. doi: 10.1186/s12943-015-0483-1.

## 11. ACKNOWLEDGEMENTS

By writing these acknowledgements, I would like to express my sincere gratitude and appreciation to all the people who have offered their generous help and support to me during my 4-year study in TUM in Germany.

I am appreciative of the executive committee of the university for carrying out my dissertation within the framework of the Doctor Med program.

I would like to thank my supervisor, Prof. Helmut Friess, for his scientific supervision and providing me with the great opportunity to join the surgical research family in TUM and introducing the beautiful German culture to me. His noble personality, profound knowledge, and rigorous academic attitude always inspire me to explore in the research and pursue my dreams.

I would like to thank my mentor, Dr. Dr. Bo Kong, for his tremendous support for my research and life during my study in Germany. He led me into the basic medical research field and trained to be an active and independent researcher with creative ideas. Without his enlightening supervising, insightful ideas and valuable suggestions, I could not complete my projects or finish this thesis.

Moreover, I would like to thank our technician, Ms Nadja Maeritz, the axis to keep our lab running perfectly, for her generous technical assistance. Besides her meticulous assistance, she serves also as the motivator of our group activities and culture exchanges. We could only have such a positive and colorful research life with her enthusiasm.

I would like to thank our postdoc, Dr. rer. nat. Kathleen Schuck, for her advices and kind help in correcting my thesis. Besides, she has helped us with a good many of tricky problems in the project and the lab routines, although she just joined us newly. Her quiet confidence always

calms me in confronting problems stressfully. I would also like to thank Dr. rer.nat Susanne Raulefs, and Dr. rer.nat Jie Qie. Although they finished their work and left our group already, they had offered me with their patient instructions and helpful comments.

I would like to thank my other colleagues of our pancreas research group, including Dr. Mingyue Hu, Yuanyuan Yu, Zhiheng Zhang, Yamin Zhao for their generous support during my work.

I am sincerely grateful to the China Scholarship for funding and supporting me during my stay in Germany for the past four years.

In the end, I would like to thank my parents, Mr Dongya Cao and Mrs Ying Huang. I am deeply indebted to them for their endless devotion and encouragement. Their selfless love and care warm and inspire me all the time across half of the world and encourages me to exert my best during my study. And I would also like to thank my beloved boyfriend Xiaobo Wang, who companies me, consoles me and encourages me in both happy and frustrated time during my research study.